TRANSPORT.PDF

Environmental Engineering Science

William W Nazaroff and Lisa Alvarez-Cohen
Department of Civil and Environmental Engineering
University of California, Berkeley

John Wiley & Sons, Inc.
New York / Chichester / Weinheim / Brisbane / Singapore / Toronto

4

Transport Phenomena

Transport phenomena are encountered in almost every aspect of environmental engineering science. In assessing the environmental impacts of waste discharges, we seek to predict the impact of emissions on contaminant concentrations in nearby air and water. Contaminant transport must be understood to evaluate the effect of wastewater discharge to a river on downstream water quality or the effect of an incinerator on downwind air pollutant levels. In waste treatment technologies, contaminant transport within the control device influences the overall efficiency. In many instruments used to measure environmental contamination, performance depends on the effective transport of contaminants from the sampling point to the detector.

The physical scales of concern for contaminant transport span an enormous range. At the low end, we are interested in phenomena that occur over molecular dimensions, such as the transport of a contaminant into the pore of an adsorbent. At the upper extreme, we consider the transport of air and waterborne contaminants over

global distances. This range of linear dimensions encompasses approximately 15 orders of magnitude. Not surprisingly, some phenomena that are important at one end of the spectrum are irrelevant at the other.

Transport phenomena also are important in other fields of study, notably chemical and mechanical engineering. In these fields, the subject is often subdivided into fluid mechanics, heat transfer, and mass transfer. In environmental engineering, where the focus is on the movement of contaminants in air and water, elements of all three of these branches are considered. The essential ingredients for understanding contaminant transport processes are knowledge of the basic physical phenomena coupled with the analytical tools of engineering mathematics.

Because of the importance of both molecular and particulate impurities in environmental fluids, the dominant transport processes of both molecules and particles will be discussed in this chapter. We consider both the movement of impurities *with* fluids and their movement *relative to* fluids. In Chapter 5, we will explore how the transformation mechanisms studied in Chapter 3 and the transport mechanisms explored in this chapter are combined to predict system behavior using mathematical models.

4.A BASIC CONCEPTS AND MECHANISMS

4.A.1 Contaminant Flux

Transport of both molecules and particles is commonly quantified in terms of *flux density,* or simply *flux.* Flux is a vector quantity, comprising both a magnitude and a direction. The flux vector points in the direction of net contaminant motion, and the magnitude indicates the rate at which the contaminant is moving.

For example, think of an environmental fluid as depicted in Figure 4.A.1. Imagine a small square frame suspended in this fluid and centered at a point of interest. The frame is oriented so that the transport of contaminants through it is maximized. Then the flux vector points in a direction normal to the frame, aligned with the direction of contaminant transport. The magnitude of the flux vector is the net rate of contaminant transport per unit area of the frame. Since the flux can vary from one position to another, the flux at a point represents the net transport through the frame per area in the limit of the frame becoming infinitesimally small. The common units of flux are mass or moles per area per time. We will use the symbol J to represent flux. An arrow is written above J when we wish to emphasize its vector character. Contributions to flux

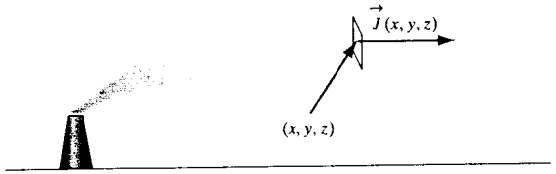

Figure 4.A.1 Flux, $\vec{J}$, is a vector quantity whose value varies with position (x, y, z). The contaminant flux vector points in the direction of transport, and its magnitude is the quantity transported (usually mass or moles) per area per time.

Table 4.A.1 Dominant Mechanisms That Cause Transport of Molecules and Particles in Environmental Fluids

Transport mechanism	Species[a]	Description	1-D flux[b]
Advection	m, p	Movement with fluid	$J_a = CU$
Gravitational settling	p	Transport induced by gravity	$J_g = Cv_t$
Molecular diffusion or Brownian motion[c]	m, p	Transport caused by random thermal motion	$J_d = -D\frac{dC}{dx}$
Turbulent diffusion	m, p	Transport caused by apparently random fluid velocity fluctuations in turbulent flow	$J_t = -\varepsilon_t\frac{dC}{dx}$
Shear-flow dispersion	m, p	Transport caused by nonuniform fluid flow with position	$J_s = -\varepsilon_s\frac{dC}{dx}$
Hydrodynamic dispersion (porous media)	m, p	Transport caused by nonuniform flow through porous material	$J_h = -\varepsilon_h\frac{dC}{dx}$
Electrostatic drift[d]	m, p[e]	Movement of charged species in an electric field	$J_e = Cv_e$
Inertial drift	p	Transport associated with acceleration of a fluid	$J_f = Cv_f$

[a] m = molecule, p = particle.

[b] C = species concentration, U = fluid velocity, v_t = settling velocity, D = molecular or Brownian diffusivity, ε_t = turbulent diffusivity, ε_s = shear-flow dispersivity, ε_h = dispersion coefficient, v_e = electrostatic drift velocity, v_f = inertial drift velocity, J = flux.

[c] Molecular diffusion and Brownian motion apply to molecules and particles, respectively; both occur from the same fundamental process.

[d] See §7.C.

[e] Electrostatic drift applies to charged species only.

may be caused by several mechanisms (Table 4.A.1). A major thrust of this chapter is to explore the basic physical mechanisms that cause contaminant flux.

4.A.2 Advection

Advection is the transport of material caused by the net flow of the fluid in which that material is suspended. Whenever a fluid is in motion, all contaminants in the fluid, including both molecules and particles, are advected along with the fluid.

Figure 4.A.2 shows how an advective flux can be evaluated. Consider a fluid flowing through a tube with a uniform velocity. Assume that the fluid contains a uniform concentration, C, of some contaminant. Focus on the amount of contaminant in a slice of fluid of thickness ΔL. As shown in the upper part of the diagram, at time t, the leading edge of the slice has just reached position x. At some later time, $t + \Delta t$ (see the lower part of the diagram), the trailing edge of the slice passes position x.

The advective flux vector for this contaminant points along the axis of the tube, in the same direction as the velocity vector. The magnitude of the flux vector at position x is obtained by dividing the amount of contaminant that passes position x by the cross-sectional area of the tube (A) and by the time interval required (Δt). The amount of contaminant that passes position x is the contaminant concentration (C) times the volume of the depicted slice ($\Delta L \times A$). Note that the time interval (Δt) is equal to the thickness of the slice divided by the fluid velocity ($\Delta L/U$). So, for this case, the advective flux magnitude, J_a, is the quantity of contaminant passing position x per area

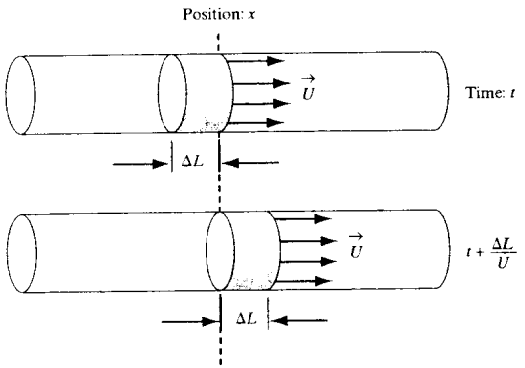

Figure 4.A.2 Advective flux of contaminant through a tube. The two pictures represent the same tube at two points in time, t and $t + \Delta t$, where $\Delta t = \Delta L/U$.

per time:

$$J_a = \frac{C \times \Delta L \times A}{A(\Delta L/U)} = CU \tag{4.A.1}$$

In general, the three-dimensional advective flux vector is the product of the contaminant concentration and the fluid velocity:

$$\vec{J}_a(x, y, z) = C(x, y, z) \times \vec{U}(x, y, z) \tag{4.A.2}$$

4.A.3 Molecular Diffusion

The molecules in air and water are constantly moving. If it could be viewed at a molecular scale, this movement would appear random and chaotic. Molecular movement in gases is particularly frenzied. In air at ordinary environmental conditions, a typical molecule, moving at a speed of ~400 m s^{-1}, collides with other molecules on the order of 10 billion times per second. Each collision involves an exchange of momentum between the participants, causing them to change direction and speed. Every cubic centimeter of air has a phenomenally large number of molecules (~25 million trillion at $T = 298$ K and $P = 1$ atm) participating in this dance. In water, where the molecules are packed a thousand times more densely, molecular motion is less frenetic, but still extremely energetic.

Although the molecular-scale motion seems hopelessly disordered, the macroscopic effects are well understood and predictable. Qualitatively, the random motion of fluid molecules causes a net movement of species from regions of high concentration to regions of low concentration. This phenomenon is known as *molecular diffusion*. The rate of movement depends on the concentration difference, with larger differences leading to higher rates of transport. The rate also varies according to how far the species must travel from high to low concentration: The longer the distance, the lower the flux. The rate of transport varies according to the molecular properties of the species, particularly size and mass, with larger size and larger mass resulting in slower transport. The properties of the fluid itself play a key role: Molecular diffusion

is much slower in water than in air because of the much closer packing density of water molecules.

Our discussion is restricted to conditions in which the diffusing species is present at a low mole fraction ($\ll 1$), referred to as the *infinite dilution* condition. In most environmental engineering applications, this assumption is appropriate. At high concentrations, diffusion can cause significant net flow of the bulk fluid (Bird et al., 1960; Cussler, 1984).

Fick's Law

To better understand diffusion, it is useful to think about a specific physical system, such as the one depicted in Figure 4.A.3. A glass bulb at 25 °C contains a liquid with a moderate vapor pressure, such as ethylbenzene (1280 Pa at 25 °C; see Table 3.B.1). The bulb is open to the air through a thin cylindrical glass tube. Ethylbenzene molecules evaporate from the liquid, maintaining a partial pressure in the gas phase of the bulb equal to the saturation vapor pressure. Because of their random motion, the ethylbenzene molecules gradually migrate through the tube and escape into the open air. After a short transient period, the net rate of transport of ethylbenzene molecules through the tube will reach a steady value that will be maintained as long as there is liquid ethylbenzene in the bulb. The escape rate of ethylbenzene from the tube varies in inverse proportion to tube length, in proportion to the cross-sectional area of the tube, and in proportion to the partial pressure of the species in the bulb. These characteristics can be expressed quantitatively by the relationship

$$J_d \propto -\frac{\Delta C}{\Delta x} \tag{4.A.3}$$

where J_d is the diffusive flux density (moles per cross-sectional area of the tube per time), ΔC is the change in concentration of ethylbenzene molecules across the tube, and Δx is the tube length. The minus sign appears in this relationship to remind us that the diffusive flux proceeds in the direction of decreasing concentration.

By introducing the proportionality constant, D, this expression can be converted to an equation:

$$J_d = -D\frac{\Delta C}{\Delta x} \tag{4.A.4}$$

The constant, D, is called the *diffusion coefficient*, or *diffusivity*. It is a property of the diffusing species (ethylbenzene in this case), the fluid through which it is diffusing

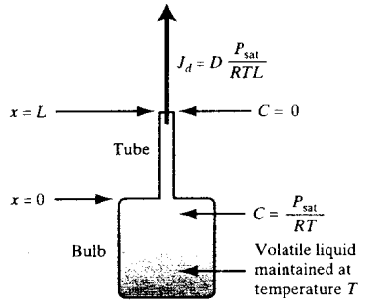

Figure 4.A.3 Apparatus for producing a controlled diffusive flux of a volatile species. P_{sat} is the saturation vapor pressure of the species at temperature T. Provided that the time scale for evaporation and condensation is much more rapid than the time scale for diffusion through the tube, a molar concentration P_{sat}/RT will be attained throughout the bulb. The vapor molecules will diffuse through the tube with a net diffusive flux J_d.

(air), and environmental conditions such as temperature and pressure. The diffusion coefficient has dimensions of length squared per time; typically, D is reported in units of $cm^2\ s^{-1}$. For molecules in air, a characteristic diffusivity is 0.1 $cm^2\ s^{-1}$. In water, molecular diffusivities are on the order of 10^{-5} $cm^2\ s^{-1}$.

If we treat a fluid as a continuous substance, and take the limit of equation 4.A.4 as the distance Δx becomes infinitesimally small, we can replace $\Delta C/\Delta x$ by the derivative dC/dx and write

$$J_d = -D\frac{dC}{dx} \tag{4.A.5}$$

For applications in three dimensions, the general equation for diffusive flux can be written as follows:

$$\vec{J_d}(x, y, z) = -D\left(\frac{\partial C}{\partial x}, \frac{\partial C}{\partial y}, \frac{\partial C}{\partial z}\right) \tag{4.A.6}$$

In words, equation 4.A.6 states that each component of the flux vector is proportional to the partial derivative of concentration in that coordinate direction, and the proportionality constant is $-D$ for each direction. So diffusive flux occurs in the direction opposite to the concentration gradient at a rate that is proportional to its magnitude. Equations 4.A.5 and 4.A.6 are known as Fick's first law of diffusion, or simply Fick's law. See Exhibit 4.A.1 for more details about the system depicted in Figure 4.A.3.

Significance of Diffusion

Diffusion is a slow transport process. Albert Einstein showed that the characteristic distance a molecule (or a particle) will travel by diffusion in time t is given by

$$x \sim \sqrt{2Dt} \tag{4.A.7}$$

So a gas molecule with a diffusivity of 0.1 $cm^2\ s^{-1}$ can be expected to move a characteristic distance of 5 mm in a second, 3 cm in a minute, 30 cm in an hour, and 1 m in a day. Molecules in water, with diffusivities lower by a factor of 10^{-4}, will travel only 1 percent as far on these time scales.

Another perspective is gained by comparing the simple form of Fick's law (equation 4.A.4) with the simple advective flux expression (equation 4.A.1). If a species concentration diminishes from C to zero over some distance Δx, then diffusion causes transport at a rate equivalent to advection at a velocity $D/\Delta x$. Given the small values of D for air and especially for water, we see that the effective diffusive velocity is very small except when the concentration changes by a large fractional amount over a very small distance.

Although molecular diffusion is a slow process, it plays a very important role in contaminant transport and fate. Diffusion is particularly important at interfaces, for example between two fluids such as air and water, or at solid-fluid interfaces. There can be no fluid advection at an interface in the direction normal to the surface. So impurities cannot be transported by advection all the way to an interface. Instead, some other transport mechanism must convey the species through a small distance, known as a *boundary layer*, to the interface. For uncharged molecular impurities, diffusion is the dominant mechanism of transport through boundary layers. For ions and particles, diffusion always contributes, although other mechanisms such as electrostatic drift and gravitational settling may also play a role. These details are important because impurities may be removed from a fluid by deposition or other transformation processes that occur on surfaces. Often, the rate of transport to the surface governs the overall removal rate.

EXHIBIT 4.A.1 *An Application of Diffusion*

Let's further explore the behavior of the system depicted in Figure 4.A.3. Devices like this are used to release a volatile substance at a constant rate. By diluting the emissions from the top of the tube with a known flow rate of contaminant-free air, one generates an air stream with a constant, known concentration of the volatile substance. This air stream can be used for instrument calibration among other purposes.

When liquid is first placed into the bulb, some time must elapse before the diffusive flux leaving the tube reaches a steady value. An estimate of this time is obtained by rearranging equation 4.A.7 (substituting $\tau_{diffusion}$ for t and L for x):

$$\tau_{diffusion} \sim \frac{L^2}{2D} \tag{4.A.8}$$

This expression yields an estimate of the time required for a molecule to diffuse through some distance L. It is a good estimate for the characteristic time required to establish a steady concentration profile throughout the tube length. For typical values in a device of this sort, $L \sim$ 5 cm and $D \sim 0.1$ $cm^2\ s^{-1}$, so $\tau_{diffusion} \sim 2$ min. With conditions held steady for a time $t \gg \tau_{diffusion}$, the flux will approach a steady value that will be maintained as long as liquid remains in the bulb.

The characteristic time for the liquid to completely evaporate is obtained as the number of moles of liquid in the bulb divided by the molar rate of escape by diffusion:

$$\tau_{evaporation} \sim \frac{\left(\frac{\rho V}{MW}\right)}{J_d A} \tag{4.A.9}$$

where ρ is the liquid density, V is the liquid volume, MW is the molecular weight of the diffusing species, and A is the cross-sectional area of the tube. For the case of ethylbenzene, we can estimate an evaporation time, $\tau_{evaporation} \sim 4 \times 10^7$ s ~ 500 d. We have assumed the following values for the input data: ρV = 1 g, MW = 106 g mol^{-1}, $J_d = 7.2 \times 10^{-9}$ mol $cm^{-2}\ s^{-1}$ (D = 0.07 $cm^2\ s^{-1}$, P_{sat} = 1280 Pa, $R = 8.31 \times 10^6$ cm^3 Pa K^{-1} mol^{-1}, T = 298 K, and L = 5 cm), and A = 0.031 cm^2 (0.2 cm inner tube diameter). For times t that satisfy $\tau_{diffusion} \ll t \ll \tau_{evaporation}$, the diffusive flux from the tube into the air will be constant. During this time interval, the concentration profile within the tube will also be constant, varying linearly with position x, as shown in Figure 4.A.4.

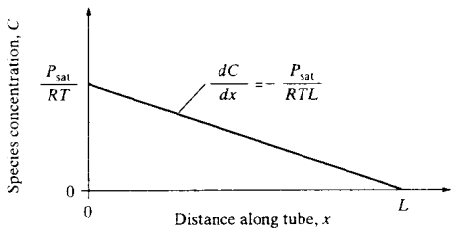

Figure 4.A.4 Steady concentration profile within the tube shown in Figure 4.A.3, valid for times t that satisfy $\tau_{diffusion} \ll t \ll \tau_{evaporation}$.

Diffusivity of Molecules in Air

Predictions of diffusive flux depend on the selection of an appropriate diffusion coefficient, D. Measured diffusion coefficients for selected species in air are presented in Table 4.A.2. This table emphasizes species of environmental interest, with air at ordinary environmental temperatures and pressures as the background fluid. Note that there are discrepancies in the data reported from different sources (e.g., ammonia).

Table 4.A.2 Measured Diffusion Coefficients for Species in Air at 1 atm

Species	Formula	T (K)	D ($cm^2\ s^{-1}$)	Reference[a]
Ammonia	NH_3	273	0.198	Bretsznajder, 1971
		273	0.216	McCabe et al., 1993
Benzene	C_6H_6	273	0.077	McCabe et al., 1993
		298.2	0.096	Cussler, 1984
Carbon dioxide	CO_2	273	0.138	McCabe et al., 1993
		317.2	0.177	Cussler, 1984
Ethanol	C_2H_5OH	273	0.102	McCabe et al., 1993; Cussler, 1984
		313	0.147	Reid et al., 1987 (pressure = 1 bar)
Helium	He	276.2	0.624	Cussler, 1984
Hydrogen	H_2	273	0.611	Cussler, 1984; McCabe et al., 1993
Methane	CH_4	273	0.196	Cussler, 1984
Methyl alcohol	CH_3OH	273	0.133	McCabe et al., 1993
n-Octane	C_8H_{18}	273	0.051	McCabe et al., 1993
Naphthalene	$C_{10}H_8$	273	0.051	McCabe et al., 1993
		303	0.087	Reid et al., 1987
Oxygen	O_2	273	0.178	Cussler, 1984; McCabe et al., 1993
Toluene	C_7H_8	273	0.071	McCabe et al., 1993
		299.1	0.086	Cussler, 1984
Water	H_2O	273	0.219	Bretsznajder, 1971; McCabe et al., 1993
		289.1	0.282	Cussler, 1984
		298.2	0.260	Cussler, 1984
		312.6	0.277	Cussler, 1984
		313	0.292	Reid et al., 1987

[a]When two sources disagree by less than 5 percent, only one value is listed.

The data in Table 4.A.2 show that the diffusivity of gases in air varies over about an order of magnitude from about 0.05 $cm^2\ s^{-1}$ for large organic molecules (*n*-octane and naphthalene) to about 0.6 $cm^2\ s^{-1}$ for helium and hydrogen. Diffusivities increase with increasing temperature because of the higher kinetic energy of the molecules.

Diffusivities of Molecular Species in Water

Experimental data for selected species in water are presented in Table 4.A.3. These data exhibit a range of about a factor of 5.

4.A.4 Dispersion

Our everyday experience tells us that impurities released into open air or water do not remain confined at high concentration in a small volume for very long. Cooking odors, incense, and cigarette smoke all become detectable throughout an indoor space within minutes of their release. The visible smoke plume from a fire can be seen to spread significantly as it travels downwind. The rate of contaminant spreading is of substantial interest in environmental engineering. And although fundamentally it occurs as a result of advection and diffusion, the rate of spreading is much more rapid than might be inferred from the discussion so far.

Table 4.A.3 Measured Diffusion Coefficients for Species in Water

Species	Formula	T (K)	D ($cm^2\ s^{-1}$)	Reference[a]
Benzene	C_6H_6	298	1.02×10^{-5}	Cussler, 1984
Hydrogen	H_2	298	3.36×10^{-5}	Bretsznajder, 1971
		298	4.50×10^{-5}	Cussler, 1984
Air		298	2.00×10^{-5}	Cussler, 1984
Methane	CH_4	275	0.85×10^{-5}	Reid et al., 1987
Carbon dioxide	CO_2	298	2.00×10^{-5}	Reid et al., 1987
Methanol	CH_3OH	288	1.26×10^{-5}	Reid et al., 1987
		298	0.84×10^{-5}	Cussler, 1984
Ethanol	C_2H_5OH	288	1.00×10^{-5}	Reid et al., 1987
		298	0.84×10^{-5}	Cussler, 1984
Ethylbenzene	C_8H_{10}	293	0.81×10^{-5}	Reid et al., 1987
Oxygen	O_2	298	2.60×10^{-5}	Bretsznajder, 1971
Vinyl chloride	C_2H_3Cl	298	1.34×10^{-5}	Reid et al., 1987

[a]When two sources disagree by less than 5 percent, only one value is listed.

Uniform, steady advection does not cause pollutant spreading, and we have seen that molecular diffusion is a slow process. Consider the following situation (Cussler, 1984). Imagine that a thin stream of smoke particles is released along the western coast of the United States and is steadily advected at a constant, uniform wind speed of 5 m s^{-1} to the eastern coast. Assume that particles have a diameter of 0.1 μm. How much spreading of the plume will occur by diffusion during this transcontinental travel? The time required for the wind to travel that distance is $\sim 10^6$ s or 12 d (5000 km ÷ 5 m s^{-1}). In Example 4.B.3 it will be shown that a 0.1 μm particle has a diffusivity in air of 7×10^{-6} $cm^2\ s^{-1}$. The plume spread caused by diffusion is estimated to be the characteristic distance traveled due to Brownian motion, which, according to equation 4.A.7, is roughly 4 cm. Clearly, this is not an accurate description! It is entirely contrary to our experience to think that we could even detect a smoke plume at a distance of 5000 km from its source. Yet this example accurately applies the tools and concepts we have introduced. What went wrong?

Our error was made in assuming that the wind speed is uniform and steady. It is a property of most fluid flows, including winds and ocean currents, that they are neither constant nor uniform. When fluid velocity varies with time or position, contaminants in the fluid tend to be transported from high concentration to low concentration. The spreading of contaminants by nonuniform flows is called *dispersion*.* It is not a fundamentally distinct transport process. Instead, dispersion is caused by nonuniform advection and influenced by diffusion.

Figure 4.A.5 illustrates why it is important to incorporate dispersion into the analysis of environmental transport. Pollutants are shown being released from an elevated stack and blowing downwind. The left-hand figures show that in the case of weak dispersion, the plume spreads slowly. Downwind of the source, the peak concentrations remain very high near the plume centerline and the pollutants do not spread rapidly to the ground. On the right, dispersion is strong. The concentrations within the plume are diminished rapidly by dispersion, but the plume reaches the ground much nearer to the source. This trade-off is characteristic of the effect that

*We will use the term *dispersion* to include both shear-flow dispersion and turbulent diffusion.

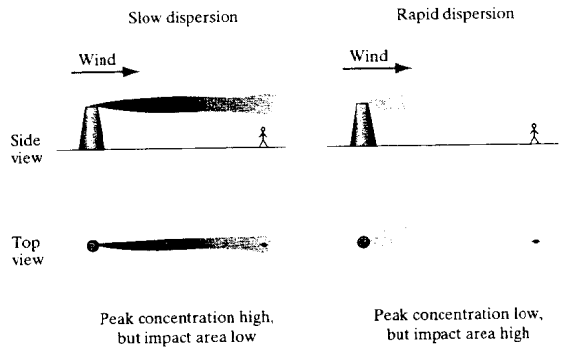

Figure 4.A.5 Effect of dispersion on pollutant concentrations downwind of a localized source. If the release rate of pollutants and mean wind speed are the same in the left- and right-hand frames, then the total flow of pollutants is the same in the two cases. Rapid dispersion leads to smaller peak concentrations but a larger impact area.

dispersion has in all environmental settings: High dispersion rates reduce average concentrations at the expense of increasing the area or duration of impact. A common challenge in environmental transport modeling is to predict concentrations in the region downwind or downstream of a pollution source. To make these predictions in the face of dispersion phenomena, we must solve two problems. First, we must have a model that describes pollutant concentration fields in the presence of dispersion. Second, we must be able to determine how the rate of dispersion varies with environmental conditions.

In complex flow fields, it is impossible (or at least impractical) to describe fluid velocity exactly as a function of space and time. Without this information, dispersion cannot be accurately described in terms of the fundamental mechanisms of advection and molecular diffusion. As an alternative, dispersion can be treated as a random process, analogous to molecular diffusion, by applying Fick's first law of diffusion with the molecular diffusion coefficient replaced by a dispersion coefficient. So in one dimension, we would write

$$J_{\text{dispersion}} = -\varepsilon \frac{dC}{dx} \tag{4.A.10}$$

where ε is a *dispersion coefficient*, obtained through a combination of empirical data and theoretical equations.

Although equation 4.A.10 has the same form as Fick's first law, it is important to bear in mind the great distinction between diffusion and dispersion. Diffusivities are properties of the contaminant and the fluid, depending weakly on environmental conditions (such as temperature) but not at all on fluid flows. Dispersion coefficients, on the other hand, are primarily a function of the fluid flow field. Environmental flows are highly variable and very complex. Dispersion in environmental flows is far less well understood than molecular diffusion. One should not expect a high degree of accuracy from any models that must account for dispersion, especially when applied to environmental transport.

Dispersion phenomena arise in all three branches of environmental engineering discussed in this text. Figure 4.A.5 illustrates one of many instances that arise in air quality engineering. In water quality, the impact of wastewater discharges on contaminant concentrations in rivers, lakes, or oceans depend on dispersion. In hazardous waste management, dispersion controls the movement of contaminants in groundwater.

Several types of dispersion phenomena are encountered in environmental engineering. In this section, two common types are introduced: *shear-flow dispersion* and *turbulent diffusion.*

Shear-Flow Dispersion

In a shear flow, the fluid speed varies with position in a direction that is perpendicular to the fluid velocity. If contaminant concentrations in a shear flow vary in the direction of flow, then dispersion will occur, leading to a net transport of contaminants from regions of high concentration to areas of low concentration.

Shear-flow dispersion is generally important when there is a short-term release of contaminants, such as a spill, in environments in which the velocity gradients are large, such as a river, an estuary influenced by tides, or the near-ground atmosphere. Let's consider a relatively simple example: shear-flow dispersion in fully developed laminar flow through a circular tube or pipe (Figure 4.A.6). The velocity profile of the fluid flow is parabolic because of wall friction. At time $t = 0$, some mass, M, of contaminant is injected into the tube at position $x = 0$ and instantaneously mixed laterally so that its concentration is uniform across the tube. We then observe the contaminant as it is advected past some position, L, downstream. The upper frame in the figure shows the initial condition. The lower frame shows the tube at a subsequent time, $t = L/U_0$. At the later time, the contaminant pulse is centered on downstream position $x = L$, but it has been substantially stretched because those molecules that lie close to the centerline of the tube are advected at a higher velocity than those near the wall. At the same time, contaminant molecules positioned near the leading edge of the pulse and near the center of the tube tend to diffuse toward the walls, reducing their average forward velocity. Conversely, contaminant molecules located near the trailing edge of the pulse along the tube walls tend to diffuse toward the center, increasing their forward velocity. Therefore, surprisingly, the net effect of molecular diffusion is to slow the rate of dispersion, in this case.

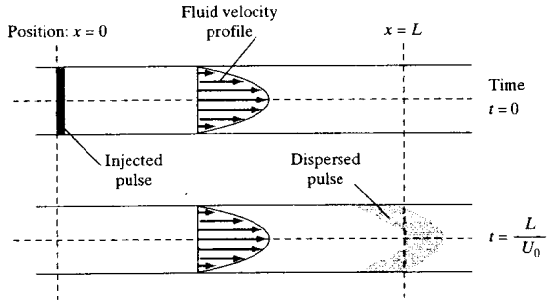

Figure 4.A.6 Schematic of a model problem illustrating the effects of shear-flow dispersion.

For the situation depicted in Figure 4.A.6, the contaminant flux in the direction of flow can be described as the sum of two components: (1) advection, which transports the overall pulse through the tube, and (2) shear-flow dispersion, which causes the pulse to become stretched as it travels. The flux in the direction of flow caused by shear-flow dispersion is written as

$$J_s = -\varepsilon_s \frac{dC(x)}{dx} \tag{4.A.11}$$

where ε_s is the shear-flow dispersivity and $C(x)$ represents the contaminant concentration averaged over a cross-section of the tube at position x.

Shear-flow dispersion is most commonly applied to predict the transport of contaminants in systems in which the flow is confined. In addition to pipe or tube flow, shear-flow dispersion is applied to study pollutant transport in rivers and in estuarine environments influenced by tides.

Turbulent Diffusion

In most systems encountered in environmental engineering, fluid flows are *turbulent* rather than *laminar*. Whereas for laminar flows we can determine the fluid velocity field at each instant and each position, turbulent flows fluctuate in such a manner that predictions are nearly impossible. Instead, we describe turbulent flows in terms of their statistical properties, such as the mean speed and the average size of the fluctuations.

Like molecular diffusion, the apparently random motion that is characteristic of turbulent flows causes a net flux of a contaminant from high to low concentrations. This flux is often described by an equation that is analogous to Fick's law:

$$J_t = -\varepsilon_t \frac{dC}{dx} \tag{4.A.12}$$

where ε_t is the *turbulent diffusion coefficient* and C now denotes the time-averaged value of concentration. For application in three dimensions, this expression can be generalized to vector form:

$$\vec{J_t} = -\left(\varepsilon_{tx}\frac{\partial C}{\partial x}, \varepsilon_{ty}\frac{\partial C}{\partial y}, \varepsilon_{tz}\frac{\partial C}{\partial z}\right) \tag{4.A.13}$$

Here ε_{tx}, ε_{ty}, and ε_{tz} represent the *turbulent diffusion coefficients*, or *eddy diffusivities* in the x, y, and z directions, respectively. Typically, for turbulent transport in the atmosphere or in natural waters, the coordinate system is arranged so that x and y lie in the horizontal plane and z is vertical. Vertical eddy diffusivity generally differs from horizontal eddy diffusivity. Usually, though, it is assumed that $\varepsilon_{tx} = \varepsilon_{ty}$.

To help visualize the impact of turbulence on pollutant dispersion, ignite something that will generate a visible smoke plume, such as a cigarette or some incense. Place the smoldering object indoors in still air with lighting that permits good observation of the plume. (For example, position a high-intensity desk lamp on the opposite side of the plume from you, but just out of your line of sight, and direct the light at the plume.) If the air is sufficiently still so that the buoyancy of the plume controls its motion, you will see the plume rise in a steady, narrow stream for a distance on the order of 10–30 cm, then buckle, and finally break up into turbulent eddies. The flow in the lower portion of the plume is laminar, and the flow in the upper portion is turbulent. If you now imagine that the concentration of smoke particles is to be determined on a

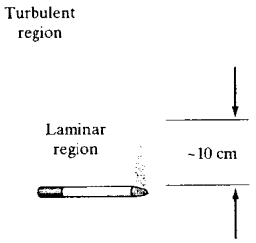

Figure 4.A.7 Schematic representation of time-averaged smoke plume rising from a smoldering cigarette in still air.

time-averaged basis, over a minute or so, you should arrive at a picture like the one shown in Figure 4.A.7. The broadening of the plume in the turbulent region is a direct consequence of turbulent air motion. The mean fluid flow is still upward, but there are fluctuating horizontal components of the flow that cause rapid pollutant dispersion in the horizontal direction. For environmental engineering applications, this is a key property of turbulence: In unbounded flow, turbulent diffusion controls the transport of pollutants in directions normal to the mean flow.

Figure 4.A.8 depicts a plume spreading from a point source discharging either to water or to air. A horizontal slice through the center of the plume is shown from above, and the mean fluid velocity is oriented from left to right. The coordinates are oriented so that x is aligned with the mean velocity and y represents the horizontal distance from the plume centerline. The origin is positioned at the source.

Assume that the rate of pollutant discharge is constant and the mean fluid velocity is independent of position and time. Then Figure 4.A.8 represents the average conditions over some period, such as an hour. On this basis, the plume spreads fairly smoothly and symmetrically from the source. The coordinate axes at right show the time-averaged concentration profile plotted against y at some distance away from the source. The peak concentration occurs at $y = 0$ and gradually approaches zero as the distance from the centerline increases. The spreading of the plume in the y-direction is controlled by turbulent diffusion.

A practical challenge in the use of equation 4.A.13 is to determine the turbulent diffusivities. These parameters vary not only with flow conditions, but also with position and direction. For example, turbulent diffusivities diminish to zero at rigid fluid boundaries, because the fluid velocity itself goes to zero. Correlations exist for

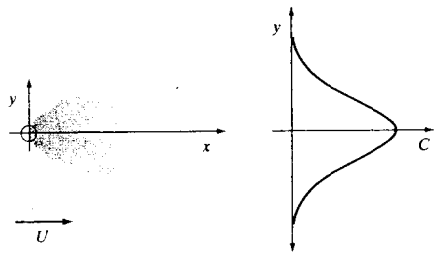

Figure 4.A.8 Plume spreading from a point source. The pollutant discharge rate is constant and the mean fluid velocity is steady and uniform, but the flow is turbulent.

predicting turbulent diffusivities, but these should be used cautiously, as the supporting experimental data are limited.

Turbulent diffusivities are higher in rivers than in regular channels because the irregularities in the river channel create additional irregularities in the flow, which tend to enhance mixing. Turbulent diffusivities in rivers are an order of magnitude smaller than longitudinal (shear-flow) dispersion coefficients. Consequently, studies of transport and mixing in rivers typically account for transport across the flow by turbulent diffusion and along the flow by advection and shear-flow dispersion. Vertical transport is assumed to occur very rapidly, since most rivers are much wider than deep.

In the atmosphere, turbulent diffusion is especially important in the vertical direction. Most pollutants are emitted near the ground, and the rate and extent of vertical turbulent diffusion strongly influences ground-level concentrations. Atmospheric stability, as will be discussed in §7.D, has a very strong influence on turbulent diffusivities, especially in the vertical direction. In unstable conditions, which are characterized by strong heating of the ground by the sun, vertical velocity fluctuations are strong and turbulent diffusivities are high.

Typical turbulent diffusivity values for both rivers and the atmosphere exceed by many orders of magnitude molecular diffusivities of contaminants. This observation reinforces the point that pollutant dispersion away from fluid boundaries is controlled by a combination of shear-flow dispersion and turbulent diffusion, and not by molecular or Brownian motion.

SKIP "PARTICLE MOTION", PICK UP AGAIN ON p 182

4.C MASS TRANSFER AT FLUID BOUNDARIES

Several important phenomena occur at the boundaries of fluids. The rate of contaminant transport to and from these boundaries may have a strong influence on contaminant concentration. This influence occurs in both natural and engineered systems. Contaminants can enter or leave a fluid at a boundary, and they may also undergo chemical transformations there. The boundaries of interest include air-water interfaces as well as boundaries between either air or water and (a) soil, (b) other solid surfaces, or (c) nonaqueous liquids such as fuels and solvents.

There is a close relationship between the transport phenomena explored in this section and the transformation processes involving phase change discussed in §3.B. In fact, the distinction between transport and transformation is somewhat blurred here. The kinetics of phase change processes depend, in general, both on the rate of transport to or from the fluid boundary and the kinetics of the transformation processes. Transport and transformation processes occur serially, so the slower process governs the overall rate.

Transport across air-water interfaces is of particular interest in environmental engineering. Several treatment technologies involve transferring pollutants from one phase

to the other. For example, scrubbers remove acid gases such as sulfur dioxide and hydrochloric acid from waste air streams by transferring them to water, where they can easily be neutralized. Air strippers remove volatile organic compounds from water. Once the organic molecules are transferred to the gas phase, they can be more easily captured by sorption or destroyed by oxidation processes. In nature, air-water exchanges are also important. The transfer of oxygen from air to water supports aquatic life. The ultimate fate of many air pollutants involves transfer to cloud or rainwater followed by deposition to the earth's surface. The uptake of carbon dioxide by the oceans plays a key role in moderating the impact of fossil fuel combustion on climate.

Transport to a fluid boundary may occur by a variety of mechanisms. Diffusion is always present and often is the rate-limiting process because, at rigid boundaries, flow velocities diminish to zero. Advection usually plays a role in controlling the thickness of the layer through which diffusion must occur. For particles, gravitational settling, electrostatic drift, inertial drift, and other mechanisms may dominate transport near boundaries.

For engineering analysis of transport processes at fluid boundaries, we seek a description that captures the overall effects, that does not violate central principles such as mass conservation, and that is practical to apply. We will employ models that link flux to concentrations and may include an empirical parameter. In the case of turbulent diffusion, we used an equation inspired by Fick's law of diffusion, and the empirical parameter was turbulent diffusivity. For mass transfer at boundaries, similarly inspired flux equations will be written that incorporate a mass-transfer coefficient as the empirical parameter.

4.C.1 Mass-Transfer Coefficient

The net rate of mass flux between a fluid and its boundary is commonly expressed in this form:

$$J_b = k_m(C - C_i) \tag{4.C.1}$$

Here J_b is the net flux to the boundary (amount of species per area per time). When J_b is greater than zero, the flux direction is from the fluid to the boundary; when J_b is less than zero, the flux is directed from the boundary to the fluid. The concentration terms C and C_i, respectively, represent the species concentration in the bulk fluid far from the boundary and the species concentration in the fluid immediately adjacent to the boundary. The other parameter in this equation, k_m, is known as a *mass-transfer coefficient*. The mass-transfer coefficient commonly has units of velocity (length per time).

Figure 4.C.1 shows a simple system for which a mass-transfer coefficient can be directly derived. A glass cylinder is partly filled with a pure volatile liquid (with a sat-

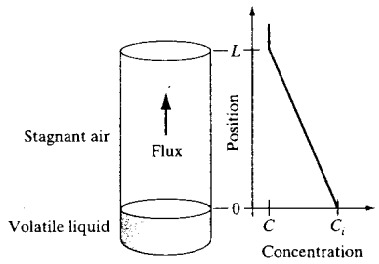

Figure 4.C.1 A simple system in which a mass-transfer coefficient can be directly determined.

uration vapor pressure $\ll$ 1 atm). The remainder of the cylinder contains stagnant air. Molecules of the liquid evaporate, diffuse through the cylinder, and escape from the open top into the free air. Provided that diffusion is not too rapid, the gas-phase concentration of the diffusing species at the liquid-gas interface will be determined directly as $P_{sat}/(RT)$, where P_{sat} is the equilibrium vapor pressure of the liquid. Assume that the concentration at the top of the cylinder is maintained at some value, C, determined by processes occurring in the open air. After an initial transient period, during which the gas-phase concentration profiles may change, a steady-state linear profile will be established, as depicted in Figure 4.C.1. The diffusive flux through the tube, J_d, is given by Fick's law as

$$J_d = D\frac{C_i - C}{L} \tag{4.C.2}$$

The net transport rate from the air to the liquid is equal to the negative of the diffusive flux, J_d. Comparing equation 4.C.2 with equation 4.C.1, we see that the mass-transfer coefficient for this system is

$$k_m = \frac{D}{L} \tag{4.C.3}$$

This is a general result, provided that the concentration profile is steady: For pure diffusion through a stagnant layer, the mass-transfer coefficient is given by the diffusivity divided by the thickness of the layer.

A second case is illustrated in Figure 4.C.2. Particles are suspended in a fluid above a horizontal boundary. The fluid is motionless, the particle concentration is uniform, and the particles migrate only because of gravitational settling. All particles are assumed to have the same settling velocity, v_t. The concentration of particles in the fluid at the interface is taken to be zero. This may seem peculiar, since the particles accumulate on the bottom boundary. However, provided resuspension does not occur (as it will not in a stagnant fluid), once the particles strike the boundary, they are no longer suspended in the fluid, and so it is reasonable to assign $C_i = 0$. The gravitational flux to the surface, J_g, is then given by

$$J_g = v_t C \tag{4.C.4}$$

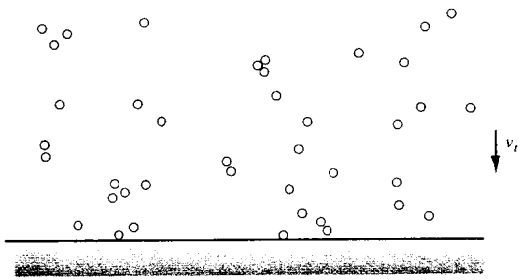

Figure 4.C.2 In a uniform suspension of monodisperse particles settling through a stagnant fluid onto a horizontal surface, the mass-transfer coefficient is equal to the settling velocity.

Comparing this result with equation 4.C.1, we see that for this case the mass-transfer coefficient is equal to the particle settling velocity:

$$k_m = v_t \tag{4.C.5}$$

This too is a general result. Whenever contaminant transport to a surface occurs solely because of a net migration velocity, the mass-transfer coefficient is equal to that velocity.

These examples yield exact expressions for the mass-transfer coefficient. However, in most applications, the use of a mass-transfer coefficient is a simplified description of what is a very complicated set of processes. Therefore, a high degree of precision should not be expected in problems involving mass transfer at boundaries.

Applying equation 4.C.1 wisely requires a sound understanding of the meaning of each of the four variables. First, let's consider the concentration at the interface, C_i. In many cases, C_i can be taken to be zero. This is appropriate when a transformation process that is fast and irreversible occurs at the boundary. Particle deposition by settling is one example where C_i is zero: When a particle strikes a surface with a low incident velocity, it adheres essentially immediately. Chemical transformations can also produce an interface concentration of zero if transport, rather than surface-reaction kinetics, is the rate-limiting step. In some cases, such as that shown in Figure 4.C.1, the interface concentration can be determined by assuming local equilibrium at the boundary.

An important issue arises concerning the species concentration in bulk fluid, C: Where should it be determined? The issue is easily resolved when the fluid is well mixed outside of a thin boundary layer (see Figure 4.C.3). Then C is the concentration anywhere outside the boundary layer. However, some circumstances arise in environmental engineering in which species concentrations vary strongly with position throughout the fluid. In such cases, the use of a mass-transfer coefficient may yield no more than a rough approximation of the mass-transfer rate at surfaces.

A complication arises when the fluid boundary occurs at a surface that has a complex texture. If J_b represents the quantity of contaminant transferred *per area* per time, how do we define the area? Typically, the flux to rough surfaces is determined on the basis of a superficial or apparent area. In other cases, rather than determining the interface area and the mass-transfer coefficient separately, their product is determined and the mass-transfer equation is rewritten in terms of total net transfer of species (flux times area) rather than in terms of flux.

The final issue to address is how an appropriate mass-transfer coefficient is determined for a given situation. There are two main approaches, and both are widely used. For systems with fairly regular geometries, the mass-transfer coefficient is calculated using existing correlations based on theory or experimental data. Some of these correlations are presented below. A second approach, commonly used for more complex systems, is to calculate mass-transfer coefficients based on experiments conducted in laboratory or field settings.

Film Theory

The simplest model system that includes fluid flow divides the fluid into two layers. Adjacent to the surface is a stagnant layer, or film, through which species must diffuse. The concentration profile within the film is assumed to be linear, corresponding to steady diffusive flux. In the second layer, the fluid is well mixed and the species concentration is uniform everywhere.

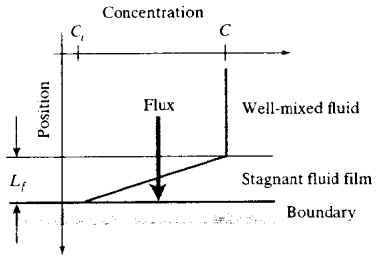

Figure 4.C.3 Schematic of mass transfer to a surface according to film theory.

Mass transfer from the fluid to a surface, according to film theory, is depicted in Figure 4.C.3. This situation is almost identical to that depicted in Figure 4.C.1, and so, in analogy with equation 4.C.3, it should be clear that the mass-transfer coefficient for this case is

$$k_m = \frac{D}{L_f} \tag{4.C.6}$$

where L_f is the film thickness. Film theory suggests that for given flow conditions, the mass-transfer coefficient should scale in direct proportion to species diffusivity ($k_m \propto D$). Experiments consistently demonstrate that, in systems with fluid flow, the mass-transfer coefficient flow increases in proportion to D^{α}, with $\alpha < 1$. The key weakness of film theory is its dependence on a specific value of the film thickness, L_f. In most circumstances, there is no practical way to determine L_f that is independent of a measurement of mass transfer (or heat transfer) to a surface. Furthermore, the effective thickness of the film through which species must diffuse varies with species diffusivity: A higher diffusion coefficient results in a larger film thickness. Still, although not entirely accurate, film theory provides a helpful conceptual picture of interfacial mass transfer.

Penetration Theory

Recall (equation 4.A.8) that the characteristic time required for a steady-state concentration profile to be established by diffusion is given by $L^2(2D)^{-1}$ where L is the distance over which diffusion occurs. In film theory, the boundary must be in contact with the fluid for a minimum time of $\tau \sim L_f^2(2D)^{-1}$ for the concentration profile to approach the constant-slope condition depicted in Figure 4.C.3. In some circumstances, the contact time between a boundary and a fluid is not long enough for film theory to apply. A second conceptual model, known as penetration theory, has been developed to address this case.

The model is based on transient diffusion in one dimension. At time $t = 0$, the concentration in the fluid is assumed to be uniform everywhere except at the position of the boundary, where it is C_i. Then diffusion to the surface begins and a boundary layer begins to grow (Figure 4.C.4). Fluid motion affects the contact time between the fluid and the boundary.

Analysis of time-dependent diffusion to a flat surface yields the following expression for the mass-transfer coefficient:

$$k_m(t) = \left[\frac{D}{\pi t}\right]^{1/2} \qquad \text{instantaneous} \tag{4.C.7}$$

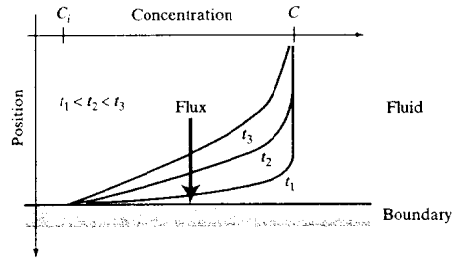

Figure 4.C.4 Schematic of mass transfer to a surface according to penetration theory.

This is the instantaneous mass-transfer coefficient at time t. Because the distance through which species must diffuse increases with time, k_m decreases as t increases. If the contact period is maintained for some interval t^*, the time-averaged mass-transfer coefficient is obtained by integration:

$$k_m = \frac{1}{t^*}\int_0^{t^*} k_m(t)\,dt = 2\left[\frac{D}{\pi t^*}\right]^{1/2} \qquad \text{average} \tag{4.C.8}$$

From equation 4.C.8, we see that penetration theory predicts that the mass-transfer coefficient should increase in proportion to the square root of species diffusivity. By contrast, we have just seen that film theory predicts that the mass-transfer coefficient is proportional to diffusivity. The reason for the difference lies in the assumptions about the distance through which species must diffuse. In film theory, the film thickness is assumed to be constant and so is independent of D. In penetration theory, the diffusion distance increases with time, and the rate of growth depends on species diffusivity.

Boundary-Layer Theory: Laminar Flow along a Flat Surface

Transport from moving fluids to boundaries is caused by simultaneous advection and diffusion, with advection being stronger far from the boundary and diffusion dominating adjacent to the boundary. Film and penetration theories simplify the analysis by decoupling advection from diffusion. Boundary-layer theory can predict mass-transfer coefficients for simple flows and geometries while simultaneously accounting for the effects of both transport mechanisms.

Let's consider the case of laminar fluid flow at velocity U, parallel to a flat surface (see Figure 4.C.5). The species concentration is C_i at the surface and is C far from the surface. Within the boundary layer there is a concentration gradient, which gives rise to diffusion toward the surface. There are also advective velocity components in

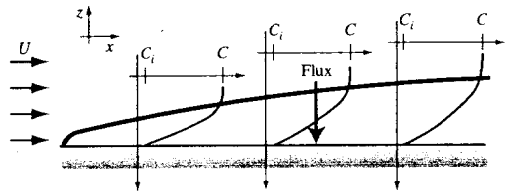

Figure 4.C.5 Schematic of mass transfer to a surface according to boundary-layer theory for the case of a flat surface parallel to a uniform, laminar fluid flow.

the x-direction (relatively strong) and the z-direction (relatively weak) that affect the concentration profile. The characteristic thickness of the boundary layer for a contaminant species is the distance from the surface over which the concentration increases to approximately C. As shown in Figure 4.C.5, the boundary-layer thickness grows with increasing distance downstream of the leading edge. The thickness of this boundary layer at any x-position is a function of species diffusivity, with higher diffusivity causing a thicker boundary layer. For any given species, a thicker boundary layer means slower mass transfer to the surface. Because of species loss at the surface, the boundary-layer thickness grows with downstream distance and the rate of mass transfer correspondingly decreases.

This problem is analyzed using equations that describe the conservation of fluid mass, momentum, and species in the boundary layer (Cussler, 1984; Bejan, 1984). The result is a mass-transfer coefficient calculated at a specific position x downstream of the leading edge of the surface:

$$k_m(x) = 0.323\left(\frac{U}{x}\right)^{1/2} \nu^{-1/6} D^{2/3} \qquad \text{local} \qquad (4.C.9)$$

where ν is the kinematic fluid viscosity. (Recall that $\nu = \mu/\rho$, where μ is the dynamic fluid viscosity and ρ is the fluid density.) The overall mass-transfer coefficient to the surface is obtained by averaging over the length of the surface:

$$k_m = \frac{1}{L}\int_0^L k_m(x)\,dx = 0.646\left(\frac{U}{L}\right)^{1/2} \nu^{-1/6} D^{2/3} \qquad \text{average} \qquad (4.C.10)$$

Equation 4.C.10 gives the average mass-transfer coefficient for this flow system for a surface from the leading edge to a distance L downstream. Note that the mass-transfer coefficient, k_m, varies with the diffusion coefficient raised to the 2/3 power. It is generally true that when advection and diffusion are combined, the mass-transfer coefficient increases with diffusivity raised to some power between 0.5 (penetration theory) and 1 (film theory).

4.C.2 Transport across the Air-Water Interface

In environmental engineering applications, the rate of transport of a molecular species across an air-water interface is described by an expression similar to equation 4.C.1:

$$J_{gl} = k_{gl}(C_s - C) \qquad (4.C.11)$$

where J_{gl} is the net flux of a species from the gas phase to the liquid phase (mass per interfacial area per time), k_{gl} is a mass-transfer coefficient (length per time), C is the concentration of the species in the bulk liquid phase, and C_s is the saturation (or equilibrium) concentration of the species in the liquid phase that corresponds to the given partial pressure of the species in the gas phase. Typically, C_s is obtained from Henry's law (see §3.B.2). When C_s exceeds the current aqueous concentration, $J_{gl} > 0$ and net transfer occurs from the gas to the liquid. Conversely, when the water is supersaturated with respect to the gas phase, $C > C_s$, so $J_{gl} < 0$, and equation 4.C.11 predicts a net rate of volatilization.

In general, the mass-transfer coefficient k_{gl} depends on fluid flow near the interface and on species diffusivity in both air and water. The film model introduced in the previous section can be extended to a two-film model, as depicted in Figure 4.C.6, with the air-water interface as the boundary. In this model, stagnant film layers exist

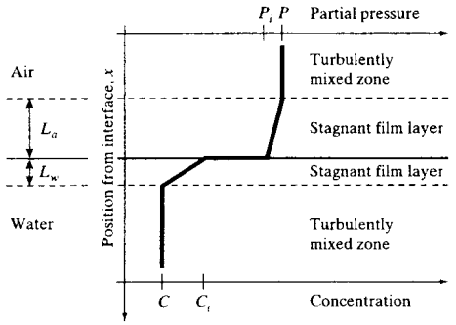

Figure 4.C.6 Schematic of the two-film model for estimating mass transport across an air-water interface.

on either side of the boundary through which species transport occurs only by molecular diffusion. Outside of its stagnant film layer, each fluid is well mixed. Immediately adjacent to the interface, the partial pressure in the gas phase, P_i, is assumed to be in equilibrium with the aqueous concentration, C_i, as described by Henry's law. As in the film model, the concentration profiles in the stagnant film layers are assumed to be linear. Also, because of mass conservation, the flux through the air layer must be equal to the flux through the water layer.

Applying Fick's law, we can write the gas-side flux (from air to the interface) as

$$J_{gl} = D_a \frac{(P - P_i)/RT}{L_a} \qquad (4.C.12)$$

where D_a is the species diffusivity through air and L_a is the thickness of the stagnant film layer in the air. Likewise, the liquid-side flux (from the interface into the water) is

$$J_{gl} = D_w \frac{C_i - C}{L_w} \qquad (4.C.13)$$

where D_w is the species diffusivity in water and L_w is the film-layer thickness in the water. Since we don't know either P_i or C_i, we would like to eliminate these parameters from the expressions. So far, we have two equations but three unknowns (J_{gl}, C_i, and P_i).

The third equation comes from the equilibrium relationship at the interface:

$$C_i = K_H P_i \qquad (4.C.14)$$

where K_H is the Henry's law constant for the species (see Table 3.B.2). Now, we can use algebra to derive an expression for flux that is in the form of equation 4.C.11. Use equation 4.C.14 to replace P_i with C_i/K_H in equation 4.C.12. Then equate the right-hand sides of equations 4.C.12 and 4.C.13 and solve for C_i to obtain

$$C_i = \frac{\alpha C_s + C}{1 + \alpha} \qquad (4.C.15)$$

where

$$\alpha = \frac{D_a L_w}{D_w L_a K_H RT} \qquad (4.C.16)$$

and

$$C_s = K_H P \qquad (4.C.17)$$

Next substitute for C_i from equation 4.C.15 into equation 4.C.13. After some algebraic manipulation, one arrives at equation 4.C.11, where

$$k_{gl} = \frac{D_w}{L_w}\left(\frac{\alpha}{1+\alpha}\right) = \frac{1}{\frac{L_w}{D_w} + \frac{L_a}{D_a}K_H RT} \tag{4.C.18}$$

The film thicknesses, L_w and L_a, cannot be measured. So for practical application, we rewrite equation 4.C.18 in this form:

$$\frac{1}{k_{gl}} = \frac{1}{k_l} + \frac{K_H RT}{k_g} \tag{4.C.19}$$

where k_l and k_g are the respective mass-transfer coefficients through the liquid and gas boundary layers near the interface, each corresponding to the diffusivity divided by the film thickness (D_w/L_w and D_a/L_a, respectively), as in equation 4.C.6. The factor K_H appears with k_g in this expression because k_{gl} is used with the aqueous concentrations to determine flux (equation 4.C.11). The factor RT is needed to convert partial pressure to molar concentration, since we write Henry's law in a way that relates aqueous molar concentration to gaseous partial pressure.

Equations 4.C.11 and 4.C.19 are together sometimes called the *two-resistance model for interfacial mass transfer*. Since species must be transported through fluid on both sides of the interface, the total resistance (k_{gl}^{-1}) is the sum of the resistance in the liquid side of the interface (k_l^{-1}) plus the resistance on the gas side ($K_H RT k_g^{-1}$).

From equation 4.C.19 we see that the relative sizes of the gas and liquid resistances vary according to the Henry's law constant, K_H. The diffusion coefficients, D, of molecular species in a given fluid vary by about one order of magnitude (§4.A.3). The film resistance terms k_l and k_g are expected to vary by no more than D to the first power (§4.C.1). The Henry's law constant, on the other hand, varies by at least eight orders of magnitude among species of interest in environmental engineering (see Table 3.B.2). Therefore, even for fixed flow conditions, the interfacial mass-transfer coefficient, k_{gl}, may vary greatly from one species to another according to the value of the Henry's law constant. This point is illustrated in Figure 4.C.7.

Liss and Slater (1974) reviewed available information on the mass transfer of species between the oceans and the atmosphere and concluded that liquid-side and gas-side mass-transfer coefficients of $k_l = 0.2$ m h^{-1} and $k_g = 30$ m h^{-1} apply for average meteorological and ocean current conditions. These coefficients are suggested to be approximately correct for species with molecular weights between 15 and 65 g/mol. Figure 4.C.7 shows how the overall mass-transfer coefficient varies with the Henry's law constant for molecular species exchange between the atmosphere and the seas. For sparingly soluble gases such as oxygen ($K_H = 0.0014$ M atm^{-1}), the resistance lies entirely on the liquid side and an overall average mass-transfer coefficient of approximately $k_{gl} = 0.2$ m/h applies. On the other hand, the resistance for a highly soluble species such as formaldehyde ($K_H = 6300$ M atm^{-1}) lies entirely on the gas side.

The liquid-side and gas-side mass-transfer coefficients can be combined with values of species diffusivities to estimate effective film thicknesses: $L_a \sim D_a k_g^{-1} \sim 2$ mm and $L_w \sim D_w k_l^{-1} \sim 20$ μm. We see from these estimates that diffusive transport over very small length scales controls the overall rate of interfacial mass transfer. The time scales required for steady-state concentration profiles to be achieved in gas and liquid films of this size are approximately $\tau_g \sim L_a^2(2D_a)^{-1} \sim 0.1$ s and $\tau_l \sim L_w^2(2D_w)^{-1} \sim 0.2$ s.

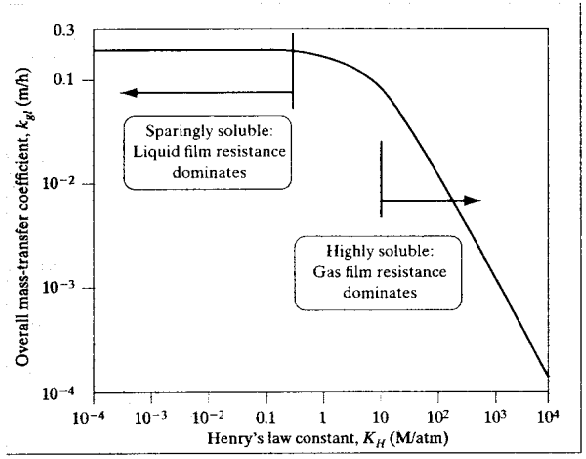

Figure 4.C.7 Dependence of the overall mass-transfer coefficient on the Henry's law constant for average conditions in large bodies of water. The curve traces equation 4.C.19 with $k_l = 0.2$ m h^{-1}, $k_g = 30$ m h^{-1}, and $T = 293$ K (Liss and Slater, 1974).

For natural bodies of water, the following expressions can be applied to estimate gas-side and liquid-side mass-transfer coefficients in relation to environmental and species conditions (Schwarzenbach et al., 1993). For the gas-phase mass-transfer coefficient,

$$k_g = \left[\frac{D_a}{0.26 \text{ cm}^2 \text{ s}^{-1}}\right]^{2/3}(7U_{10} + 11) \tag{4.C.20}$$

For oceans, lakes, and other slowly flowing waters,

$$k_l = \left[\frac{D_w}{2.6 \times 10^{-5} \text{ cm}^2 \text{ s}^{-1}}\right]^{0.57}(0.0014U_{10}^2 + 0.014) \tag{4.C.21}$$

For rivers,

$$k_l = 0.18\left[\frac{D_w}{2.6 \times 10^{-5} \text{ cm}^2 \text{ s}^{-1}}\right]^{0.57}\left(\frac{U_w}{d_w}\right)^{1/2} \tag{4.C.22}$$

In these expressions, U_{10} is the mean wind speed measured at 10 m above the water surface (units are m/s). The term U_w is the mean water velocity in the river (m/s). The mean stream depth is d_w (m). The equations are written so that k_g and k_l have units of m/h. Example 4.C.1 illustrates how these equations are used.

In general, for interfacial transfer of molecular species in any air-water flow system, the overall mass-transfer coefficient for any species can be determined by making measurements of k_{gl} for a minimum of two species with known Henry's law constants, provided one is sparingly soluble and the other is highly soluble. From these measurements, one can determine the values of k_l and k_g. Then the overall mass-transfer coefficient for any other species can be estimated using equation 4.C.19.

EXAMPLE 4.C.1 *Mass-Transfer Coefficient for Oxygen in a River*

In Nebraska, the Missouri River has a mean depth of 2.7 m and flows at a mean velocity of 1.75 m/s (Fischer et al., 1979). Assume that the wind speed at 10 m is 4 m/s. Estimate the overall mass-transfer coefficient for oxygen (O_2) from the atmosphere to the river.

SOLUTION The diffusion coefficient of O_2 in water is $D_w = 2.6 \times 10^{-5}$ cm^2 s^{-1} (Table 4.A.3). From equation 4.C.22, the liquid-side mass-transfer coefficient is estimated to be $k_l = 0.14$ m/h. The diffusion coefficient for O_2 in air is $D_a = 0.178$ cm^2 s^{-1} (Table 4.A.2). From equation 4.C.20, the gas-side mass-transfer coefficient is estimated to be $k_g = 30$ m/h. The Henry's law constant for oxygen is $K_H = 0.0014$ M atm^{-1} (Table 3.B.2). With $R = 0.0821$ atm K^{-1} M^{-1} and $T = 293$ K, we predict from equation 4.C.19 that $k_{gl} = 0.14$ m/h. As expected for a sparingly soluble gas such as oxygen, mass transfer through water adjacent to the interfacial boundary controls the overall rate of the process.

4.D TRANSPORT IN POROUS MEDIA

Porous materials are solids that contain distributed void spaces. Permeable porous materials contain an interconnected network of voids or pores that permit bulk flow of fluid through the material. Soil is a common example of a permeable porous material. Usually, the pores are highly variable in shape and size, resulting in complex flow channels.

Environmental engineers study the movement of fluids and contaminants through porous media for several reasons. Many treatment technologies for removing pollutants from water and air entail passing the fluid through a porous material. In municipal treatment plants, for example, drinking water is passed through sand filters to remove small, suspended particles. Drinking water is also sometimes treated by passing it through a column of granular activated carbon to remove dissolved organic molecules that are harmful or that may cause taste and odor problems. Air used in industrial processes is often passed through fabric filters to remove suspended particles. Filters of granular activated carbon are also used to remove volatile organic compounds from gas streams. Many hazardous waste treatment technologies also involve passing a fluid through a porous material. Much attention in hazardous waste management focuses on characterizing contaminant migration in subsurface soils, either to predict the threat to water quality or to evaluate a treatment strategy.

The aim of this section is to provide an introduction to transport in porous media, emphasizing the movement of water and air and the contaminants dissolved or suspended within these fluids. The behavior of nonaqueous-phase liquids in subsurface environments is also important in environmental engineering, but the complexities that must be addressed render it beyond the scope of this book. Application of the ideas introduced here for filtering contaminants from water are discussed in Chapter 6. Groundwater contamination is addressed in Chapter 8.

Before proceeding, we must define some basic terms and concepts that arise when dealing with transport through porous materials. One quantitative descriptor of a porous material is its *porosity*, here given the symbol ϕ and defined as

$$\phi = \frac{\text{pore volume}}{\text{total volume}} \tag{4.D.1}$$

The pores may contain both air and water (and, in general, other fluids). We define the *air-filled porosity*, ϕ_a, and the *water-filled porosity*, ϕ_w, in analogy with equation 4.D.1, but with the numerator replaced by the pore volume filled with air or water, respectively. If the air and water are the only fluids contained in the pores, the porosities must satisfy this relationship:

$$\phi = \phi_w + \phi_a \tag{4.D.2}$$

A porous material is *saturated* with a particular fluid if that fluid entirely fills the pores. So, for example, a medium is saturated with water if $\phi_w = \phi$.

Most porous materials encountered in environmental engineering are granular or fibrous. Granular materials, such as soils, typically have porosities in the range 0.3–0.7. The porosities of fibrous materials are usually higher, sometimes as high as 0.99. These materials may have two distinct classes of pores, those that are external to the grains or fibers and those that are internal. Bulk fluid flow occurs only in the external pores, but contaminants can migrate by diffusion into the internal pores and interact with the solid surfaces there. This characteristic is especially important for porous sorbents, such as activated carbon, which have large internal porosities and enormous internal surface areas. However, in this section, we will emphasize fluid and contaminant behavior in the pores that are external to grains and fibers.

Two densities are commonly defined for a porous solid. The *solids density*, ρ_s, represents the mass of solid per volume of solid (often including internal pores). The *bulk density*, ρ_b, represents the mass of solid per total volume. These measures are related by the total porosity:

$$\rho_b = \rho_s(1 - \phi) \tag{4.D.3}$$

The solids density of soil grains is fairly constant at ~2.65 g cm^{-3}. Given a range of porosities of 0.3–0.7, the bulk density would be in the range 0.8–1.9 g cm^{-3}. Soil bulk density varies with grain size, but the dependence is not strong. In soil, as in any granular material, porosity tends to be higher when grain sizes are distributed over a narrow range. With a broad distribution of grain sizes, smaller grains can fill the pores created by larger grains, reducing overall porosity.

Porosity is an area characteristic as well as a volume characteristic of granular materials. Imagine a plane slicing through a porous material. The *area porosity* is the ratio of the area of the plane that intersects pores to the total area that intersects the porous material. Conveniently, if pores are randomly distributed and the number of pores in a plane is large, then the area porosity is equal to the porosity measured on a volume basis. This conclusion is reached by considering a porous material as a collection of infinitesimally thin slices. The volume porosity of the whole is the average of the porosities of the individual slices. If these slices include a random distribution of a large number of pores, then the porosity of each slice will be close to the mean for all slices.

4.D.1 Fluid Flow through Porous Media

During the middle of the nineteenth century, Henri Darcy, a French engineer who was interested in the development of groundwater resources, studied the hydraulics of water flow through a sand column using an apparatus like that shown in Figure 4.D.1. With experiments conducted under steady flow conditions, he found that the following relationship described his results:

$$Q = KA\frac{\Delta h}{L} \tag{4.D.4}$$

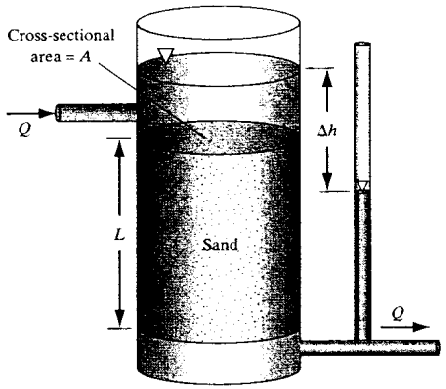

Figure 4.D.1 Apparatus similar to that used by Darcy to study the hydraulics of water flow through sand.

where Q is the volumetric flow rate ($m^3\ s^{-1}$), Δh is the change in fluid head from the inlet to the outlet of the column (m), A is the cross-sectional area of the column (m^2), and L is the length of the column (m). The parameter K, which has units of velocity, was constant for a given sand but varied from one sand sample to another, increasing with increasing grain size.

This relationship has been generalized and is now commonly known as *Darcy's law*. For water flow in one dimension through a water-saturated material, Darcy's law can be written as

$$U = -K\frac{dh}{dl} \tag{4.D.5}$$

where U is called the *Darcy velocity, filtration velocity,* or *superficial flow velocity, K* is called the *hydraulic conductivity;* and *dh/dl* is the rate of change of pressure head with distance. In relation to Darcy's experiment, U represents Q/A, and the hydraulic gradient, *dh/dl*, replaces $\Delta h/L$. The filtration velocity (U) should not be confused with the local velocity of water through the pores. Rather, it represents the average volumetric flow of water per unit *total* cross-sectional area of the porous material. Since solids occupy some area, and since water can flow only through pores, the average local velocity of water in the pores must be higher than the filtration velocity. The minus sign in Darcy's law, like the minus sign in Fick's law, reminds us that water flows from high to low pressure head, just as molecules diffuse from high to low concentration. Since head has units of length, *dh/dl* is dimensionless, and so the hydraulic conductivity must have the same units as U, velocity.

Another form of Darcy's law applies to porous media saturated with any fluid:

$$U = -\frac{k}{\mu}\frac{dP}{dl} \tag{4.D.6}$$

where k is called the *intrinsic permeability,* or simply *permeability,* of the porous material; μ is the viscosity of the fluid; and *dP/dl* is the derivative of dynamic pressure with respect to distance. This form of Darcy's law assumes that the fluid is incompressible, which, for air, would mean that the pressure drop across the medium must be much smaller than the inlet pressure.

The hydraulic conductivity in Darcy's law (equation 4.D.5) depends primarily on two properties of the system: the viscosity of the fluid and the size of the pores. Fluids

that are more viscous flow more slowly, and materials with smaller pores permit less flow. The second form of Darcy's law (equation 4.D.6) separates these two properties. The intrinsic permeability is a function only of the porous material and does not depend on the fluid properties.

Given the units of viscosity (e.g., kg $m^{-1}\ s^{-1}$), pressure derivative (kg $m^{-2}\ s^{-2}$), and velocity (m s^{-1}), we see that permeability has units of length squared. For a porous medium made up of uniform spherical grains, the permeability increases approximately in proportion to the square of the grain diameter.

The dynamic pressure (P) in equation 4.D.6 is the difference between the total pressure and the hydrostatic pressure. In the absence of motion, fluid pressure must increase with depth to support the mass of the fluid suspended above it against the acceleration of gravity. This hydrostatic change in pressure with height does not induce flow.

The difference between the two forms of Darcy's law lies primarily in the coefficients K and k. By noting that head loss corresponds to dynamic pressure drop according to $\rho_w g\Delta h = \Delta P$, where ρ_w is the density of water and g is gravitational acceleration, we can show that the hydraulic conductivity is related to the intrinsic permeability by

$$K = \frac{k\rho_w g}{\mu_w} \tag{4.D.7}$$

where μ_w is the dynamic viscosity of water.

Intrinsic permeability, k, may be expressed in ordinary area units such as m^2. However, the permeabilities of ordinary materials are so low that a special unit, the darcy, has been defined for permeability, with 1 darcy = $0.987 \times 10^{-12}\ m^2$. Figure 4.D.2 shows representative permeabilities and hydraulic conductivities of soils. Note the enormous range of values between homogeneous clays and coarse sand or gravel.

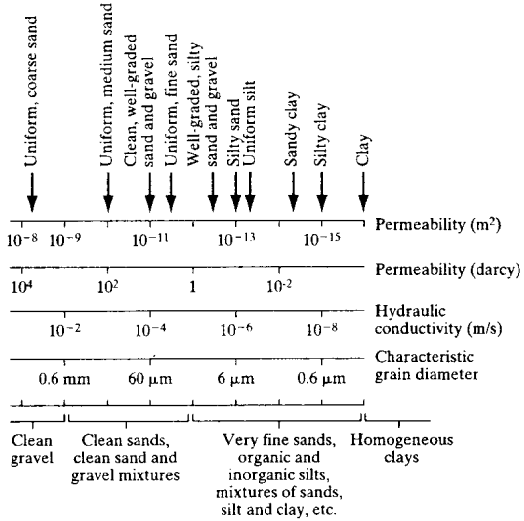

Figure 4.D.2 Permeability and hydraulic conductivity scales, indicating representative values for soils and gravel (Terzaghi and Peck, 1967; Tuma and Abdel-Hady, 1973). Characteristic grain diameters are computed from the Carman-Kozeny equation (4.D.8), assuming $\phi = 0.5$.

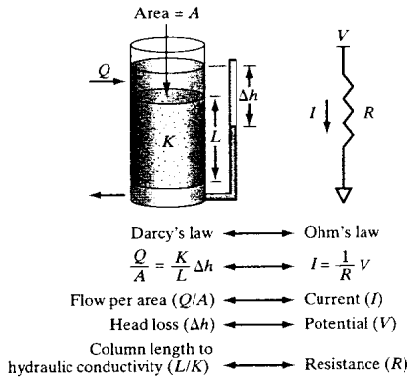

Figure 4.D.3 The analogy between Darcy's law and Ohm's law.

Fluid flow through a sand column is analogous to electrical current flow through a resistor. Figure 4.D.3 makes the comparison, showing that the ratio of the column length to hydraulic conductivity acts like a "resistor" to fluid flow driven by a loss in pressure head.

A widely used expression that relates permeability to grain size is known as the Carman-Kozeny equation. It was derived by analyzing flow through porous media in analogy to flow through a bundle of small capillaries, but with varying size and orientation (Dullien, 1979), giving

$$k = \frac{\phi^3 d_g^2}{180(1-\phi)^2} \tag{4.D.8}$$

where d_g is the grain diameter. For grains that are not spherical, d_g is replaced by $\psi\, d_{eq}$ where ψ is known as the *sphericity* of the grain and d_{eq} is the *equivalent diameter*. The sphericity is the ratio of the surface area of a sphere with the same volume as the grain to the (external) surface area of the grain. Sphericities of materials used in granular-bed filters typically range from 0.45 to 0.8 (Cleasby, 1990). The equivalent diameter is that which produces a sphere with the same volume as the grain. Example 4.D.1 shows how the Carman-Kozeny relationship is used.

EXAMPLE 4.D.1 *Hydraulics for a Granular Activated Carbon Filter*

A filter of granular activated carbon is used for treating drinking water. It has the following characteristics, which are typical for municipal water treatment (Cleasby, 1990; Snoeyink, 1990). Estimate the permeability and the head loss.

$d_{eq} = 1$ mm	Equivalent grain diameter
$\psi = 0.75$	Sphericity
$\phi = 0.5$	Porosity
$L = 1$ m	Bed depth
$U = 3$ m h^{-1}	Filtration velocity

SOLUTION Substitution into equation 4.D.8 yields an estimate of the permeability:

$$k = \frac{0.5^3(0.75 \times 1 \times 10^{-3}\text{m})^2}{180(1-0.5)^2} = 1.6 \times 10^{-9}\ \text{m}^2$$

EXAMPLE 4.D.1 *Hydraulics for a Granular Activated Carbon Filter (continued)*

From equation 4.D.7, the hydraulic conductivity is

$$K = \frac{1.6 \times 10^{-9}\text{m}^2 \times 1000\ \text{kg m}^{-3} \times 9.8\ \text{m s}^{-2}}{0.001\ \text{kg m}^{-1}\ \text{s}^{-1}} = 0.015\ \text{m s}^{-1}$$

The head loss is determined from equation 4.D.5:

$$\Delta h = L\frac{dh}{dl} = -L\frac{U}{K}$$

$$= -1\ \text{m} \times \frac{3\ \text{m h}^{-1}}{0.015\ \text{m s}^{-1}} \times \frac{1\ \text{h}}{3600\ \text{s}} = -0.06\ \text{m}$$

The head loss in this case is about 6 cm.

4.D.2 Contaminant Transport in Porous Media

All of the mechanisms that cause contaminant transport in bulk fluids also act on contaminants suspended in fluids in porous media. Contaminants are advected with the fluid flow. Molecules diffuse within the fluid through the pores. Particles settle and undergo Brownian motion. Contaminants sorb onto and within porous media grains. Chemical or biological reactions may cause generation or decay of contaminants. If both air and water are present in the pores, contaminants can partition between the two fluids and migrate within both. Additional transport mechanisms arise, such as surface diffusion, but discussion of these is beyond the scope of this text.

Because of the large surface area of solids in contact with the fluid, contaminant-surface interactions may assume a particularly important role in transport through porous media. Particles may contact and adhere to the solid grains or fibers. Molecular contaminants may sorb onto the solid surface and may undergo chemical reactions there. Our attention in this section is focused mainly on transport mechanisms that do not involve pollutant-surface interactions. The modeling of sorption and transformation reactions in porous media is discussed in §5.B, and applications of particle deposition in porous filters are described in §6.C.2 and §7.C.1.

Diffusion

Molecular diffusion through porous materials affects the migration of gases through soils. In groundwater, diffusion is slow (recall that molecular diffusivities in water are 10,000 times smaller than in air) and therefore of little importance. In treatment technologies, transport is generally dominated by advection because of the need to treat fluids quickly.

In this discussion, we will emphasize gas-phase diffusion. Fick's law relates diffusive flux through a porous medium to the concentration gradient, but requires some clarification and adjustment because of the presence of the solids. For molecular diffusion through a porous solid, Fick's law is written in one dimension as

$$J_d = -D_e\frac{dC}{dx} \tag{4.D.9}$$

For three-dimensional transport applications, Fick's law can be written in vector form:

$$\vec{J_d} = -D_e\left(\frac{\partial C}{\partial x}, \frac{\partial C}{\partial y}, \frac{\partial C}{\partial z}\right) \tag{4.D.10}$$

Here J_d, representing diffusive flux through the porous medium, gives the quantity of contaminant transported per *total* area (not just pore area) per time. The parameter D_e is an effective diffusion coefficient, and C is the species concentration in the pores (per *pore* volume, not per total volume). These equations have the same form as Fick's law for bulk fluids (equations 4.A.5–6), but each of the parameters has an altered meaning.

The effective diffusion coefficient through a porous material is smaller than the corresponding ordinary diffusion coefficient for the given contaminant/fluid combination. For gas molecules in a granular material, such as soil, the following expression is widely used to estimate the effective diffusivity (Millington, 1959):

$$D_e = D\frac{\phi_a^{10/3}}{\phi^2} \tag{4.D.11}$$

In vadose-zone soils (i.e., above the groundwater table), typical values of air-filled and total porosity are $\phi_a = 0.2$ and $\phi = 0.4$. According to equation 4.D.11, the effective diffusivity would be reduced to $0.03D$ in this case. For air-saturated pores, equation 4.D.11 reduces to

$$D_e = D\phi_a^{4/3} \qquad \phi_a = \phi \tag{4.D.12}$$

So with a typical value for dry soil of $\phi_a = 0.4$, $D_e = 0.3D$.

An alternative expression, applied in the case of water- or air-saturated pores, uses an empirical correction factor, the *tortuosity*, T, which accounts for (a) the reduced area through which diffusion can occur and (b) the longer average path a molecule must travel to move a certain distance through the pores. The effective diffusivity is related to the tortuosity by

$$D_e = \frac{D}{T} \tag{4.D.13}$$

Typical values of tortuosity are in the range 2 to 6 (Cussler, 1984), yielding effective diffusivities that are approximately consistent with predictions based on 4.D.12.

Hydrodynamic Dispersion

Hydrodynamic dispersion in porous media is similar to the shear-flow dispersion that occurs in pipes and rivers, as discussed in §4.A.4. The dispersion of a nonreactive groundwater contaminant, or *conserved tracer*, is depicted in Figure 4.D.4. At some time t_1, contamination occurs in the groundwater, as shown in the left-hand portion of the figure. The groundwater flows with a uniform filtration velocity, U, in the $+x$-direction. At some later time, t_2, the center of mass of contamination has been transported downstream to position x_2, given by

$$x_2 = x_1 + (t_2 - t_1)U \tag{4.D.14}$$

In words, the center of mass of contamination moves at the same speed as the fluid. However, the areal extent of contaminated groundwater increases, and typically this increase is much greater than can be explained by molecular diffusion alone. Because

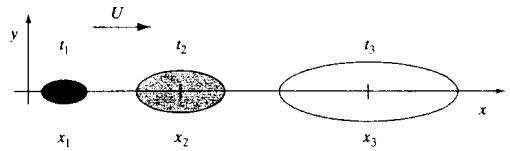

Figure 4.D.4 Transport and dispersion of a fixed quantity of a nonreactive groundwater contaminant. The figure schematically shows the areal extent of contamination at three instants in time, with $t_3 > t_2 > t_1$. The center of mass of contamination is advected in the x-direction at a rate given by the mean velocity, U. Hydrodynamic dispersion causes the contamination to spread more rapidly in the direction of flow than in the transverse direction.

the local velocity through the soil pores is not uniform, some of the contamination travels at an average speed greater than U, while other contaminant molecules travel more slowly than U. There is also some spreading in the y-direction, even though the mean velocity in that direction is zero. Since the contaminant is conserved, the greater areal extent of contamination is offset by a lower average concentration. The same characteristics prevail in the interval from t_2 to t_3.

This spreading is not caused by turbulence; it occurs even if the grain Reynolds number is much less than 1, so that the flow is stable and laminar. It is observed to occur in uniform sand columns in the laboratory, although it can be much stronger in the field if the soil contains zones of higher and lower permeability than the average.

Fundamentally, this spreading is caused by the variation of fluid velocities within the pores. At the grain surfaces, the velocities diminish to zero. In the center of a channel between two grains, the local velocity may be much higher than the volume average. Individual contaminant molecules experience independent velocity histories. When averaged over all contaminant molecules, the rate of advection matches that of the fluid, but some individual molecules may travel significantly faster or slower than the mean, causing plume dispersion.

The contaminant flux in the direction of flow caused by hydrodynamic dispersion in porous media is described by an expression analogous to Fick's law in one dimension:

$$J_h = -\varepsilon_h\frac{\partial C}{\partial x} \tag{4.D.15}$$

where ε_h is the *dispersion coefficient* and x is the direction of flow. In this expression, the dispersion coefficient includes molecular diffusion as a limiting condition:

$$\varepsilon_h = D_e + \varepsilon U \tag{4.D.16}$$

Here ε is a characteristic of the porous medium called the *dispersivity* (units of length). As defined above, U is the filtration velocity and D_e is the effective diffusivity. So, the flux J_h represents the sum of transport due to molecular diffusion and due to dispersion caused by nonuniform fluid flow. As with molecular diffusion alone, this flux represents the net rate of contaminant movement per unit *total* cross-sectional area. Similar expressions could be written for the flux components in the transverse direction, but these would require different dispersion coefficients, since it is observed that transverse dispersion is weaker than longitudinal dispersion.

1

Darcy's Law and Advective Transport

1.1 AVERAGE PARTICLE VELOCITY AND TIME OF TRAVEL

Figure 1-1 shows a pipe, one section of which is packed with sand; water of uniform density and viscosity flows through the pipe under pressure, so that the pipe remains full and the sand remains saturated. The rate of flow, in volume of water per unit time, is designated Q. Piezometers at either end of the sand section are used to measure the hydraulic head, h, or elevation of the piezometric water level above datum; the cross-sectional area of the pipe is designated A, and the length of the sand section as L. The flow rate through the sand section is given by

$$Q = -KA\frac{h_2 - h_1}{L} \tag{1-1}$$

where K is the hydraulic conductivity of the sand; h_1 the head at the upstream face and h_2 the head at the downstream face. Equation (1-1) is a form of Darcy's Law, the fundamental relation describing flow in porous media (Darcy, 1856).

Expressed in terms of the derivative or gradient of head, Darcy's law for the problem of Figure 1-1 may be written as

$$Q = -KA\frac{dh}{dl} \tag{1-2}$$

where l represents distance along the pipe.

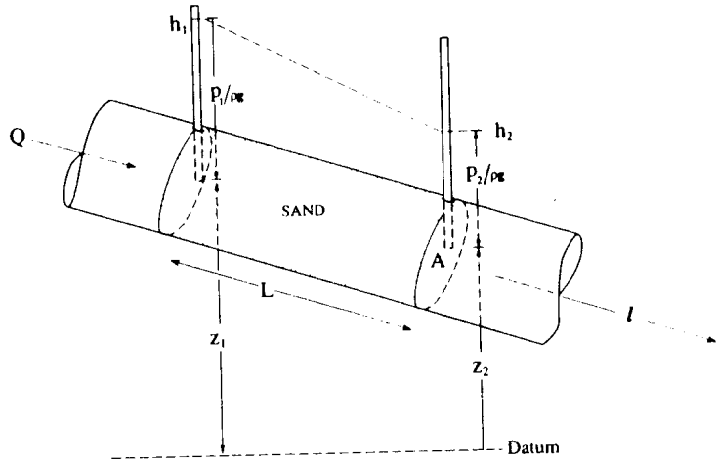

FIGURE 1-1. Sand-packed pipe section carrying a flow Q.

The head, h, measures the potential energy of a unit weight of water located at the point of measurement. Within the sand section, the loss of head between two points represents the energy or work required to move a unit weight of water between those points. Note that the head, at points within the sand, has two components, i.e.,

$$h = z + \frac{P}{\rho g} \tag{1-3}$$

where z is the elevation of the point above datum; P the pressure; ρ the mass density of the water; g the acceleration of gravity; and the term $P/(\rho g)$ is the height to which water will rise in a piezometer open at that point. Readers familiar with open flow hydraulics will note that the kinetic term $v^2/(2g)$, where v is the water velocity, is not included in equation (1-3). Velocities of flow within a porous medium are normally low enough so that this term is negligible. Darcy's Law can be stated in much more general terms (see Section 1.2), but equations (1-1) or (1-2) are adequate to describe the flow regime in the system of Figure 1-1.

Now suppose we are interested not just in the quantity of flow passing through the sand, but in the time it takes water to pass from one face of the sand section to the other. We begin by assuming that there may be some fraction of the pore space in which velocity is zero, i.e., in which the water

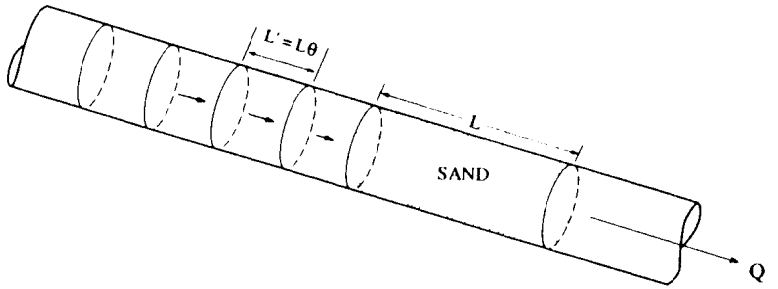

FIGURE 1-2. Pipe of Figure 1-1, showing a series of pore volumes approaching the sand section.

is completely static; examples might include "dead-end" pore space or fully isolated pores. We use the term *effective porosity* to designate the ratio of the remaining pore volume, i.e., that containing moving water, to the bulk volume of the sand. To simplify the analysis we assume initially that the velocity is completely uniform throughout this segment of the pore space. Under this assumption, the water in the sand which is free to move is totally displaced, in a certain time interval, by new water entering through the upstream sand face. The volume of moving water within the sand at any time is θAL, where θ is the effective porosity. For purposes of travel time calculation, we consider the quantity θAL to be a "pore volume," since it represents the volume of pore space in which flow occurs. We can think of the flow as a succession of discrete pore volumes moving along the pipe as shown in Figure 1-2, so that each pore volume is displaced from the sand in turn by the following pore volume. (Note that before entering the sand, or after leaving it, each pore volume occupies a distance L' along the pipe, where $L' = L\theta$.)

The displacement of a pore volume from the sand requires a certain time interval, Δt_p; and by definition, the displaced liquid volume divided by this time interval is the flow rate, Q, i.e.

$$Q = \frac{\theta AL}{\Delta t_p} \tag{1-4}$$

or

$$\Delta t_p = \frac{\theta AL}{Q} \tag{1-5}$$

If we consider the successive pore volumes in Figure 1-2 to be separated by liquid interfaces, Δt_p is obviously the time required for one of these

interfaces to move completely through the sand section; thus Δt_p can be interpreted as the time required for a fluid particle to traverse the distance L within the sand. More generally, if flow at a rate Q occurs through a given volume of aquifer V, the term $\theta V/Q$ gives the time required for movement of a fluid interface through the volume V along the path of flow.

We can define an average seepage velocity, or, interstitial velocity, v, through the sand section of Figure 1-2, as $L/\Delta t_p$, i.e.,

$$v = \frac{L}{\Delta t_p} = \frac{Q}{\theta A} \tag{1-6}$$

Substituting equation (1-2) into the above equation yields

$$v = -\frac{K}{\theta}\frac{dh}{dl} \tag{1-7}$$

In writing Darcy's Law, we frequently use the Darcy velocity, q or Q/A, i.e.,

$$q = \frac{Q}{A} = -K\frac{dh}{dl} \tag{1-8}$$

and it is important to distinguish this Darcy velocity from the seepage velocity defined in equation (1-6) or (1-7). The Darcy velocity is actually a discharge per unit bulk area of sand face, and is often referred to as specific discharge; it represents the average fluid velocity in the open pipe, outside the sand section in Figure 1-2, but is less than the seepage velocity within the sand by the factor θ. To view this in another way, the cross-sectional area of flow in the sand (θA) is smaller than that in the open pipe (A); and since the same discharge prevails in each section, velocity must be greater within the sand.

It should also be noted that even under our assumption that velocity is uniform within the effective component of the pore space, the seepage velocity, v, is not the true velocity of movement within the sand. Any fluid particle moving through the sand section must travel a greater distance than L, since the flow path must necessarily involve tortuous movement around the sand grains. Thus the actual particle velocity must exceed $L/\Delta t_p$. The seepage velocity, however, gives the apparent velocity in terms of linear distance along the exterior of the porous medium; in field or laboratory problems, this is the quantity which can be measured or calculated.

Before leaving this discussion we note that the flow distribution within the pore space is never actually as simple as that assumed above. Clearly

there is never a perfectly uniform flow velocity throughout one part of the pore space, and zero velocity in the remainder, as assumed in the preceding development; and in fact the role of porosity in solute transport is far more complex than this example would suggest. However, where an independent measure of *total porosity* (the ratio of total pore volume to bulk volume) is available, one often finds that use of this total porosity in equation (1-5) will yield a travel time which differs from the results of tracer experiments, and that some smaller porosity figure must be used to achieve agreement. This value is taken as the effective porosity. As we will see in the following chapter, flow velocities in the pore space actually vary through a wide spectrum; and in the displacement of a "pore volume" of liquid (as measured by the effective porosity) the interstitial water in some parts of the pore space may be replaced several times, while that in other parts of the pore space is only partially replaced, or is not replaced at all. Thus the term *effective porosity*, as used above, should properly be viewed as the porosity required to achieve agreement with observation in a calculation of travel time. Where seepage velocity can be estimated from the observed travel time of a tracer, effective porosity is taken as the ratio of Darcy velocity to the measured seepage velocity. This interpretation has numerous implications which can be considered more fully as our discussion of general solute transport processes is developed; further discussion of porosity in solute transport calculation is therefore deferred to Chapter 2. Unless otherwise indicated, however, the term *porosity* and the symbol θ, as used in this text, refer to effective porosity in the sense used above.

To return to the relationship between time of flow, volume of liquid and flow rate, the pipe in Figure 1-2 is analogous to a stream tube in steady-state groundwater flow, i.e., a region in a flow field which is bounded by a stream surface, or surface across which no flow occurs. If a system of stream tubes can be defined in a steady-state flow field, times of travel can readily be estimated. As in the example of Figure 1-2, this is done by dividing the volumes of water displaced in a section of the stream tube by the flow rate through the stream tube. (For a more detailed discussion of stream tubes or stream functions, see Appendix A).

1.2 GENERALIZATION OF DARCY'S LAW AND EQUATION OF GROUNDWATER FLOW

In field problems the Darcy velocity and seepage velocity are generally not unidirectional, as they are in the example in Figure 1-1; thus the simple formulations of equation (1-8) for Darcy's Law and equation (1-7) for the seepage velocity are usually not adequate. This section presents two

formulations of Darcy's Law which can be applied to a wide range of three-dimensional flow problems. More detailed discussions of Darcy's Law are available in standard groundwater texts (e.g., Freeze and Cherry, 1979; Domenico and Schwartz, 1990).

In a three-dimensional problem the Darcy velocity is expressed as a vector through the relation:

$$\mathbf{q} = q_x\mathbf{i} + q_y\mathbf{j} + q_z\mathbf{k} \tag{1-9}$$

where $\mathbf{q}$ is the Darcy velocity vector; $\mathbf{i}$, $\mathbf{j}$, and $\mathbf{k}$ are the conventional unit vectors in the x, y, and z coordinate directions; and q_x, q_y, and q_z are the scalar components of the Darcy velocity in those directions. If the porous medium is characterized by three principal axes of hydraulic conductivity, and if these principal axes are aligned with the coordinate axes, the Darcy velocity components in water of uniform density and viscosity are given by

$$q_x = -K_x\frac{\partial h}{\partial x} \tag{1-10}$$

$$q_y = -K_y\frac{\partial h}{\partial y} \tag{1-11}$$

$$q_z = -K_z\frac{\partial h}{\partial z} \tag{1-12}$$

where K_x, K_y, and K_z represent the components of hydraulic conductivity in the respective coordinate directions. If the water is not of uniform density and viscosity, the equations are usually formulated in terms of intrinsic permeabilities and pressure gradients, i.e.,

$$q_x = -\frac{k_x}{\mu}\frac{\partial P}{\partial x} \tag{1-13}$$

$$q_y = -\frac{k_y}{\mu}\frac{\partial P}{\partial y} \tag{1-14}$$

$$q_z = -\frac{k_z}{\mu}\left(\frac{\partial P}{\partial z} + \rho g\right) \tag{1-15}$$

where P is pressure; μ is the dynamic viscosity of the water; ρ is water density; k_x, k_y, and k_z represent the intrinsic permeabilities in the respective coordinate directions; g is the acceleration of gravity, which is considered a positive scalar in equation (1-15); and z is the vertical coordinate, taken positive upwards. Intrinsic permeability is a function only of the porous medium, whereas hydraulic conductivity incorporates properties of the fluid as well. The two are related by

$$K_x = \frac{k_x\rho g}{\mu} \tag{1-16}$$

for the x direction, and by similar expressions for the y and z directions. Because of the relation between hydraulic head, h, and pressure, P, as given in equation (1-3), equations (1-13) through (1-15) specialize to equations (1-10) through (1-12) when density and viscosity are independent of the spatial coordinates.

It should be noted that the hydraulic conductivity or intrinsic permeability is actually a second-rank tensor. If the principal components of hydraulic conductivity or intrinsic permeability are not aligned with horizontal and vertical coordinate axes, velocity components in each direction are a function of head or pressure gradients in all three directions, rather than solely in the direction of the velocity component. Thus, in terms of head, equations (1-10) through (1-12) must be written as

$$q_x = -K_{xx}\frac{\partial h}{\partial x} - K_{xy}\frac{\partial h}{\partial y} - K_{xz}\frac{\partial h}{\partial z} \tag{1-17}$$

$$q_y = -K_{yx}\frac{\partial h}{\partial x} - K_{yy}\frac{\partial h}{\partial y} - K_{yz}\frac{\partial h}{\partial z} \tag{1-18}$$

$$q_z = -K_{zx}\frac{\partial h}{\partial x} - K_{zy}\frac{\partial h}{\partial y} - K_{zz}\frac{\partial h}{\partial z} \tag{1-19}$$

where K_{xx}, K_{yy}, and K_{zz} are principal components of the hydraulic conductivity tensor, while K_{xy}, K_{xz}, K_{yx}, K_{yz}, K_{zx}, and K_{zy} are cross terms of that tensor. In practical applications, equations (1-17) through (1-19) are rarely used. In other words, it is generally assumed that the principal components of the hydraulic conductivity tensor can be aligned with horizontal and vertical coordinate axes so that the cross terms of the hydraulic conductivity tensor become zero.

When the Darcy velocity is calculated as a vector point function using equation (1-9), the average seepage velocity is also taken as a vector point function, and is simply the Darcy velocity vector divided by the (scalar) effective porosity, i.e.,

$$\mathbf{v} = \frac{\mathbf{q}}{\theta} = \frac{q_x}{\theta}\mathbf{i} + \frac{q_y}{\theta}\mathbf{j} + \frac{q_z}{\theta}\mathbf{k} \tag{1-20}$$

or

$$v_x = q_x/\theta$$
$$v_y = q_y/\theta \qquad (1\text{-}21)$$
$$v_z = q_z/\theta$$

The seepage velocity components in equation (1-21) are obtained by first solving the differential equation of groundwater flow to obtain head or pressure as a function of the spatial coordinates and time; then invoking equations (1-10) through (1-12) or (1-13) through (1-15) to calculate Darcy velocity components throughout the region and time span of interest; and finally converting the Darcy velocity terms to seepage velocities using the porosity. In terms of head, which is the most convenient formulation if the water is of uniform density and viscosity, the differential equation of groundwater flow takes the form (see for example Freeze and Cherry, 1979; Domenico and Schwartz, 1990):

$$\frac{\partial}{\partial x}\left(K_x \frac{\partial h}{\partial x}\right) + \frac{\partial}{\partial y}\left(K_y \frac{\partial h}{\partial y}\right) + \frac{\partial}{\partial z}\left(K_z \frac{\partial h}{\partial z}\right) + q_s = S_s \frac{\partial h}{\partial t} \qquad (1\text{-}22)$$

where q_s is the fluid sink/source term, or volumetric rate at which water is added to or removed from the system per unit volume of aquifer; S_s is the specific storage, or volume of water released from storage in a unit volume of aquifer per unit decline in head; and it is assumed that the aquifer is characterized by three orthogonal principal directions of hydraulic conductivity, with which the coordinate axes are aligned.

If viscosity and density are not uniform, the flow equation is more conveniently formulated in terms of pressure. We again assume three orthogonal coordinate axes, but now add the condition that the z axis is along the vertical. We also assume that spatial variations in density are due primarily to changes in solute concentration, and that spatial differences in the mass of pure water per unit volume due to variations of pressure are negligible in comparison. Under these assumptions, letting z represent the vertical direction and taking z positive upward, the equation of flow can be written as

$$\frac{\partial}{\partial x}\left(\frac{k_x}{\mu}\frac{\partial P}{\partial x}\right) + \frac{\partial}{\partial y}\left(\frac{k_y}{\mu}\frac{\partial P}{\partial y}\right) + \frac{\partial}{\partial z}\left\{\frac{k_z}{\mu}\left(\frac{\partial P}{\partial z} + \rho g\right)\right\} + q_s = S_{sp}\frac{\partial P}{\partial t} \qquad (1\text{-}23)$$

where S_{sp} is the specific storage in terms of pressure, or the volume of water released from storage in a unit volume of aquifer in response to a unit decline in pressure.

1.3 ADVECTIVE TRANSPORT

Section 1.1 considered the average rate of movement and time of travel of fluid particles. So long as the fluid particles in a groundwater regime are chemically and physically indistinguishable, there is little reason to be concerned with these topics. Frequently, however, the fluid particles are not all identical. Some particles, although fully miscible with the groundwater, may be "tagged"—they may represent a dissolved tracer, or water of higher salinity, or a dissolved organic contaminant. The movement of such "tagged" particles is termed solute transport; in this section we will derive equations of solute transport under the simplifying assumption of Section 1.1, that all solute particles move with the average seepage velocity of the water. Equations of this type are termed advective transport equations; equations of transport which incorporate other processes are developed in Chapters 2 and 3.

1.3.1 Mass-Balance Considerations and the Eulerian Approach to Advective Transport

We will first develop the equation of advective transport through a mass-balance approach. This approach requires that the concentration of the solute be introduced as the primary dependent variable. Suppose that the water moving through the sand of Figure 1-2 contains dissolved salt or tracer at a concentration C, in units of mass of solute per volume of water. The mass of solute transported across a plane at right angles to the pipe in the sand-packed section of Figure 1-2 is given by

$$Q_m = QC \qquad (1\text{-}24)$$

where Q_m is the mass of solute crossing the plane per unit time and Q is again the volumetric fluid discharge (volume per unit time) through the sand. Using the Darcy velocity vector, $\mathbf{q}$, as in equation (1-9), rather than the fluid discharge, Q, an advective mass flux vector may be calculated as

$$\mathbf{q}_m = \mathbf{q}C \qquad (1\text{-}25)$$

where $\mathbf{q}_m$ is a vector having the direction of the Darcy velocity and a magnitude equal to the mass of solute transported advectively per unit time across a unit area normal to the flow.

Figure 1-3 shows the apparatus of Figures 1-1 and 1-2 again, but now showing two cross-sectional planes, each normal to the flow and separated by a distance Δl; thus the two planes enclose a bulk volume $A\,\Delta l$, where A

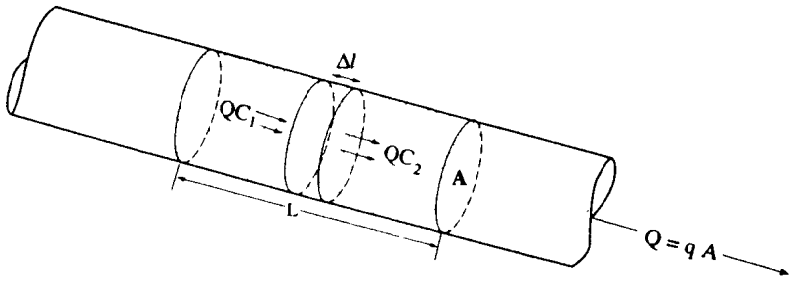

FIGURE 1-3. Pipe of Figure 1-1, showing solute mass transport into and out of a volume element.

is again the cross-sectional area of the pipe. Let us suppose that the concentration of salt or tracer in the water moving through the system varies along the pipe (but is constant over any cross-sectional plane normal to the pipe). At the upstream cross section of Figure 1-3 we designate the concentration C_1, and at the downstream cross section, C_2. The rate at which solute mass enters the volume $A\,\Delta l$ at the upstream face, Q_{m1}, is then equal to QC_1; the rate at which it leaves that volume at the downstream face, Q_{m2}, is given by QC_2. Because these two rates differ, the mass of solute within the volume $A\,\Delta l$ must change with time, at a rate equal to the difference between the rates of mass inflow and mass outflow. Letting M represent the mass of solute in the volume $A\,\Delta l$, and dM/dt the rate at which that mass changes with time,

$$\frac{dM}{dt} = QC_1 - QC_2 \tag{1-26}$$

or equivalently

$$\frac{dM}{dt} = qA(C_1 - C_2) \tag{1-27}$$

where q is the scalar magnitude of the Darcy velocity.

To simplify the analysis we assume that the solute carried in advective transport remains completely within the moving water, i.e., that there is no diffusion of solute into and from sections of the pore space which may contain static or nearly static water. In effect, we are assuming that the diffusion of solute into essentially static water (for example, along the pore walls or in dead-end pores) can be neglected, or will be addressed through some separate aspect of the analysis as discussed in the following chapter. Under this assumption, the volume of water containing solute in the bulk volume $A\,\Delta l$ is $\theta A\,\Delta l$, where again θ is effective porosity; and letting C represent the average concentration in this volume, the mass of solute between the two planes at any time is given by $\theta A\,\Delta l C$. Thus the rate at which this solute mass changes with time can be expressed in terms of the rate at which concentration changes with time as

$$\frac{dM}{dt} = \theta A\,\Delta l \frac{\partial C}{\partial t} \tag{1-28}$$

Equating the expressions for dM/dt in (1-27) and (1-28) gives

$$qA(C_1 - C_2) = \theta A\,\Delta l \frac{\partial C}{\partial t} \tag{1-29}$$

The concentration difference, $C_1 - C_2$ can be expressed in terms of the concentration gradient along the pipe, $\partial C/\partial l$, as

$$C_1 - C_2 = -\frac{\partial C}{\partial l}\Delta l \tag{1-30}$$

where l is taken positive in the direction of flow. Combining equations (1-29) and (1-30) gives

$$-qA\frac{\partial C}{\partial l}\Delta l = \theta A\,\Delta l \frac{\partial C}{\partial t} \tag{1-31}$$

or

$$-q\frac{\partial C}{\partial l} = \theta \frac{\partial C}{\partial t} \tag{1-32}$$

In a more general case we could allow for the possibility that the Darcy velocity itself might vary between the upstream and downstream faces in Figure 1-3. This would imply that the mass of water within the volume $A\,\Delta l$ was itself changing, due to elastic storage effects analogous to those observed in confined groundwater systems. Let us assume for simplicity that these storage effects involve no appreciable change in the volume $A\,\Delta l$, i.e., that the storage effects are due only to changes in the density of the water, in response to pressure change, within a rigid porous framework. Under this assumption equation (1-32) can be generalized as

$$-\frac{\partial(qC)}{\partial l} = \theta \frac{\partial C}{\partial t} \tag{1-33}$$

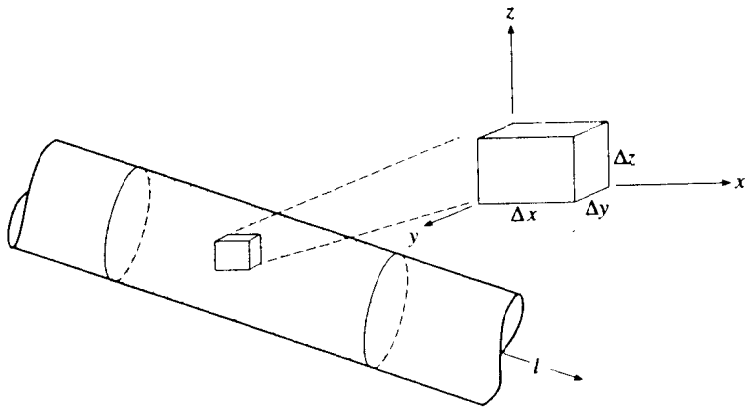

FIGURE 1-4. Volume element for development of the advective transport equation in Cartesian coordinates.

where the change in the product (qC) between the faces of the volume element is now recognized as the factor controlling solute accumulation.

An equation for advective transport under more general conditions can be obtained by considering a small volume element within the sand of Figure 1-1 which is not aligned in any way with the flow direction but rather is oriented along a conventional vertical/horizontal Cartesian coordinate system. Figure 1-4 shows this volume element, $\Delta x\,\Delta y\,\Delta z$. None of the three coordinate axes is either parallel to or normal to the pipe; thus the Darcy velocity vector, $\mathbf{q}$, has components in all three coordinate directions, and the solute concentration similarly varies in all three directions. For simplicity, we again assume that storage effects involve only changes in fluid density within a rigid porous framework. The cross-sectional area of the element normal to the x direction is $\Delta y\,\Delta z$; applying the concepts used in developing equation (1-33), the net inflow minus outflow of solute mass in the x direction for the volume element is given by

$$-\frac{\partial}{\partial x}(q_x C)\,\Delta x\,\Delta y\,\Delta z \tag{1-34}$$

where q_x is the component of the Darcy velocity in the x direction. Similar expressions can be written for the y and z directions, so that the total net inflow minus outflow of solute mass for the element is

$$-\left[\frac{\partial}{\partial x}(q_x C)+\frac{\partial}{\partial y}(q_y C)+\frac{\partial}{\partial z}(q_z C)\right]\Delta x\,\Delta y\,\Delta z \tag{1-35}$$

If the volume element of Figure 1-4 contains a fluid source through which water enters the flow regime, or a fluid sink through which water is withdrawn, an additional term is required in the expression for inflow minus outflow. Let Q_s represent the volumetric rate at which water is added or removed, where a positive sign indicates a source and a negative sign a sink, and let C_s represent the concentration of solute in the water which is added or withdrawn. The term $Q_s C_s$ thus represents the net rate at which solute mass is added to or removed from the volume element by the source or sink, expressed in dimensions of mass per unit time. This term must be added to equation (1-35), which represents inflow minus outflow for the volume element, giving

$$-\left[\frac{\partial}{\partial x}(q_x C)+\frac{\partial}{\partial y}(q_y C)+\frac{\partial}{\partial z}(q_z C)\right]\Delta x\,\Delta y\,\Delta z + Q_s C_s \tag{1-36}$$

The rate of accumulation of solute mass within the element is given by $\theta\,\Delta x\,\Delta y\,\Delta z\,\partial C/\partial t$. Equating this rate of accumulation to the expression in (1-36) gives

$$-\frac{\partial}{\partial x}(q_x C)-\frac{\partial}{\partial y}(q_y C)-\frac{\partial}{\partial z}(q_z C)+\frac{Q_s C_s}{\Delta x\,\Delta y\,\Delta z}=\theta\frac{\partial C}{\partial t} \tag{1-37}$$

where again it is assumed that any change in the volume of water within the element $\Delta x\,\Delta y\,\Delta z$ can be neglected. Equation (1-37) can be divided by porosity, converting the Darcy velocity components to seepage velocity components, v_x, v_y, and v_z. This yields the alternative form:

$$-\frac{\partial}{\partial x}(v_x C)-\frac{\partial}{\partial y}(v_y C)-\frac{\partial}{\partial z}(v_z C)+\frac{q_s}{\theta}C_s=\frac{\partial C}{\partial t} \tag{1-38}$$

where $q_s = Q_s/(\Delta x\,\Delta y\,\Delta z)$ is the volumetric inflow rate per unit volume of the aquifer due to the source or sink. Equation (1-38) can also be written in vector form as

$$-\nabla\cdot(\mathbf{v}C)+\frac{q_s}{\theta}C_s=\frac{\partial C}{\partial t} \tag{1-39}$$

or in subscript form as

$$-\frac{\partial}{\partial x_i}(v_i C)+\frac{q_s}{\theta}C_s=\frac{\partial C}{\partial t} \tag{1-40}$$

where the subscript i designates coordinate direction, and summation over all coordinate directions is implied by the notation.

Equations (1-38) through (1-40) provide a more general description of advective transport, suitable for use where the velocity and the concentration vary in three dimensions, and where fluid sinks or sources are present. As the development shows, these forms of the equation are required even where the velocity and the concentration gradient are unidirectional and colinear, if the coordinate system is not itself aligned with the direction of flow.

The development of equations (1-37) through (1-40) is based on the assumption of a rigid aquifer, i.e., the assumption that changes in the quantity of water in storage are due only to expansion or compression of the interstitial water. Confined storage is normally attributed both to changes in water density and to deformation of the aquifer (e.g., Cooper, 1966). Exact analysis of the solute mass balance in a deforming aquifer is considerably more complex than that for a rigid aquifer. If it is assumed that the aquifer is deforming, allowance must be made for the fact that the porosity, θ, must change with time. Thus in developing a solute mass balance for a fixed spatial volume element, porosity should appear under the time derivative in the expression for rate of solute mass accumulation. For example, in developing equation (1-37), the rate of solute mass accumulation within the element $\Delta x\,\Delta y\,\Delta z$ should be taken as $\partial(\theta C)/\partial t\,\Delta x\,\Delta y\,\Delta z$ rather than as $\theta\,\partial C/\partial t\,\Delta x\,\Delta y\,\Delta z$. This would lead to an exact solution for solute mass balance if the specific discharge terms on the left-hand side of equation (1-37), q_x, q_y, and q_z, represented the true liquid fluxes across the faces of the element in a deforming aquifer.

However, because the volume element $\Delta x\,\Delta y\,\Delta z$ is assumed to be fixed in space, and because the solid grains of a porous medium are essentially incompressible, aquifer deformation and change in porosity can occur only if there is some movement of solid grains across the boundaries of the element, at some finite grain velocity which we designate w_g. This in turn implies that some pore space, and the interstitial water within that pore space, are also carried across the element boundaries at the velocity w_g in the deformation process. As noted by Cooper (1966), the Darcy velocity and the associated seepage velocity are actually velocities relative to the grains, or solid matrix, of the porous medium. Thus in a deforming aquifer, the total velocity of the interstitial water relative to a fixed frame of reference is the sum of the seepage velocity and the grain velocity; the total specific discharge, or flow per unit cross-sectional area, is similarly the sum of the Darcy velocity and $w_g\theta$, the product of grain velocity and porosity. These total velocity or total specific discharge terms would therefore have to be used in the expression for net solute inflow, e.g., the left-hand sides of equations (1-38) through (1-40), in order to derive an exact mass balance equation for the deforming system.

In practical problems, the effect of confined storage on solute mass balance is usually very small, and transport equations developed under the rigid-aquifer assumption are an adequate approximation. Where this is not the case, the effect of confined storage can be simulated by including an artificial sink/source term in the governing transport equation, where the source strength is varied to equal the rate of storage accumulation or release associated with aquifer deformation, i.e., the rate of storage accumulation or release in excess of that which would occur in a rigid aquifer.

The most significant storage process observed in the field is unconfined storage, i.e., storage due to movement of the water table or free surface. In terms of the differential equation of groundwater flow, water table storage actually represents a time-varying boundary condition. In practical calculations, however, water table effects are usually treated as an internal storage accumulation or release occurring in the upper part of an aquifer, rather than as a boundary condition. Thus they are represented by the right-hand side of equation (1-22), but using a high value of specific storage, usually taken as the specific yield divided by the thickness of the hydrogeologic interval in which the water table occurs. The solute mass balance in a volume of aquifer which includes the water table cannot be fully represented by equations (1-38) through (1-40), which were derived for a fully saturated volume element in the interior of an aquifer, and contain no term to account for solute gain or loss associated with a rising or falling free surface. In transport simulation, however, the approximating equations at cells or nodes containing a free surface are formulated in terms of the saturated thickness, rather than in terms of a fixed thickness, Δz. The saturated thickness is updated at each time step as the water level changes; thus the volume of water accumulating in or released from storage, and the associated solute mass accumulation or release, can be accounted for in the calculation.

Equations (1-38) through (1-40), in which the partial derivative, $\partial C/\partial t$, indicates the rate of change in solute concentration, C, at a fixed point in space, are called Eulerian expressions (e.g., Daily and Harleman, 1966). Equations of this kind can be used directly in standard numerical solution methods based on the mass-balance approach. Unfortunately, direct solution of the Eulerian form of the advective transport equation is plagued by a serious problem, known as *numerical dispersion*. While we will provide a detailed discussion on this and other topics related to numerical methods for transport simulation in Chapters 5 and 6, we present here an intuitive demonstration of the numerical dispersion phenomenon.

Consider again the apparatus of Figure 1-3, and suppose that initially water having a salt concentration of 10 milligrams per liter (mg/l) circulates

through the system. Suppose that the Darcy velocity in the sand is 10 cm/hr, and the cross-sectional area of the pipe is 100 cm^2, so that the rate of flow through the sand is 1000 cm^3 per hour, or 1 liter per hour. Assume that the length Δl is 100 cm, and the porosity of the sand is 0.1; thus the pore volume of the element $A\,\Delta l$ is 1000 cm^3, or 1 liter, and the flow rate could be expressed as one pore volume per hour. Finally, assume that the salt concentration of water entering the upstream face is changed abruptly at a time t_0 to 100 mg/l.

Now considering the application of the mass-balance approach over the full volume $A\,\Delta l$. Prior to t_0 salt is transported across the upstream face at a mass rate of 10 milligrams per hour (mg/hr), and is transported out of the volume at the downstream face at the same rate; thus the rate of accumulation of salt mass within the volume is zero. At time t_0 the concentration at the upstream face is changed to 100 mg/l, and the mass rate of salt inflow increases to 100 mg/hr. We apply equation (1-33) to the problem, representing the time derivative, $\partial C/\partial t$, as a finite-difference term, $\Delta C/\Delta t$, where ΔC represents the change in average salt concentration within the volume $A\,\Delta l$ over a finite time interval, Δt, which we take as 6 minutes or 0.1 hr; and we assume that the concentration of the water leaving the volume at the outflow face during each time step is equal to the average concentration within the volume at the beginning of the time step. Thus during the first six-minute time step after t_0 we calculate a mass inflow of 100 mg/hr, and a mass outflow of 10 mg/hr. This leads to a rate of mass accumulation in the first time step of 90 mg/hr; at this rate the mass of salt in the volume $A\,\Delta l$ increases by 9 mg during the initial time step, causing an increase in concentration of 9 mg/l during that period. In this way we calculate an average concentration of 19 mg/l at the end of the time step. For the second time we again use a mass inflow rate of 100 mg/hr, but we now assume that the outflow concentration is 19 mg/l; thus the mass outflow during the second time step occurs at a rate of 19 mg/hr, and mass accumulation within the volume is calculated as 81 mg/hr. Table 1-1 shows calculated values of average concentration within the volume at the end of each time step using this approach.

In the process of calculation described above we have actually used a finite-difference approach to solve equation (1-33), employing a forward-difference approximation to the time derivative (see Chapter 6). Because we assume that the concentration at the outflow face is equal to the average concentration in volume $A\,\Delta l$, Table 1-1 can be taken as a summary of the calculated outflow concentration as a function of time. If we plot the concentration in Table 1-1 versus time, as shown in Figure 1-5, the result is a smooth curve with the outflow concentration gradually increasing from 10 mg/l and eventually approaching that of the inflow, 100 mg/l.

TABLE 1-1 Calculated Concentration at the Outflow Face for the Mass-Balance Example

Time (hr)	Concentration (mg/l)
0.1	19.0
0.2	27.1
0.3	34.4
0.4	41.0
0.5	46.9
0.6	52.2
0.7	56.9
0.8	61.2
0.9	65.1
1.0	68.6
1.1	71.4
1.2	74.2
1.3	76.8
1.4	79.1
1.5	81.2
1.6	83.1
1.7	84.7
1.8	86.2
1.9	87.5
2.0	88.7

Theoretically, the concentration change at the outflow face for this problem, assuming only advective transport, should show a sharp change from 10 mg/l to 100 mg/l at 1 hour after t_0 (see Figure 1-5). It is clear that the mass-balance method of calculation has introduced a smearing of the concentration-time curve, or "breakthrough" curve, at the outflow face. As we will see in the next chapter, breakthrough curves in nature are never perfectly sharp; there is always a certain amount of spreading, or dispersion, associated with natural velocity variation. The computational effect which we see here mimics this behavior, and hence the term numerical dispersion. It should be pointed out, however, that the numerical dispersion is an artifact of the computation, and is fundamentally unrelated to any physical mechanism.

If instead of using the entire volume $A\,\Delta l$ of Figure 1-3 as the basis of our calculation, we were to break that volume into a series of thin slices normal to the pipe, and apply the mass-balance approach in sequence to those slices, we could achieve a better result. Similarly, if we retained the full volume $A\,\Delta l$ but happened to use a time step of 1 hour, or in any case a time step closer to the travel time of a fluid particle through the volume of

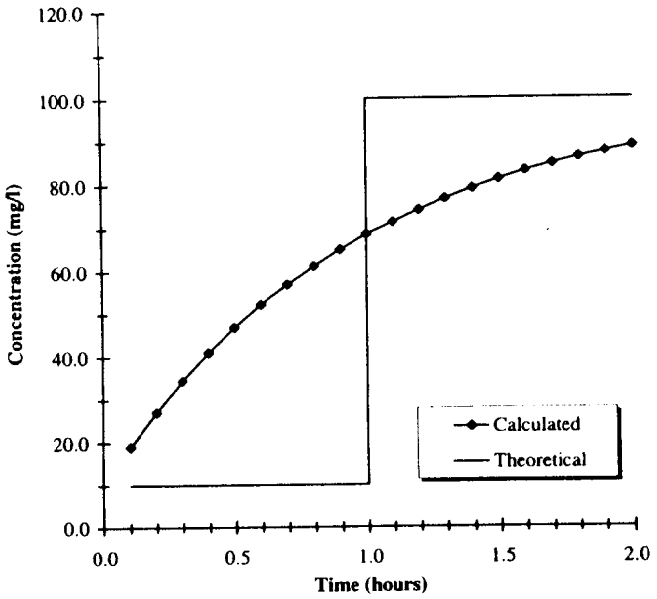

FIGURE 1-5. Outflow concentrations calculated for the purely advective transport example, compared with theoretical outflow concentrations (a constant inflow concentration is assumed).

calculation, we could reduce the numerical dispersion effect. This shows that the numerical dispersion effect is affected by both spatial and temporal discretizations.

1.3.2 The Particle Tracking Approach to Advective Transport

Because of the numerical dispersion effect associated with the mass-balance approach, an alternative method based on fluid particle tracking is often used to solve advective transport problems. In this method a concentration value is associated with individual particles of fluid, and the advance of those particles through the region of interest is calculated from an analysis of the flow field. The particle tracking approach is based on the Lagrangian point of view (e.g. Daily and Harleman, 1966; Bear, 1972), in which concentration is associated not with fixed points or volume elements in space, but rather with fluid elements or particles which move with the prevailing flow velocity.

A Lagrangian equation for advective transport can be developed from the mass-balance equation in subscript form, i.e., equation (1-40), if it is kept in mind that C now refers to the concentration identified with a fluid element or particle which moves with the flow. We may expand the first term on the right side of equation (1-40) using the chain rule as follows:

$$\frac{\partial}{\partial x_i}(v_i C) = v_i \frac{\partial C}{\partial x_i} + C \frac{\partial v_i}{\partial x_i} \tag{1-41}$$

Note that because the subscript notation implies summation over the coordinate directions, the term $\partial v_i/\partial x_i$ actually represents the flow divergence, or net outflow rate per unit pore volume. In steady-state flow, this term must be equal to the sink/source term q_s/θ, which gives the volumetric rate of gain or loss of fluid from sources or sinks, per unit pore volume, i.e.,

$$\frac{\partial v_i}{\partial x_i} = \frac{q_s}{\theta} \tag{1-42}$$

Substituting equations (1-41) and (1-42) into (1-40) and rearranging yields

$$\frac{\partial C}{\partial t} + v_i \frac{\partial C}{\partial x_i} = \frac{q_s}{\theta}(C_s - C) \tag{1-43}$$

The terms on the left side of equation (1-43) define the rate of change of concentration identified with a particle or element of fluid which is moving along a pathline (also referred to as a characteristic curve) of the flow field. The sum of the two terms is referred to as the *substantial derivative* and is designated DC/Dt, i.e.,

$$\frac{DC}{Dt} = \frac{\partial C}{\partial t} + v_i \frac{\partial C}{\partial x_i} \tag{1-44}$$

Thus equation (1-43) can be written as

$$\frac{DC}{Dt} = \frac{q_s}{\theta}(C_s - C) \tag{1-45}$$

Equation (1-45) can be simplified further by recalling that under the Lagrangian interpretation the concentration, C, is identified with a moving element or particle; and by noting that in purely advective transport, the concentration carried by particles emerging from a source must be the same

as the concentration associated with the source, and the concentration carried by a particle which enters a sink must be equal to the concentration associated with that particle immediately outside the sink. Thus the terms C and C_s of equation (1-45), as interpreted in the Lagrangian context, are equal. Equation (1-45) therefore becomes simply

$$\frac{DC}{Dt} = 0 \tag{1-46}$$

Equation (1-46) is a statement that the concentration identified with a fluid particle does not change with time as the particle traverses a pathline, provided the transport is purely advective. Rather, the particle's concentration at the starting point of the pathline remains its concentration at every point along that pathline. Because particles emanating from a source follow a pathline which originates at the source, they retain the concentration associated with the source along the entire length of the pathline; similarly, particles entering a sink follow a pathline which terminates at the sink, and enter it with the concentration they have carried along the entire pathline. Thus the solution to a problem of purely advective transport using a Lagrangian approach is a matter of defining the pathlines of individual solute particles in the flow regime.

We now return to the problem considered in the previous section, involving the movement of saline water through the apparatus of Figure 1-2; we approach the problem from the Lagrangian point of view, through particle tracking. We begin by placing a number of particles on the planar interface representing the abrupt change in concentration from 10 mg/l to 100 mg/l. We then simply calculate the advance of this planar interface through the sand, beginning at t_0 and moving at a seepage velocity of 100 cm/hr; we interpret the concentration ahead of the interface as 10 mg/l and that behind it as 100 mg/l. Following this method, we calculate the concentration at the outflow face as 10 mg/l until one hour after t_0, at which time it increases abruptly to 100 mg/l. Note that during the calculation process, no numerical dispersion is introduced, and the results should agree more closely with observation than those obtained using the mass-balance (Eulerian) approach if the transport is predominantly advective.

In the above example there are only two regions, separated by a planar interface which advances uniformly through the sand-packed pipe of Figure 1-2; within each region, concentration has only one value. However, the particle tracking approach has much wider application than this example suggests. For example, in a problem in which the solute distribution is described by a series of three-dimensional surfaces of equal concentration, each of these surfaces may be taken as an interface. The concepts of seepage velocity and travel time may then be applied to calculate the position of each of these isoconcentration surfaces at successive times, generating a new concentration distribution for each time of calculation. However, even though new concentration distributions are obtained, concentration itself never appears as a variable of calculation under this approach; the calculation involves only the positions, velocities, and times of travel of fluid particles marking the various interfaces.

The effort involved in calculating the advance of an interface depends on the geometry of the interface and the complexity of the flow pattern. In the apparatus of Figure 1-2, an interface would always be a plane at right angles to the pipe; its advance would follow a known direction at a uniform velocity. In a field problem where the flow field is three-dimensional and varying with time, interfaces may advance irregularly and change shape continuously. Calculation of the advance of an interface involves determining the sequence of positions of a large number of particles marking its surface. In the apparatus of Figure 1-2, the velocity is constant in time and the same for all particles. A single calculation of velocity is therefore sufficient, and there is no requirement for bookkeeping to keep track of the positions of a large number of particles at successive times. In the case of a complex three-dimensional interface in the field, the velocities of individual particles on the interface differ from one another and vary through time. Thus the velocity of each particle must be calculated separately, in general using the three-dimensional vector form of Darcy's Law, equations (1-9) through (1-12); and the calculations must be repeated at successive times for all particles. The position of each particle must be updated after each time increment using the velocity, the time increment, and the particle's prior position; and a large amount of computer memory may be needed to store the required information on particle position. However, while the process is more cumbersome, the approach is basically similar to that of calculating the advance of an interface through the pipe of Figure 1-2.

The particle tracking approach and existing computer codes for solving purely advective transport problems are discussed in detail in Chapter 5.

2

Dispersive Transport and the Advection-Dispersion Equation

2.1 INTRODUCTION

The theory of dispersive transport, or hydrodynamic dispersion, addresses the effects of the departure of individual particle velocities from the average seepage velocity as defined in equation (1-7). In the preceding chapter we assumed that all fluid particles moved with this average seepage velocity of the water. In fact the velocity of an individual particle may differ from the average seepage velocity for a number of reasons. Solute particles are subject to diffusion in the presence of a concentration gradient; while this is often a very small term relative to advective movement, in problems where velocities are extremely low it may be significant. Individual particle velocities also deviate from the average seepage velocity because of the microscopic heterogeneity and tortuosity associated with the pore structure. Finally, virtually all natural porous media exhibit heterogeneity on a macroscopic scale, most of which remains hidden from observation. The hydraulic properties assumed in velocity calculation are average or bulk values; locally, within any volume for which velocity is calculated, hydraulic conductivity may differ from the average values used in velocity calculation. Thus the true local velocity of a fluid particle, even in a macroscopic sense, will generally differ from the average seepage velocity calculated from hydraulic parameters.

Macroscopic heterogeneity has been recognized in recent years as the primary reason for the departure of observed solute movement from the results of advective calculation in field situations. Historically, however, the development of a theory to account for these departures focused first on considerations of microscopic or pore-scale phenomena, perhaps because

these are of primary importance in laboratory settings. In this discussion we will follow the historical model in developing the concepts, and focus first on microscopic processes. While many workers have contributed to the development of hydrodynamic dispersion, the contributions of Scheidegger (1954, 1958, 1961), de Josselin de Jong (1958), Saffman (1959, 1960), Bear (1960, 1961), and Bachmat and Bear (1964) are of particular note. Detailed discussions of the theory are given by Bear et al. (1968) and Bear (1972).

2.2 MICROSCOPIC DISPERSIVE PROCESSES

2.2.1 Mechanism of Hydrodynamic Dispersion

If we consider flow within a single pore as illustrated in Figure 2-1, the velocity must vary from a maximum along the centerline of the pore to essentially zero along the pore walls. At a slightly larger scale, looking at the velocity distribution in an assemblage of pores as shown in Figure 2-2, fluid particles must necessarily follow tortuous flow paths around the sand grains, and velocity must therefore vary in direction from one point to another. Moreover, the magnitude of the velocity must be greater in large pores than in small pores; and we must allow for the possibility of totally isolated pores or "dead-end" pores, in which velocity is zero.

In calculations of groundwater flow, the focus is never on these microscopic velocities. The seepage velocity of equation (1-7) and the Darcy velocity of equation (1-8) actually represent average or bulk quantities, even though they are commonly treated as vector point functions. In effect, we assume that in the sand of Figure 1-1, any small volume element large enough to allow a practical determination of discharge or velocity would necessarily contain a very large number of pores; and we assume that in terms of fluid

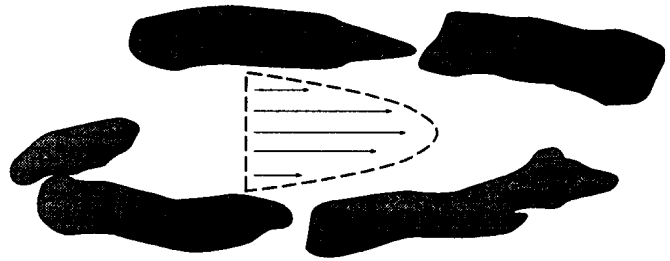

FIGURE 2-1. Diagram illustrating theoretical variation of velocity within an individual pore.

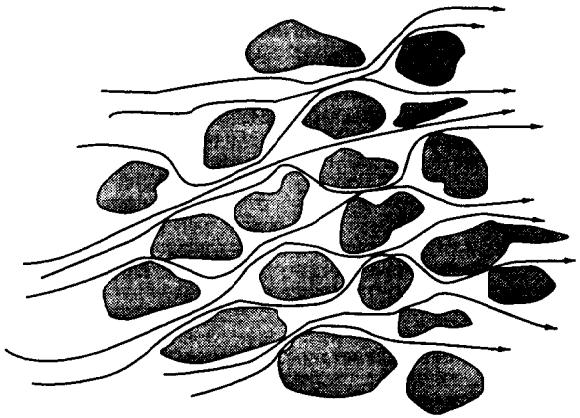

FIGURE 2-2. Diagram illustrating tortuous branching and reconnection of microscopic flow paths in a porous medium.

discharge, the microscopic velocity components within such an element cancel except in one resultant direction of movement. The volumetric discharge through a unit area normal to that direction is then the Darcy velocity through the element, and is divided by effective porosity to yield the seepage velocity.

But while the Darcy velocity, by definition, gives a good representation of volumetric flow through the sand of Figure 1-1, the seepage velocity cannot yield the resultant path of movement of each individual fluid particle, nor can it yield the travel time of every individual particle traversing the sand. Each particle must experience a sequence of velocities as it moves through the sand; and because the sequence differs or different particles, the outcome in terms of final position and travel time will not be the same for all particles.

To see what this means in terms of the movement of solute or tracer, assume that a point source of water containing dye or other tracer is located at the center of the upstream face of the sand section, as shown in Figure 2.3. Further assume that this source is activated instantaneously, emitting a pulse of "tagged" water at a time t_0, i.e., assume that a small volume of water, containing tracer at a concentration C_0, enters the flow at the center of the upstream face, within a brief time interval centered on t_0. Finally, assume the tracer to be chemically inert and identical to water in its hydraulic properties, and imagine that sensors capable of measuring its concentration are positioned at various points within the sand and on the downsteam face.

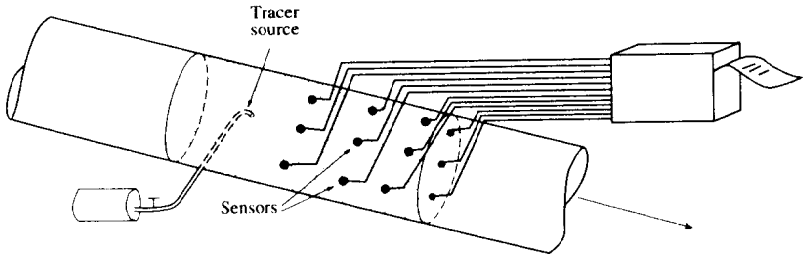

FIGURE 2-3. Sand-packed pipe equipped with tracer source and detectors.

If the assumptions of the simple displacement model of Section 1-1 were valid, we should expect most of the tracer mass (except for the effects of molecular diffusion) to remain within the injected volume of water; and we should expect that injected volume to move cohesively along the centerline of the sand, with no sensible change in its shape or in its tracer concentration. A sensor positioned on the centerline of the sand should give the response shown in Figure 2-4, i.e., concentration should rise abruptly from zero to the injected value, C_0, and then drop rapidly back to zero as the volume of

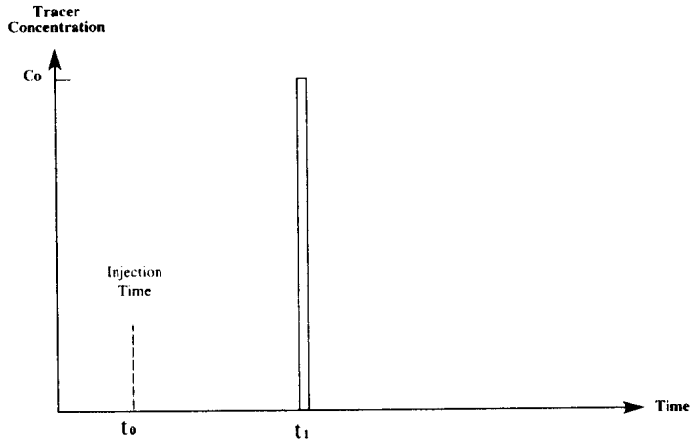

FIGURE 2-4. Response of a sensor located along a streamline from the tracer injection point, assuming purely advective transport; distance of sensor from source is $v(t_1 - t_0)$, where v is the seepage velocity.

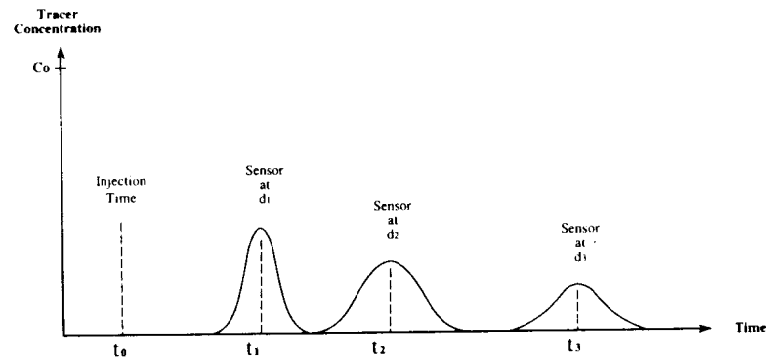

FIGURE 2-5. Responses of successive sensors located along a streamline from the tracer injection point. Midpoints of tracer concentration peaks occur at $t_n = t_0 + d_n/v$, where d_n is distance to the sensor and v is seepage velocity.

"tagged" water passes. This concentration pulse should be observed at a time t_1 such that $t_1 - t_0$ is equal to d_1/v, where d_1 is the distance from the injection point to the sensor, and v is the seepage velocity. Sensors positioned off the centerline should show no response at all.

In fact, of course, something else is observed. Successive sensors along the centerline will show responses such as those illustrated in Figure 2-5. With increasing distance from the source, the maximum concentration decreases and the concentration-time curve becomes broader, indicating that the tracer is no longer confined to the small volume of water into which it was injected, or that the volume of water has itself been mixed with a much greater volume of water as it traverses the sand. The peak of the concentration-time curve must still represent the arrival of a large number of tracer particles in the vicinity of a sensor; but some particles have clearly arrived earlier, and some continue to arrive after the peak concentration has passed, causing the gradual rise and fall of concentration with time at each sensor. This effect becomes more pronounced with distance downstream—the maximum concentration decreases progressively, and the width of the time-response curve becomes broader. Along the centerline, the peak of the concentration pulse moves with the seepage velocity v.

In addition, sensors positioned off the centerline will show a response as the repeated branching of flow paths shown in Figure 2-2 causes increasing lateral spread of the tracer with distance downstream. Note that in general, at any point away from the centerline, division of the flow around an individual sand grain should cause tracer to be diverted back toward the centerline as well as away from it. Because of this, if we examine the tracer

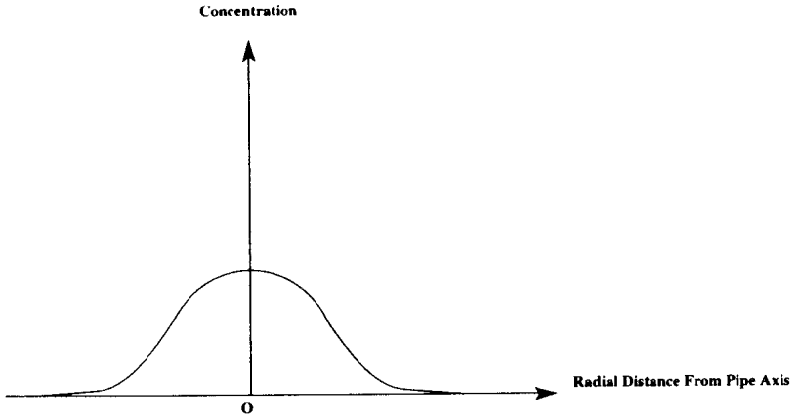

FIGURE 2-6. Tracer concentration vs. radial distance from pipe axis at a downstream point.

concentration in any cross section normal to the flow, the highest concentration will still be found along the centerline; concentration will decrease steadily with radial distance from the centerline, as shown in Figure 2-6.

The responses illustrated in Figures 2-5 and 2-6 arise because the velocity experienced by individual fluid particles is not uniform. Every particle in the flow experiences an overall tendency to move parallel to the pipe at the seepage velocity of equation (1-7). However, the actual motion of a particle at any point or time will generally deviate from this overall or average movement. This suggests that the velocity of an individual fluid particle at any point in the flow may be viewed as a vector sum of two components: the average seepage velocity of equation (1-7) and a deviation or difference from that average velocity.

Under this approach, assuming that the flow regime within the sand of Figure 2-3 is at steady state, the seepage velocity is a constant or uniform vector, always having the same direction and magnitude. The velocity deviation is similarly a vector, but one whose magnitude and direction vary from one point to another. To simplify the problem, we will assume that this difference vector is always two-dimensional, i.e., that it can be described in terms of two components—a *longitudinal* component in the direction of the flow, and a *transverse* component normal to the flow. Figure 2-7 shows these two components, the resultant difference vector, and the particle velocity vector obtained by adding the difference vector to the seepage velocity. Since ours is a steady-state problem, any process controlling the velocity of an individual particle should be a function only of position within the porous

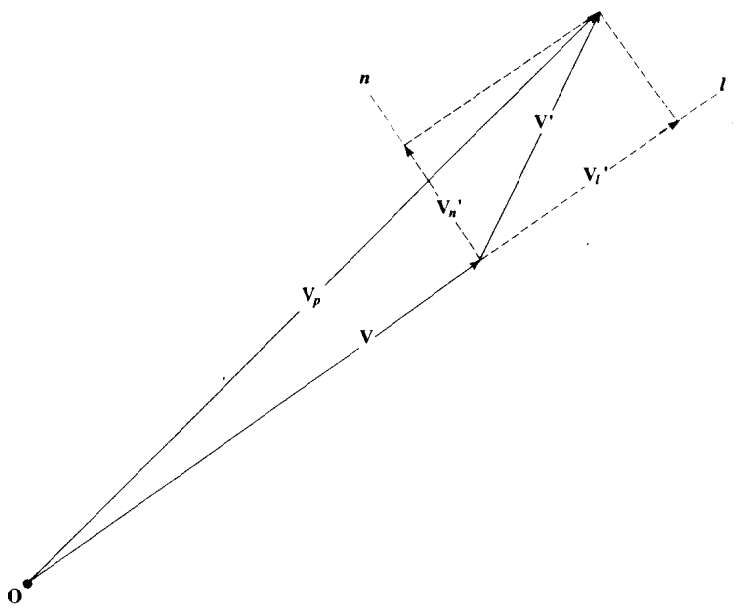

FIGURE 2-7. Vector representation of fluid particle velocity: $\mathbf{v}$ is a vector representing average seepage velocity at the point O; $\mathbf{v}_p$ is a vector representing the actual velocity of a fluid particle at point O; $\mathbf{v}'$ is the vector difference, with components v_l' and v_n' parallel and normal to $\mathbf{v}$.

network; if our knowledge of that network and its properties were sufficiently detailed, we might be able to calculate the components of the difference vector of Figure 2-7 at any point, just as we can calculate the uniform seepage velocity. This would in theory allow us to calculate the actual sequence of velocities experienced by every particle in the flow, which in turn would permit a complete description of the tracer distribution at any time after the initial release.

In reality, of course, it is impossible to know either the details of the pore structure or the way in which these may influence the velocity of an individual fluid particle. As an alternative, therefore, we treat the difference vector of Figure 2-7 as a random quantity, i.e., a term which can be known only within certain limits, in a probabilistic sense, at any given point. More exactly, we treat the longitudinal and transverse components of the difference vector as separate random terms, since the factors causing longitudinal velocity departures may differ from those causing transverse velocity components.

Whereas the porous medium imposes on each fluid particle a sequence of deterministic velocities, or as we are viewing it a sequence of deterministic departures from the seepage velocity, our model assumes a sequence of random departures from the seepage velocity. Our assumption is that over a large enough sample of the sand, the vector field generated in this way will mimic the actual velocity distribution in the sand, at least to the extent that the net effect on tracer transport will be the same.

In effect, we are separating the tracer transport problem into two parts—a motion described by the seepage velocity of equation (1-7), and a departure from that motion which we consider random. The first component represents advective transport, which we considered in the previous chapter; the second component is referred to as *hydrodynamic dispersion* or *dispersive transport*. While it is customary to discuss dispersion as though it were a transport *process*, the mechanism involved is primarily advective, i.e., movement of dissolved matter due to fluid velocity. To the limited extent that molecular diffusion contributes to dispersive transport, dispersive transport does in fact represent an independent transport process; to the extent that hidden variations in fluid velocity are responsible for the observed phenomena, dispersive transport is more correctly viewed as a method of adjusting the advective transport calculation for recognized deficiencies in the description of the velocity field.

2.2.2 The Analogy between Dispersive Transport and Molecular Diffusion

As we have noted, molecular diffusion is a contributing process (though usually a minor one) to dispersive movement. However, molecular diffusion is of interest to us here for a further reason; our representation of dispersive transport in terms of random motion is directly analogous to the way in which diffusive transport is characterized in the classical theory of diffusion; that analogy is utilized in the following discussion to develop a general understanding of the dispersive transport concept.

The classical diffusion model supposes that all ions or molecules within a fluid system are subject to random movement (e.g., Scheidegger, 1974; Cussler, 1984); where this movement occurs in the presence of a gradient in the concentration of a particular dissolved substance, it results in a net flux or transport of that substance. Consider for example the system shown in Figure 2-8(a); a container is divided into two parts by an impervious but removable plate. Distilled water is present on one side of the plate while a salt solution is present on the other. The two liquids are at the same level, and we assume the density difference between them to be negligible. The initial salt concentration in the saline water is C_0. Molecules of water on

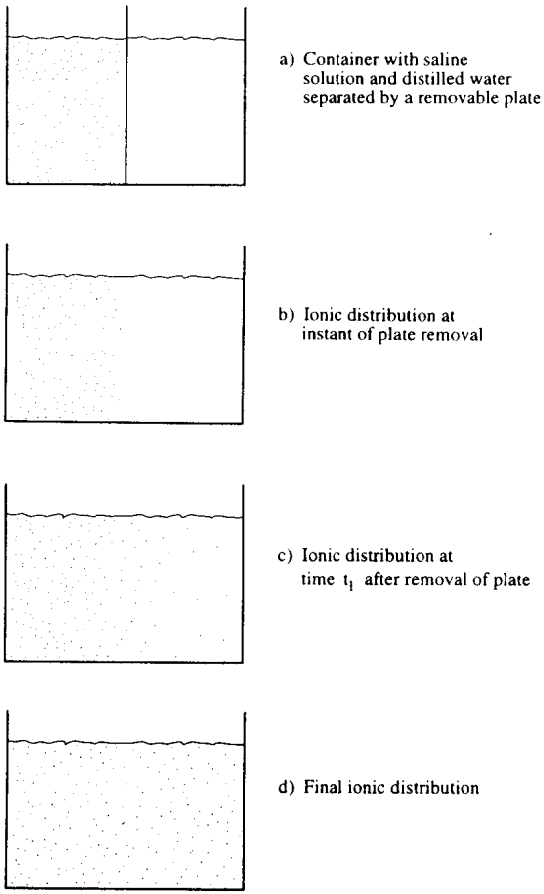

FIGURE 2-8. Experiment illustrating ionic diffusion.

both sides of the plate, and salt ions on the saline side, are in random motion associated with the thermal energy of the liquids.

At a certain instant the plate is withdrawn; at this instant a very steep concentration gradient, from C_0 on the saline side to zero in the distilled water side, exists in the region vacated by the plate, as shown in Figure 2.8(b). The random movement of salt ions in this region causes some ions to move from the saline side to the distilled water side. The number of ions

crossing the boundary is a function of the concentration difference; if a high concentration of salt is present initially at the boundary, a very large number of ions will be shifted across the boundary by random movements in a very short time; at lower initial concentrations, the number of ions moved in a given time will be less. In any case, after a short period of time the diffusive process causes the sharp transition to erode, leading to the more gradual transition shown in Figure 2-8(c). Now the concentration difference across the original boundary plane is smaller. Random motion causes less movement of salt ions in the direction of decreasing concentration, and causes some transport of ions back across the boundary; the net ion transport in the direction of decreasing concentration is therefore lower than under the conditions of Figure 2-8(b). Figure 2-8(d) shows the situation after diffusion has resulted in a completely uniform distribution of salinity through the container. Because concentration is now everywhere the same, random motion causes as many salt ions to move in one direction as in the other, and there is no net transport across the original interface.

Figure 2-9 shows how classical diffusion theory approaches the problem we have described. The section originally occupied by the plate has an area A and a width Δs. An assumption is made that the diffusive transport across this section at any time will be proportional to the difference in concentration

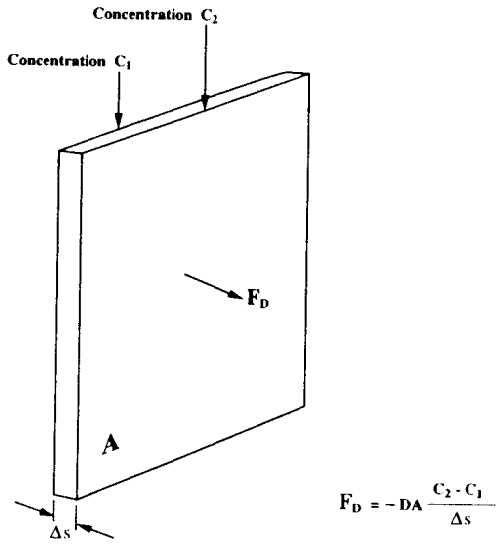

FIGURE 2-9. Diagram illustrating the terms in Fick's Law of diffusion.

across it and to the area, A, and inversely proportional to the distance of separation, Δs. The constant of proportionality is termed the diffusion coefficient, D. The concentrations on either side of Δs are C_1 and C_2; because s is considered positive toward the right of the figure, the difference in concentration is taken as $C_2 - C_1$. Thus the expression for diffusive transport is

$$F_D = -DA\frac{C_2 - C_1}{\Delta s} \tag{2-1}$$

where F_D represents the rate, in mass per unit time, at which salt is transported across area A, from the C_1 side to the C_2 side; the negative sign indicates that transport is in the direction of decreasing concentration. The term $(C_2 - C_1)/\Delta s$ is an approximation to the concentration gradient; and the equation tells us that the sharper this gradient, i.e., the greater the change in concentration per unit distance, the greater the diffusive transport will be. Using the derivative notation, equation (2-1) can be written as

$$F_D = -DA\frac{dC}{ds} \tag{2-2}$$

Equations (2-1) and (2-2) are expressions of Fick's Law of diffusion (e.g., Cussler, 1984) for the case of a unidirectional concentration gradient. We see that the required condition for diffusive transport is random motion in the presence of a concentration gradient—the same combination of factors which characterizes our model of dispersive tracer transport in the sand of Figure 2-3. The analogy between diffusion and dispersive transport can be carried a step further by noting that in moving fluids, diffusive transport is assumed to be superimposed on the transport arising from the fluid velocity, just as we imagine dispersive transport to be superimposed in the advective transport associated with the seepage velocity.

These conditions lead us to the conclusion that the mathematics of diffusion can be applied, perhaps with some modification, to describe the process of hydrodynamic dispersion in porous media. By analogy with diffusion, we assume that dispersive transport in a porous medium can be considered proportional to the product of concentration gradient and cross-sectional area. More precisely we assume that dispersive transport through a unit area normal to the longitudinal direction is proportional to the longitudinal component of the concentration gradient, and that dispersive transport through a unit area normal to the transverse direction is similarly proportional to the transverse component of the concentration gradient. However, we assume that a different coefficient of proportionality prevails in the two directions, in keeping with the inference that the factors

contributing to longitudinal disperson may differ from those contributing to transverse dispersion. There is one more important difference between our treatment of hydrodynamic dispersion and the example of diffusion in a static fluid. In both the longitudinal and transverse directions, we assume dispersive transport to be proportional to the magnitude of the seepage velocity vector. This follows from our assumption that dispersive transport is generated by the aggregate deviation of individual particle velocities from the seepage velocity. As overall flow velocities in the system are increased, the magnitude of these velocity deviations from the average seepage velocity should increase as well, giving rise to a greater dispersive transport effect.

2.2.3 Dispersive Flux and Dispersion Coefficient in Two Dimensions

In this section we will develop an expression for dispersive transport in two dimensions. This will be done first in terms of the direction of flow and the direction normal to the flow; an expression in these terms is simple to formulate, and adequate for unidirectional flow problems. Following this, a more general expression, in terms of a fixed Cartesian coordinate system, will be derived. An expression of the latter kind is clearly necessary in problems where the direction of flow may vary spatially or temporally. However, the more general form is considerably more cumbersome, in that dispersive transport in each coordinate direction now depends on components of the velocity and concentration gradient in both directions. As the development will show, matrix notation provides a convenient vehicle for this form of the dispersive transport term.

Because dispersive transport occurs both in the direction of flow and the direction normal to the flow, the resultant dispersive movement will be the vector sum of components in these two directions, and will in general be neither aligned with the flow, nor normal to it. It is convenient to define a vector, **W**, having the direction of resultant dispersive transport, and having a magnitude equal to the dispersive mass flux of solute, i.e., the mass of solute, in excess of that given by advective calculation, crossing a unit area of fluid normal to **W** in a unit time. **W** then has two components, W_l and W_n, where l is the direction of flow and n is the direction transverse to the flow. In the example of Figure 2-3, l represents distance along the pipe and n the distance transverse to the pipe (we assume that n is measured from the centerline of the pipe and that radial symmetry prevails in dispersion normal to the flow, so that the dispersive process can be considered two-dimensional). In keeping with the assumptions outlined above we consider the dispersive flux in each component direction to be proportional to the derivative of concentration in that direction, and to the magnitude of

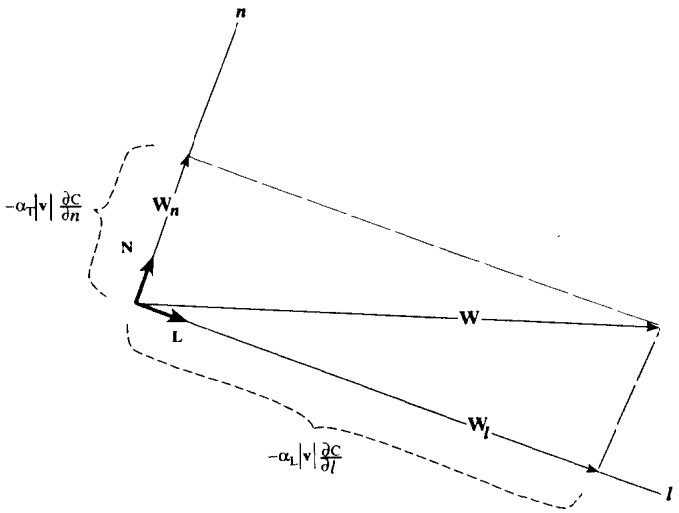

FIGURE 2-10. Representation of the net dispersive flux vector using longitudinal and transverse components, $\mathbf{W}_l$ and $\mathbf{W}_n$. **N** and **L** are unit vectors; $|v|$ is the magnitude of the seepage velocity, $\partial C/\partial l$ and $\partial C/\partial n$ are components of the concentration gradient in the l and n directions; α_L is the longitudinal dispersivity; and α_T is the transverse dispersivity.

the average seepage velocity, i.e.,

$$\mathbf{W}_l = -\alpha_L|\mathbf{v}|\frac{\partial C}{\partial l}\mathbf{L} \tag{2-3}$$

$$\mathbf{W}_n = -\alpha_T|\mathbf{v}|\frac{\partial C}{\partial n}\mathbf{N} \tag{2-4}$$

where as shown in Figure 2-10, **L** is a unit vector in the direction of flow, l; **N** is a unit vector in the transverse direction, n; α_L is the longitudinal dispersivity, a property of the porous medium describing dispersive transport in the direction of flow; α_T is the transverse dispersivity, a similar property of the porous medium describing dispersive transport normal to the direction of flow; $|\mathbf{v}|$ is the magnitude of the seepage velocity; and as before C is the concentration of solute, expressed as mass of solute per unit volume of fluid. $\partial C/\partial l$ and $\partial C/\partial n$ are the derivatives of concentration in the l and n directions, respectively, and the negative signs indicate that transport occurs in the directions of decreasing concentration. Inspection of equations (2-3) and (2-4) will show that α_L and α_T must have the dimension of length. Note that

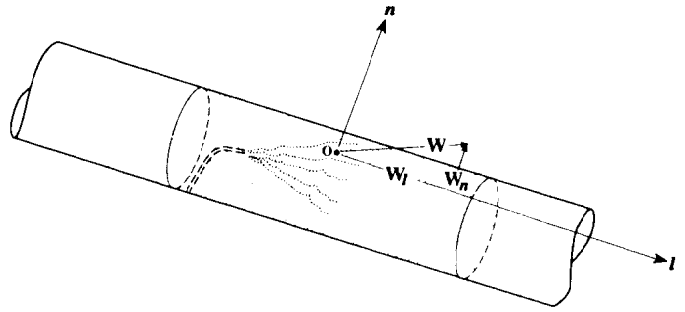

FIGURE 2-11. Components of the dispersive flux vector near the edge of the tracer plume; $\mathbf{W}_l$ and $\mathbf{W}_n$, as calculated in equations (2-3) and (2-4), are added to yield the dispersive flux vector.

$\mathbf{W}_l$ and $\mathbf{W}_n$ give the mass transport per unit cross-sectional area of fluid. Thus mass transport is calculated by combining these terms with fluid area (i.e., the product of porosity and bulk area).

Equations (2-3) and (2-4) may be applied to calculate the dispersive flux components at any point in the flow regime, for example, point o in Figure 2-11, which is located near the edge of the spreading plume of tracer in the experimental setup of Figure 2-3. Concentration gradients in both the longitudinal and transverse directions are present at this point; thus components in both directions are calculated, giving rise to the resultant dispersive flux vector shown in Figure 2-11. This dispersive flux may then be combined with an advective flux vector to calculate the resultant vector describing the tracer movement at point o. As shown in Figure 2-12 this resultant transport vector is virtually parallel to the edge of the tracer plume, reflecting the fact that point o is located close to the edge of the plume.

In the example of Figures 2-3, 2-11, and 2-12, the direction of flow, l, and the transverse direction, n, are known and fixed. Thus there is no particular difficulty in using equations (2-3) and (2-4) to calculate the components of dispersive transport anywhere in the system. In a field problem, on the other hand, we would expect the flow direction to change from one location to another, and perhaps from one time to another; to address these situations the dispersive flux equations must be framed in terms of a conventional coordinate system. To do this, assuming for simplicity that the flow field is two-dimensional, the units vectors **L** and **N** must be expressed in terms of their x and y components; $\partial C/\partial l$ must be expressed in terms of the directional derivatives of concentration in the x and y directions, $\partial C/\partial x$ and $\partial C/\partial y$; and $\partial C/\partial n$ must similarly be expressed in terms of $\partial C/\partial x$ and

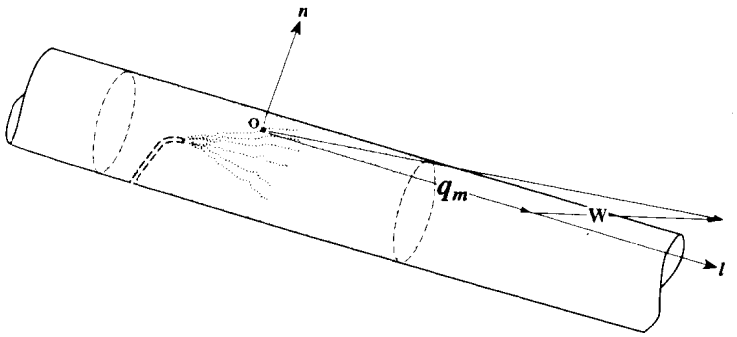

FIGURE 2-12. Resultant advective-dispersive mass flux vector near the edge of the tracer plume; resultant vector at point O is formed by adding the dispersive flux vector $\mathbf{W}$ to the advective flux vector $\mathbf{q}_m$.

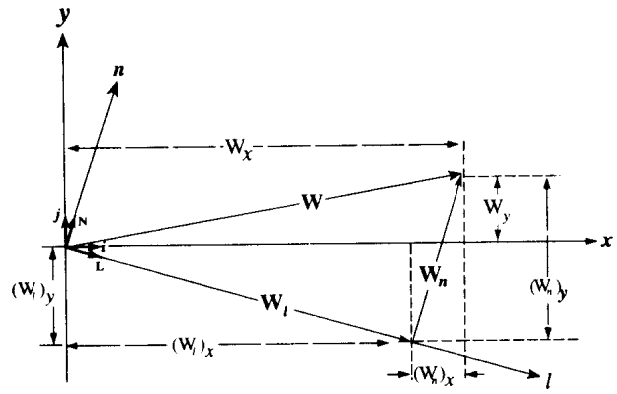

FIGURE 2-13. Components of the dispersive flux vector. $(W_l)_x$ and $(W_l)_y$ are scalar components of the longitudinal dispersive flux vector, $\mathbf{W}_l$; $(W_n)_x$ and $(W_n)_y$ are scalar components of the transverse dispersive flux vector, $\mathbf{W}_n$; W_x and W_y are scalar components of the resultant dispersive flux vector, $\mathbf{W}$; $\mathbf{N}$ and $\mathbf{L}$ are unit vectors in the l and n directions; $\mathbf{i}$ and $\mathbf{j}$ are conventional Cartesian unit vectors.

$\partial C/\partial y$. This in effect resolves $\mathbf{W}_l$ into x and y components, $(W_l)_x$ and $(W_l)_y$ and similarly, resolves $\mathbf{W}_n$ into x and y components, $(W_n)_x$ and $(W_n)_y$, as shown in Figure 2-13. Ultimately the two x components, $(W_l)_x$ and $(W_n)_x$, are combined to form W_x, the x component of the resultant dispersion vector $\mathbf{W}$; similarly the y components, $(W_l)_y$ and $(W_n)_y$, are combined to form W_y, the y component of the resultant dispersion vector. As the analysis is

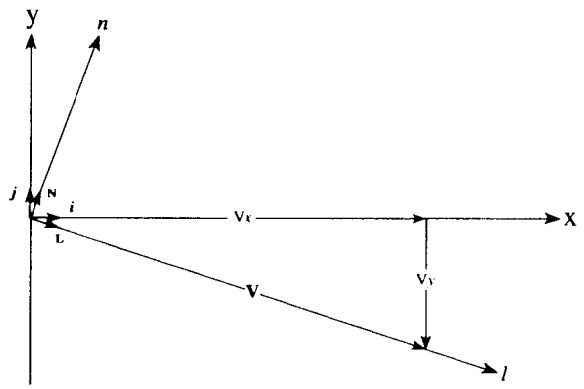

FIGURE 2-14. Components of the seepage velocity vector. $\mathbf{i}$, $\mathbf{j}$, $\mathbf{N}$, and $\mathbf{L}$ are unit vectors.

carried out, it turns out that $(W_l)_x$ depends on both $\partial C/\partial x$ and $\partial C/\partial y$, as does $(W_n)_x$; thus W_x must also depend on both $\partial C/\partial x$ and $\partial C/\partial y$. Similarly $(W_l)_y$ depends on both $\partial C/\partial x$ and $\partial C/\partial y$, as does $(W_n)_y$; thus W_y also depends on both $\partial C/\partial x$ and $\partial C/\partial y$. This leads ultimately to a matrix expression for the dispersion term.

Figure 2-14 shows the seepage velocity vector, $\mathbf{v}$, extending in the direction of flow, l; v_x and v_y are the scalar components of $\mathbf{v}$ in the x and y directions. Using the conventional unit vectors, $\mathbf{i}$ and $\mathbf{j}$ along the x and y axes, $\mathbf{v}$ can be represented as

$$\mathbf{v} = v_x\mathbf{i} + v_y\mathbf{j} \tag{2-5}$$

The magnitude of the velocity is given by

$$|\mathbf{v}| = \sqrt{v_x^2 + v_y^2} \tag{2-6}$$

Because $\mathbf{L}$ is a unit vector in the direction of the velocity, an expression for $\mathbf{L}$ can be obtained by multiplying the velocity vector, $\mathbf{v}$, by the inverse of its scalar magnitude, i.e.,

$$\mathbf{L} = \frac{v_x}{|\mathbf{v}|}\mathbf{i} + \frac{v_y}{|\mathbf{v}|}\mathbf{j} \tag{2-7}$$

Because $\mathbf{N}$ is a unit vector normal to $\mathbf{L}$, an expression for $\mathbf{N}$ can be obtained by interchanging the components of $\mathbf{L}$ while changing the sign of one

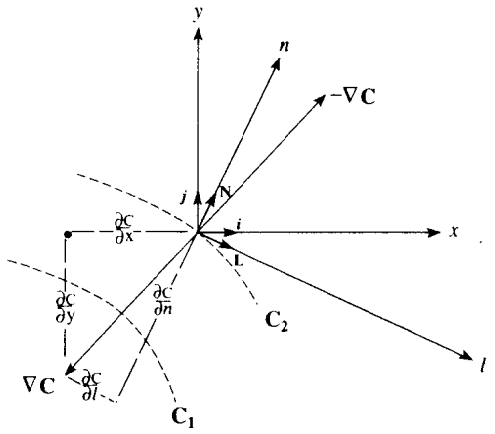

FIGURE 2-15. Components of the concentration gradient vector. Dashed lines represent isoconcentration contours; **i**, **j**, **N**, and **L** are unit vectors; $\partial C/\partial l$ and $\partial C/\partial n$ are directional derivatives of concentration parallel to and normal to the flow velocity; $\partial C/\partial x$ and $\partial C/\partial y$ are directional derivatives of concentration in the coordinate directions.

component, i.e.,

$$\mathbf{N} = \frac{v_y}{|\mathbf{v}|}\mathbf{i} - \frac{v_x}{|\mathbf{v}|}\mathbf{j} \tag{2-8}$$

The gradient vector of the solute concentration, ∇C, shown in Figure 2-15 is given by

$$\nabla C = \frac{\partial C}{\partial x}\mathbf{i} + \frac{\partial C}{\partial y}\mathbf{j} \tag{2-9}$$

The directional derivative of C in the direction, l, $\partial C/\partial l$, is the component of ∇C in the direction l; this in turn is the scalar product of ∇C with the unit vector **L**:

$$\frac{\partial C}{\partial l} = \nabla C \cdot \mathbf{L} = \frac{v_x}{|\mathbf{v}|}\frac{\partial C}{\partial x} + \frac{v_y}{|\mathbf{v}|}\frac{\partial C}{\partial y} \tag{2-10}$$

Similarly, the directional derivative of concentration in the direction normal to the velocity is the component of ∇C in the direction n, which in turn is the scalar product of ∇C with the unit vector **N**:

$$\frac{\partial C}{\partial n} = \nabla C \cdot \mathbf{N} = \frac{v_y}{|\mathbf{v}|}\frac{\partial C}{\partial x} - \frac{v_x}{|\mathbf{v}|}\frac{\partial C}{\partial y} \tag{2-11}$$

Substituting equations (2-7) and (2-10) into (2-3), the longitudinal vector component of the dispersive flux vector is given by

$$\begin{aligned}\mathbf{W}_l &= -\alpha_L|\mathbf{v}|\frac{\partial C}{\partial l}\mathbf{L} \\ &= -\left(\alpha_L|\mathbf{v}|\frac{\partial C}{\partial l}\right)\left(\frac{v_x}{|\mathbf{v}|}\mathbf{i} + \frac{v_y}{|\mathbf{v}|}\mathbf{j}\right) \\ &= -\alpha_L\frac{v_x v_x}{|\mathbf{v}|}\frac{\partial C}{\partial x}\mathbf{i} - \alpha_L\frac{v_x v_y}{|\mathbf{v}|}\frac{\partial C}{\partial y}\mathbf{i} - \alpha_L\frac{v_y v_x}{|\mathbf{v}|}\frac{\partial C}{\partial x}\mathbf{j} - \alpha_L\frac{v_y v_y}{|\mathbf{v}|}\frac{\partial C}{\partial y}\mathbf{j}\end{aligned} \tag{2-12}$$

Similarly, substituting equations (2-8) and (2-11) into (2-4), the transverse vector component of the dispersive flux vector is found to be

$$\begin{aligned}\mathbf{W}_n &= -\alpha_T|\mathbf{v}|\frac{\partial C}{\partial n}\mathbf{N} \\ &= -\left(\alpha_T|\mathbf{v}|\frac{\partial C}{\partial n}\right)\left(\frac{v_y}{|\mathbf{v}|}\mathbf{i} - \frac{v_x}{|\mathbf{v}|}\mathbf{j}\right) \\ &= -\alpha_T\frac{v_y v_y}{|\mathbf{v}|}\frac{\partial C}{\partial x}\mathbf{i} + \alpha_T\frac{v_y v_x}{|\mathbf{v}|}\frac{\partial C}{\partial y}\mathbf{i} + \alpha_T\frac{v_x v_y}{|\mathbf{v}|}\frac{\partial C}{\partial x}\mathbf{j} - \alpha_T\frac{v_x v_x}{|\mathbf{v}|}\frac{\partial C}{\partial y}\mathbf{j}\end{aligned} \tag{2-13}$$

The resultant dispersion vector, **W**, is formed as the vector sum of $\mathbf{W}_l$ and $\mathbf{W}_n$, by segregating the x component terms involving $\partial C/\partial x$, the x component terms involving $\partial C/\partial y$, the y component terms involving $\partial C/\partial x$ and the y component terms involving $\partial C/\partial y$, i.e.,

$$\begin{aligned}\mathbf{W} = \mathbf{W}_l + \mathbf{W}_n &= W_x\mathbf{i} + W_y\mathbf{j} \\ &= -\left(\alpha_L\frac{v_x v_x}{|\mathbf{v}|} + \alpha_T\frac{v_y v_y}{|\mathbf{v}|}\right)\frac{\partial C}{\partial x}\mathbf{i} - \left(\alpha_L\frac{v_x v_y}{|\mathbf{v}|} - \alpha_T\frac{v_y v_x}{|\mathbf{v}|}\right)\frac{\partial C}{\partial y}\mathbf{i} \\ &\quad -\left(\alpha_L\frac{v_y v_x}{|\mathbf{v}|} - \alpha_T\frac{v_x v_y}{|\mathbf{v}|}\right)\frac{\partial C}{\partial x}\mathbf{j} - \left(\alpha_L\frac{v_y v_y}{|\mathbf{v}|} + \alpha_T\frac{v_x v_x}{|\mathbf{v}|}\right)\frac{\partial C}{\partial y}\mathbf{j}\end{aligned} \tag{2-14}$$

We now introduce the terms

$$D_{xx} = \alpha_L\frac{v_x v_x}{|\mathbf{v}|} + \alpha_T\frac{v_y v_y}{|\mathbf{v}|} \tag{2-15}$$

$$D_{xy} = D_{yx} = \alpha_L\frac{v_x v_y}{|\mathbf{v}|} - \alpha_T\frac{v_y v_x}{|\mathbf{v}|} = (\alpha_L - \alpha_T)\frac{v_x v_y}{|\mathbf{v}|} \tag{2-16}$$

and

$$D_{yy} = \alpha_L \frac{v_y v_y}{|\mathbf{v}|} + \alpha_T \frac{v_x v_x}{|\mathbf{v}|} \tag{2-17}$$

Using these terms, an equation for the components of the dispersive flux can be expressed as

$$\begin{aligned} W_x &= -D_{xx}\frac{\partial C}{\partial x} - D_{xy}\frac{\partial C}{\partial y} \\ W_y &= -D_{yx}\frac{\partial C}{\partial x} - D_{yy}\frac{\partial C}{\partial y} \end{aligned} \tag{2-18}$$

or in matrix form

$$\begin{pmatrix} W_x \\ W_y \end{pmatrix} = -\begin{pmatrix} D_{xx} & D_{xy} \\ D_{yx} & D_{yy} \end{pmatrix} \begin{pmatrix} \dfrac{\partial C}{\partial x} \\ \dfrac{\partial C}{\partial y} \end{pmatrix} \tag{2-19}$$

where D_{xx}, D_{xy}, D_{yx} and D_{yy} now form the components of a *dispersion coefficient* tensor. Equations (2-18) and (2-19) express the net dispersive flux in terms of components in the x and y coordinate directions, rather than in terms of the directions l and n, which vary with the flow direction. To calculate dispersive mass transport in the x direction through an area $\Delta y\,\Delta z$, we would multiply W_x by the fluid area, $\theta\,\Delta y\,\Delta z$; for the y direction we would similarly form the product of W_y and $\theta\,\Delta x\,\Delta z$.

Note that in a uniform flow field, it would be possible to align an axis, say the x axis, with the direction of the velocity vector. In this case, the cross terms D_{xy} and D_{yx} are equal to zero and the expression given in equation (2-18) reduces to simpler form

$$\begin{aligned} W_x &= -D_{xx}\frac{\partial C}{\partial x} \\ W_y &= -D_{yy}\frac{\partial C}{\partial y} \end{aligned} \tag{2-20}$$

where in this case W_x represents the scalar magnitude of the longitudinal dispersive flux vector and W_y represents the scalar magnitude of the transverse dispersive flux vector; compare with equations (2-3) and (2-4). In matrix form equation (2-20) becomes

$$\begin{pmatrix} W_x \\ W_y \end{pmatrix} = -\begin{pmatrix} D_{xx} & 0 \\ 0 & D_{yy} \end{pmatrix} \begin{pmatrix} \dfrac{\partial C}{\partial x} \\ \dfrac{\partial C}{\partial y} \end{pmatrix} \tag{2-21}$$

In the preceding analysis we focused on dispersive transport due to differences between actual particle velocities and the seepage velocity used for advective transport calculation. In most problems this represents the dominant contribution to dispersion. As noted above, however, molecular diffusion may be a significant mechanism of transport in cases where flow velocities are very low. Because the component of diffusive transport in any direction is proportional to the (negative) component of the concentration gradient in that direction, diffusion can be included in the transport calculation in an isotropic medium by adding an effective coefficient of diffusion, D^*, to the terms D_{xx} and D_{yy} of the dispersion coefficient tensor, i.e.,

$$D_{xx} = \alpha_L \frac{v_x v_x}{|\mathbf{v}|} + \alpha_T \frac{v_y v_y}{|\mathbf{v}|} + D^* \tag{2-22}$$

$$D_{yy} = \alpha_L \frac{v_y v_y}{|\mathbf{v}|} + \alpha_T \frac{v_x v_x}{|\mathbf{v}|} + D^* \tag{2-23}$$

The term "effective" and the superscript notation (*) are used to indicate that the diffusion coefficient differs from that in open water because of the effect of the porous medium in reducing diffusive movement. At very low velocities both the advective transport and the terms D_{xx}, D_{xy}, D_{yx} and D_{yy} of the dispersion coefficient tensor may be so small that the diffusion term D^* is significant in comparison.

2.2.4 Dispersive Flux and Dispersion Coefficient in Three Dimensions

For the three-dimensional case, the dispersion coefficient tensor contains nine terms. An equation for the components of the dispersive flux can be

expressed as

$$W_x = -D_{xx}\frac{\partial C}{\partial x} - D_{xy}\frac{\partial C}{\partial y} - D_{xz}\frac{\partial C}{\partial z}$$

$$W_y = -D_{yx}\frac{\partial C}{\partial x} - D_{yy}\frac{\partial C}{\partial y} - D_{yz}\frac{\partial C}{\partial z} \qquad (2\text{-}24)$$

$$W_z = -D_{zx}\frac{\partial C}{\partial x} - D_{zy}\frac{\partial C}{\partial y} - D_{zz}\frac{\partial C}{\partial z}$$

or in matrix form

$$\begin{pmatrix} W_x \\ W_y \\ W_z \end{pmatrix} = -\begin{pmatrix} D_{xx} & D_{xy} & D_{xz} \\ D_{yx} & D_{yy} & D_{yz} \\ D_{zx} & D_{zy} & D_{zz} \end{pmatrix} \begin{pmatrix} \frac{\partial C}{\partial x} \\ \frac{\partial C}{\partial y} \\ \frac{\partial C}{\partial z} \end{pmatrix} \qquad (2\text{-}25)$$

As in the two-dimensional case, dispersive transport is calculated as the product of W_x, W_y, W_z and fluid area normal to the coordinate direction, for example $\theta\,\Delta y\,\Delta z$. If the effective diffusion term, D^*, is included, the components of the three-dimensional dispersion coefficient tensor in equations (2-24) and (2-25) are given by

$$D_{xx} = \alpha_L\frac{v_x^2}{|\mathbf{v}|} + \alpha_T\frac{v_y^2}{|\mathbf{v}|} + \alpha_T\frac{v_z^2}{|\mathbf{v}|} + D^* \qquad (2\text{-}26)$$

$$D_{yy} = \alpha_L\frac{v_y^2}{|\mathbf{v}|} + \alpha_T\frac{v_x^2}{|\mathbf{v}|} + \alpha_T\frac{v_z^2}{|\mathbf{v}|} + D^* \qquad (2\text{-}27)$$

$$D_{zz} = \alpha_L\frac{v_z^2}{|\mathbf{v}|} + \alpha_T\frac{v_x^2}{|\mathbf{v}|} + \alpha_T\frac{v_y^2}{|\mathbf{v}|} + D^* \qquad (2\text{-}28)$$

$$D_{xy} = D_{yx} = (\alpha_L - \alpha_T)\frac{v_x v_y}{|\mathbf{v}|} \qquad (2\text{-}29)$$

$$D_{xz} = D_{zx} = (\alpha_L - \alpha_T)\frac{v_x v_z}{|\mathbf{v}|} \qquad (2\text{-}30)$$

$$D_{yz} = D_{zy} = (\alpha_L - \alpha_T)\frac{v_y v_z}{|\mathbf{v}|} \qquad (2\text{-}31)$$

Again, in a uniform flow field, it would be possible to align an axis, say the x axis, with the direction of the velocity vector. In this case, all cross terms are equal to zero and equations (2-24) become

$$W_x = -D_{xx}\frac{\partial C}{\partial x}$$

$$W_y = -D_{yy}\frac{\partial C}{\partial y} \qquad (2\text{-}32)$$

$$W_z = -D_{zz}\frac{\partial C}{\partial z}$$

or in matrix form:

$$\begin{pmatrix} W_x \\ W_y \\ W_z \end{pmatrix} = -\begin{pmatrix} D_{xx} & 0 & 0 \\ 0 & D_{yy} & 0 \\ 0 & 0 & D_{zz} \end{pmatrix} \begin{pmatrix} \frac{\partial C}{\partial x} \\ \frac{\partial C}{\partial y} \\ \frac{\partial C}{\partial z} \end{pmatrix} \qquad (2\text{-}33)$$

Note that throughout this development we have assumed that the porous medium is isotropic with respect to dispersion. Under this assumption, the dispersion coefficient tensor is based on only two dispersivities, i.e., longitudinal dispersivity, α_L, and the transverse dispersivity, α_T, both of which are independent of coordinate direction. If isotropic conditions cannot be assumed, i.e., if the structure of the porous medium is such that dispersive effects are greater when the flow is in one direction than in another, the definition of the dispersion coefficient tensor requires more dispersivity terms. Bear (1979) indicates that formation of a dispersion coefficient tensor for an anisotropic medium requires five dispersivities. However, Burnett and Frind (1987b) suggest an approximate formulation which requires specification of only three dispersivities. Their approach is based on the recognition that transverse dispersivity is generally much smaller in the vertical direction than in the horizontal direction; they propose using a longitudinal dispersivity, α_L, a horizontal transverse dispersivity, α_{TH}, and a vertical transverse dispersivity, α_{TV}. Their expressions for the components of the dispersion

coefficient tensor are

$$D_{xx} = \alpha_L \frac{v_x^2}{|\mathbf{v}|} + \alpha_{TH} \frac{v_y^2}{|\mathbf{v}|} + \alpha_{TV} \frac{v_z^2}{|\mathbf{v}|} + D^* \tag{2-34}$$

$$D_{yy} = \alpha_L \frac{v_y^2}{|\mathbf{v}|} + \alpha_{TH} \frac{v_x^2}{|\mathbf{v}|} + \alpha_{TV} \frac{v_z^2}{|\mathbf{v}|} + D^* \tag{2-35}$$

$$D_{zz} = \alpha_L \frac{v_z^2}{|\mathbf{v}|} + \alpha_{TV} \frac{v_x^2}{|\mathbf{v}|} + \alpha_{TV} \frac{v_y^2}{|\mathbf{v}|} + D^* \tag{2-36}$$

$$D_{xy} = D_{yx} = (\alpha_L - \alpha_{TH}) \frac{v_x v_y}{|\mathbf{v}|} \tag{2-37}$$

$$D_{xz} = D_{zx} = (\alpha_L - \alpha_{TV}) \frac{v_x v_z}{|\mathbf{v}|} \tag{2-38}$$

$$D_{yz} = D_{zy} = (\alpha_L - \alpha_{TV}) \frac{v_y v_z}{|\mathbf{v}|} \tag{2-39}$$

When the horizontal transverse and vertical transverse dispersivities are equal, as in isotropic media, equations (2-34) through (2-39) specialize to equations (2-26) through(2-31).

2.2.5 Porosity in Solute Transport Calculation

The question of the porosity required in solute transport calculation was addressed briefly in Section 1.1. In this section we discuss this question further in relation to the concepts of dispersive transport, and in relation to the role of porosity in a full transport calculation.

Note that because dispersive transport is described in terms of random departures from the seepage velocity, the concentration peak of Figure 2-5 should move through the sand at the seepage velocity, v, i.e., at the Darcy velocity divided by an effective porosity term. If the problem were one involving change from an initial concentration C_1 to some final concentration C_2, an interface marking the mean concentration, $(C_1 + C_2)/2$, should similarly move through the sand at the seepage velocity. Historically, in situations where both seepage velocity measurements and measurements of total porosity, i.e., the ratio of total pore volume to bulk volume, have been available, the observed seepage velocity has often exceeded the velocity calculated using the total porosity. The concept of effective porosity, as used in the development of equation (1-6), evolved because of this phenomenon.

Clearly, no fluid movement can occur in pore space which is totally

isolated from the remaining pore space of an aquifer, and no tracer can enter such pore space. As stated in Chapter 1, however, the problem is never simply that one part of the pore space is effective in transmitting groundwater and one part is not, as assumed in the development of equation (1-5). As our discussions of dispersive transport suggest, the distribution of flow through the pore space can more accurately be described in terms of a continuous spectrum, in which velocity varies from zero to values considerably greater than the velocity of the centroid of solute mass. The nature of that flow distribution necessarily influences the porosity figure required to yield the observed centroid velocity in calculation. For example, if a very high fraction of the flow is concentrated in a very small percentage of the pore space, the porosity needed to reproduce the observed centroid velocity will differ from that required in a medium of the same total porosity, but with a relatively uniform flow distribution. In more general terms, the centroid velocity may be influenced by some of the same factors which influence dispersive flux, for example, pore-scale diffusion of solute into regions of negligible velocity. One implication of this is that effective porosity and dispersivity may not be independent.

However, the question of the porosity required in transport simulation is broader than the question of the porosity required in seepage velocity calculation. As we saw in the development of equation (1-32) and equations (1-37) through (1-40), porosity enters transport calculations not only in the seepage velocity term, but also in expressions for the solute mass in a given volume of aquifer and the rate at which that mass changes with time. In the analysis of Chapter 1, advection was assumed to be the only transport process. This implies that storage of solute mass can occur only within the mobile portion of the interstitial water. As a result, the effective porosity used in calculating seepage velocity is also the porosity assumed to govern solute mass accumulation in equation (1-32) and equations (1-37) through (1-40). When dispersive transport is considered, however, it appears that two different values of porosity might be required in the sense that pore-scale diffusion can cause solute to spread into portions of the interstitial water in which there is little or no fluid movement. In other words, one porosity may be required for seepage velocity calculation while another may be needed for evaluating the rate of mass accumulation. De Marsily (1986) shows that if the mixing of solutes caused by diffusion from mobile to immobile portions of the pore water is assumed to be instantaneous, these two porosities are both equivalent to the total porosity. At the other end of the spectrum, if the mixing is assumed to be negligible (as in the analysis of Chapter 1), the two porosities are both equivalent to the effective porosity as defined in Chapter 1, or the "kinematic" porosity, as it is defined by de Marsily (1986).

Rather than invoking two porosity terms, the convention in advection-dispersion transport analysis has been to use a single value of porosity, except in certain dual porosity approaches to very specialized situations. Thus in effect a single lumped effective porosity is defined for calculating both seepage velocity and rate of solute mass accumulation. As we have stressed previously, the effective porosity is difficult to determine in practice and generally must be interpreted as the parameter which, in model calibration, gives the closest representation both of plume movement and of observed solute accumulation effects. In some cases, particularly where two very different porosities (e.g., fracture and matrix) occur in close association, it may be impossible to define a single effective porosity which fills both roles. In these cases, a dual porosity approach can be considered.

2.3 MACROSCOPIC DISPERSION

Our discussion of dispersion began by considering departures of the magnitude and direction of the actual flow velocity from the calculated seepage velocity, as caused by the microscopic heterogeneity and tortuosity of a granular porous medium. These factors appear to determine dispersivity at the scale of laboratory experiments. The resultant dispersion is generally limited; longitudinal dispersivities in the range 0.01 to 1 cm are not uncommon in laboratory experiments. However, dispersivities from two to four orders of magnitude larger are typically required to account for observed dispersion in field situations. This disparity arises because dispersion at the field scale is caused primarily by macroscopic heterogeneities, rather than by pore-scale heterogeneity.

In any advective transport calculation, the seepage velocity is assumed to be uniform or to vary in some simple way over certain regions or domains of the flow regime. If the velocity field used for advective calculation is derived from an analytical solution, velocity will generally be constant, or will be a smoothly varying function, throughout the problem domain. More commonly, numerical solution of the flow equation is invoked, using finite-difference or finite-element simulation; and velocities are calculated at a fixed number of points corresponding in some way to the nodes or elements of the simulation mesh. Velocity may then be considered constant over a region surrounding each point of calculation, or may be defined through interpolation between those points. The result is that the calculated velocity is constant or varies smoothly over regions that typically measure thousands of square feet in map area, and extend vertically through some significant part of the local hydrogeologic section.

Clearly, regions of this size can contain macroscopic heterogeneities at a variety of scales, characterized by values of hydraulic conductivity and

porosity which differ markedly from the values used in the flow simulation. The result is that while the calculated seepage velocity may approximate the average velocity for the entire region represented by a model cell or element, the actual seepage velocity may vary widely from one location to another within that region. Fluid particles traversing the region thus experience a sequence of different velocities at the macroscopic scale; and fluid particles entering the region at different points experience a different sequence of macroscopic velocities. The microscopic velocity variation associated with the pore structure is superposed on the macroscopic variation, and its effect is usually minor in comparison. Depending on the spatial distribution of macroscopic heterogeneities, flow may tend to concentrate along pathways of higher conductivity, to diverge around areas of low conductivity, and to be refracted at conductivity boundaries. If the heterogeneities are not represented in the hydraulic conductivity distribution used in simulation, no effects of this kind are represented in the advective transport calculation.

If a tracer or solute is present, and if its concentration varies spatially within the volume represented by a model cell or element, macroscopic velocity variations will necessarily cause both longitudinal and transverse spreading of the tracer, in a way which may mimic, but on a much larger scale, the effects of velocity variation at the pore scale. In general, the macroscopic spreading of a tracer tends to increase as the number of heterogeneities increases, or as the range of hydraulic conductivity contrast increases. Figure 2-16 shows the effect that macroscopic heterogeneities, in this case high conductivity inclusions a few feet long in a sandbox experiment, can have on tracer distribution.

As noted above, the velocity distributions used in advective transport calculations are frequently supplied through numerical solution of the flow

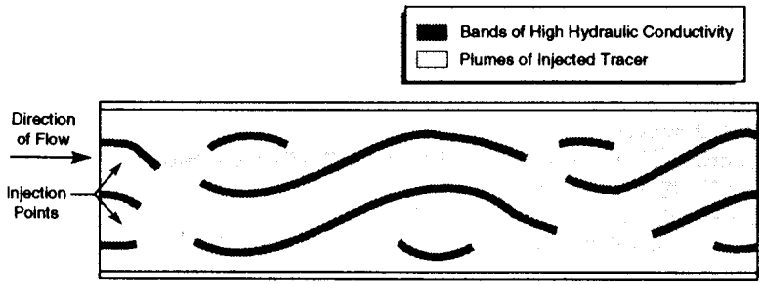

FIGURE 2-16. Results of a laboratory experiment to determine the effects of macroscopic heterogeneity on a tracer (modified from Skibitzke and Robinson, 1963).

equation, using finite-difference or finite-element simulation. Clearly, the more closely a simulation can represent the actual distribution of hydraulic conductivity in the field, the more closely the advective calculation will mirror actual solute transport, and the smaller the dispersive transport term will be. In most cases, however, when data collection has reached its practical limit, only a small fraction of the heterogeneities present in the field will have been identified; and many heterogeneities, identified or not, will be at too small a scale to be represented explicitly as an element or cell in simulation. Thus some method is necessary to account for the influence of these features on solute transport. In almost all practical solute transport studies undertaken to date, dispersive transport calculation has been used for this purpose; in general the practice has been to adjust dispersivities in calibration to achieve the best match between observed and calculated concentration distributions.

It should also be noted that while the preceding and subsequent discussions focus primarily on heterogeneity of the aquifer properties (i.e., hydraulic conductivity and porosity), heterogeneity in other properties or processes which influence velocity can have similar effects. For example, temporal and spatial variations in recharge and discharge may cause variations in velocity, which in turn generate solute transport effects; and advective transport calculation which treats recharge and discharge as uniform in space and time will fail to reproduce those transport effects, and in practice they are usually accounted for only through the dispersive transport calculation.

Like the early use of dispersive transport theory to account for microscopic or pore-scale velocity variation, its use to account for macroscopic heterogeneity or velocity variation is an attempt to adjust the advective calculation for factors and influences which are known to exist, but which cannot be incorporated explicitly because of inadequate data and unrealistic computation requirements. Again, therefore, the transport mechanism itself should be recognized primarily as solute movement with the moving fluid, and the dispersive calculations as an empirical correction, even though it is common usage to speak of a dispersive transport process.

The dispersive transport equations outlined above were developed by assuming the departures of actual particle velocity from the advective velocity to be similar to the movement of ions in diffusion. This appears to be a reasonable assumption for velocity variations associated with pore-scale heterogeneity. As the scale of heterogeneity increases, and particularly if it approaches the scale of the region used in advective calculation (e.g., an element or cell used in simulation), the assumption of random departure may come into question. Intuitively we would expect a large number of heterogeneities within the region of a single cell or element to generate velocity departures in all directions, covering a continuous range of magnitudes. Under these circumstances a calculation based on the diffusive

analogy should yield a result in reasonable agreement with observation. On the other hand, if the heterogeneity within an element is dominated by a few major features, covering a significant fraction of the region represented by the element, the velocity departure may be biased consistently toward a particular direction or magnitude. For that cell at least, a calculation which assumes random departure may not produce agreement with observation. Again, however, we might expect intuitively that over a large number of elements, effects of this kind would tend to cancel, and that calculations based on the diffusive analogy should therefore give better results as the area covered by the solute movement expands.

In a general sense, the influence of macroscopic heterogeneity on solute movement, and the use of dispersive transport theory to account for that influence, imply that the advective and dispersive calculations are interdependent. Effects which can be described through the advective calculation, at a given scale, need not be addressed in the dispersive calculation; conversely, effects which cannot be accommodated in the advective calculation must be accounted for through the dispersive calculation. The scale of the flow simulation determines to some extent what can and cannot be accommodated in the advective calculation, and so influences the role that dispersive calculation must play. In addition, scale may influence the magnitude of the dispersivity in the sense that in a simulation which uses a coarse mesh spacing, more and larger heterogeneities are included in each element or cell than in a simulation which uses a close spacing. Thus for the same field problem, the dispersivities needed to achieve agreement with observed solute movement may tend to be larger at larger node spacings. However, one would also expect intuitively that at some point further increases in spacing would no longer change the distribution of heterogeneities within an individual cell, and would therefore produce no further increase in dispersivity. This implies that the concept of representative elemental volume, or REV (Bear, 1972) may be applied to macroscopic heterogeneity, as suggested by Domenico and Schwartz (1990).

Skibitzke and Robinson (1963), who obtained the experimental results shown in Figure 2-16, were among the first to recognize the effect of macroscopic heterogeneity on solute transport in groundwater. Mercado (1967) analyzed the effect of an important category of heterogeneity, internal geologic stratification within a section which is considered a single layer in sampling or calculation. In more recent years, there has been general recognition of the dominant role of heterogeneity in causing field-scale dispersive effects. This has led to extensive research efforts, both to develop a sound theoretical description of the macrodispersive process, and to find tractable methods of representing that process in calculation. Some of the significant contributions are those of Gelhar et al. (1979); Matheron

and de Marsily (1980); Dagan (1982a, b; 1984); Cushman (1983); Gelhar and Axness (1983); Wheatcraft and Tyler (1988); and Neuman and Zhang (1990). The most active line of research has focused on stochastic approaches, in which hydraulic conductivity is considered a random variable in space. The calculated seepage velocity is thus also a random variable, and generates a dispersive effect in the calculated solute concentration. Depending on the assumptions that are made regarding the conductivity distribution, the dispersive effect may or may not turn out to be similar to diffusion as calculated by Fick's Law. However, a number of stochastic approaches predict that the diffusive model will be approximated asymptotically, and that macroscopic dispersivity will approach a constant value, as the distance of transport becomes large. Other approaches to macrodispersion research have focused on volume averaging, rather than on stochastic theory (e.g., Plumb and Whitaker, 1988). Thus equations are developed in terms of average values of concentration and velocity over volumes of the aquifer which incorporate macroscopic heterogeneities. Again, depending on the nature and scale of the heterogeneities and the scale at which the volume averaging is done, the resulting description of macrodispersive transport may or may not approximate the diffusion model.

At present, the transport simulation codes in most common use in the field treat dispersive effects as obeying the diffusive (Fick's Law) model. Intuitive reasoning, as well as the results of much of the research that has been done, indicate that this should be a satisfactory approximation provided the scale of the heterogeneities is small relative to the distance of transport or scale of calculation. Thus the question of the scale of heterogeneity versus the scale of calculation deserves consideration whenever a conventional transport model is applied. However, if these scales, and the nature of the heterogeneity, are such that the use of a model based on the diffusive approach appears justified, there is still the problem of assigning dispersivity terms which will adequately represent macrodispersive effects. In theory, if enough information on the spatial variation of hydraulic conductivity is available, it becomes possible to calculate dispersivities using the statistics of the hydraulic conductivity distribution (e.g., Sudicky, 1986; Rehfeldt et al., 1992). In practice the requisite information is rarely available for an attempt of this sort; the choice of dispersivity is usually based on model calibration, or is made more or less arbitrarily on the basis of general experience with aquifer materials of similar type. The difficulties inherent in calibration, and in the assignment of model parameters in general, are discussed in subsequent chapters. However, a few remarks are appropriate at this point.

The closer the actual hydraulic conductivity variations are represented in a model, the smaller the macrodispersive effect will be. For this reason, an effort should be made in all transport simulations to define the spatial

variation of hydraulic conductivity as completely as possible, both in the map view and in the vertical. Where persistent spatial patterns can be recognized in the results of hydraulic conductivity testing, and in particular where those patterns are supported by geologic inference, the simulation mesh should be designed in such a way that these conductivity variations can be incorporated. In many cases, however, the results of field testing may provide no information on spatial patterns of variation, and may serve only to indicate a general range of hydraulic conductivity variation. In these cases it may be a mistake to overspecify hydraulic conductivity, particularly in the absence of geological supporting evidence.

Where hydraulic conductivity variations can be identified with confidence, their representation in a model will generally create certain requirements as to mesh spacing. At any mesh spacing, unrecognized conductivity variations will remain within the volume represented by each cell or element of the model; and these must be accounted for through the dispersive calculation. At fine mesh spacings, the chance is greater that individual heterogeneities will approach the scale of the spacing, and that a diffusive model of macrodispersion may fail to represent the local concentration departures caused by those heterogeneities. Thus while many factors necessarily influence the choice of mesh design, the user of a simulation code should at least remain aware of potential problems arising from the scale of the heterogeneity versus the scale of calculation.

In any calibration exercise, nonuniqueness is a major obstacle; more than one array of parameters can generally yield a satisfactory match with observed data. This would be a significant problem in calibrating to determine dispersivity even where no other unknown parameters were involved. It is exacerbated by the fact that in most field problems hydraulic conductivity, porosity, and other transport terms may also be targets of the calibration exercise. For this reason the importance of acquiring as much field data as possible on all relevant parameters cannot be overstated.

2.4 ADVECTIVE-DIFFUSIVE SYSTEMS

In a common form of macroscopic heterogeneity, intervals of very high permeability are closely interspersed with intervals of very low permeability. In these cases, solute transport may occur primarily by advection in the high permeability zones, but primarily by molecular diffusion in the low permeability zones. For example, in a fractured bedrock system, advective transport may dominate within the fracture network, while molecular diffusion may be the dominant process in the matrix blocks between fractures. Heterogeneous glacial deposits, in which layers or lenses of sand and gravel are interspersed with low permeability clays, provide another example. Within

the clays, velocities may be so low that molecular diffusion dominates solute transport, whereas in the sand or gravel advection may dominate.

In systems of this sort, diffusion of solute into the low permeability zones reduces the mass of solute moving advectively in the higher permeability intervals, reducing the tendency for solute to "finger" preferentially for long distances along those intervals. The result, particularly where the high permeability features are closely spaced, is a more uniform solute distribution and a slower solute advance than would be predicted considering only advective movement in the high permeability features. The results are in some ways analogous to those of sorption (see Chapter 3), in that mass is removed from the advective regime when concentrations in the high permeability zone exceed those in the adjacent low permeability material, but diffuses back into the high permeability regime if concentration gradients are subsequently reversed. Thus the removal of contaminants in a system of this sort may require much longer times than in a uniform advective-dispersive system.

When the process described here occurs in a fractured rock environment, it is commonly referred to as *matrix diffusion*, reflecting the fact that solute movement into the rock matrix is controlled by diffusion (Freeze and Cherry, 1979); the more general term *advective-diffusive transport* has been used where the process occurs in heterogeneous unconsolidated deposits (Gillham and Cherry, 1982).

The advective-diffusive model represents a special case in which the result of macroscopic heterogeneity is to separate the transport regime into local zones dominated either by advection or by molecular diffusion. In theory, if the spatial distribution of these zones were fully defined, it would be possible to represent the individual advective and diffusive zones using the cells or elements of a simulation mesh; transport parameters could then be specified for each element reflecting either the advective or diffusive dominance. In practice, again, this approach is generally precluded both by the lack of detailed field information and by unrealistic computational requirements. As an alternative, the system can be viewed in terms of a dual porosity model, in which a predominantly advective regime and a predominantly diffusive regime are assumed to coexist over the same volume (e.g., Grisak and Pickens, 1980; Huyakorn et al., 1983). Equations are developed for concentration as a function of space and time in each regime, with each equation including terms to describe the transfer of solute between the regimes; these terms couple the equations into a system which can be solved jointly. Finally, an advective-diffusive system can be approached through a conventional advective-dispersive simulation, if it is possible to choose transport parameters which adequately reproduce observed results. As in any application of the advective-dispersive model to a macroscopically heterogeneous system,

however, questions may arise as to whether the underlying assumption of random deviation from an average seepage velocity actually represents the physical reality.

2.5 DEVELOPMENT OF THE ADVECTION-DISPERSION EQUATION

A combined transport equation can be obtained by adding the dispersive flux terms to the advective transport equation. To simplify this development we consider first a small volume element having the dimensions $\Delta m\, \Delta n\, \Delta l$, within the sand-packed pipe, as shown in Figure 2-17, where Δl is parallel to the pipe, and Δm and Δn represent mutually orthogonal directions normal to the pipe. Because velocity is only in the direction l, we need consider advective transport only in that direction. The area of flow through the element, normal to l, is $\Delta m\, \Delta n$, and the advective transport through that area is $qC\, \Delta m\, \Delta n$. The net difference between advective inflow at the upstream face and outflow at the downstream face of the element is therefore

$$-\frac{\partial}{\partial l}(qC)\, \Delta l\, \Delta m\, \Delta n \tag{2-40}$$

where as before, the velocity is included under the derivative to allow for the possibility that the magnitude of the velocity may vary over the distance Δl. (Again it is assumed that storage effects are limited to compression of the water with a rigid porous framework.)

The formulation of dispersive transport terms is simplified in this problem

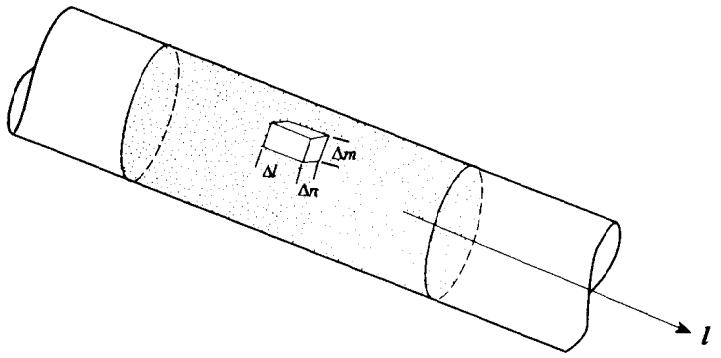

FIGURE 2-17. Volume element $\Delta l\, \Delta n\, \Delta m$ aligned with the direction of flow, l.

because the direction of flow is fixed, and because the volume element we have chosen is aligned with the flow direction and the two transverse directions. Longitudinal dispersion occurs only through the area ($\Delta m\,\Delta n$) of the upstream and downstream faces of the element; the dispersive mass transport is given by

$$-D_l \frac{\partial C}{\partial l}\theta\,\Delta m\,\Delta n \tag{2-41}$$

where D_l is the coefficient of longitudinal dispersion, and the concentration gradient $\partial C/\partial l$ may vary between the faces. Note that the possibility that velocity may vary through the element implies that D_l may also vary between the upstream and downstream faces. Under these assumptions the change in dispersive mass transport between the upstream and downstream faces is determined by the change in the product $D_l\,\partial C/\partial l$. Thus the expression for the difference between mass inflow and mass outflow due to longitudinal dispersion is

$$\frac{\partial}{\partial l}\left(D_l \frac{\partial C}{\partial l}\right)\theta\,\Delta l\,\Delta m\,\Delta n \tag{2-42}$$

Dispersion normal to the flow occurs in both the n and m directions; we assume the coefficient of transverse dispersion to be the same in these two directions. Thus the rate of dispersive mass transport in the n direction is

$$-D_n \frac{\partial C}{\partial n}\theta\,\Delta m\,\Delta l \tag{2-43}$$

and the net difference between dispersive mass inflow and outflow in that direction is

$$\frac{\partial}{\partial n}\left(D_n \frac{\partial C}{\partial n}\right)\theta\,\Delta n\,\Delta l\,\Delta m \tag{2-44}$$

Similarly, for transverse dispersion in the m direction, the net difference between mass inflow and outflow is

$$\frac{\partial}{\partial m}\left(D_m \frac{\partial C}{\partial m}\right)\theta\,\Delta m\,\Delta l\,\Delta n \tag{2-45}$$

where we assume $D_m = D_n$.

The rate of mass accumulation in the element is

$$\theta\,\Delta l\,\Delta m\,\Delta n \frac{\partial C}{\partial t} \tag{2-46}$$

Equating this term to the sum of the four terms describing the difference between mass inflow and mass outflow gives

$$\theta\,\Delta l\,\Delta m\,\Delta n \frac{\partial C}{\partial t} = -\frac{\partial}{\partial l}(qC)\,\Delta l\,\Delta m\,\Delta n + \left\{\frac{\partial}{\partial l}\left(D_l \frac{\partial C}{\partial l}\right) + \frac{\partial}{\partial m}\left(D_m \frac{\partial C}{\partial m}\right) + \frac{\partial}{\partial n}\left(D_n \frac{\partial C}{\partial n}\right)\right\}\theta\,\Delta l\,\Delta m\,\Delta n \tag{2-47}$$

or, dividing by $\theta\,\Delta l\,\Delta m\,\Delta n$ and recalling that the term q/θ is equivalent to the seepage velocity, v,

$$\frac{\partial C}{\partial t} = -\frac{\partial}{\partial l}(vC) + \frac{\partial}{\partial l}\left(D_l \frac{\partial C}{\partial l}\right) + \frac{\partial}{\partial n}\left(D_n \frac{\partial C}{\partial n}\right) + \frac{\partial}{\partial m}\left(D_m \frac{\partial C}{\partial m}\right) \tag{2-48}$$

Equation (2-48) is the differential equation for advective-dispersive transport in unidirectional flow where no sources or sinks are present, and where one coordinate is taken in the direction of flow.

Again, however, an equation in the form of (2-48) cannot be applied in general situations where the direction of flow is variable. To develop the advection-dispersion transport equation in terms of the conventional Cartesian coordinate system, consider the volume element of Figure 1-4, $\Delta x\,\Delta y\,\Delta z$, which is shown again in Figure 2-18 and is aligned with coordinate directions

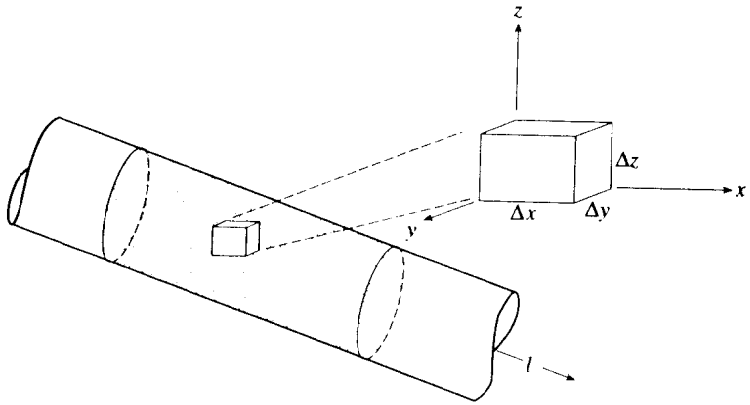

FIGURE 2-18. Volume element for development of the advection-dispersion equation in Cartesian coordinates.

that are neither parallel nor normal to the pipe. In effect, this could be considered simply a rotation of the volume element $\Delta l\,\Delta m\,\Delta n$ of Figure 2-17. Clearly the transport processes have not changed, and the flow through the system is still fixed and unidirectional; however, the fact that the coordinate directions are no longer parallel/normal to the flow leads to a more cumbersome expression of the transport equation. In addition, we will allow for the possible presence of sources or sinks within the volume element. As in the development of equation (1-36), the presence of Darcy velocity components in all three coordinate directions leads to the expression:

$$-\left\{\frac{\partial}{\partial x}(q_x C) + \frac{\partial}{\partial y}(q_y C) + \frac{\partial}{\partial z}(q_z C)\right\}\Delta x\,\Delta y\,\Delta z + Q_s C_s \qquad (2\text{-}49)$$

for the difference between inflow and outflow of solute mass due to advection and fluid sinks or sources, where again Q_s is the flow rate and C_s the concentration associated with the source or sink.

Because the x direction is neither parallel nor normal to the flow, dispersive transport through the area $\Delta z\,\Delta y$ involves both longitudinal and transverse components. Using equation (2-24) this dispersive transport in terms of mass per unit time is given by

$$F_x = W_x\theta\,\Delta y\,\Delta z = -\left(D_{xx}\frac{\partial C}{\partial x} + D_{xy}\frac{\partial C}{\partial y} + D_{xz}\frac{\partial C}{\partial z}\right)\theta\,\Delta y\,\Delta z \qquad (2\text{-}50)$$

The difference between inflow and outflow of mass due to dispersion in the x direction for the element $\Delta x\,\Delta y\,\Delta z$ is therefore

$$\frac{\partial}{\partial x}\left(D_{xx}\frac{\partial C}{\partial x} + D_{xy}\frac{\partial C}{\partial y} + D_{xz}\frac{\partial C}{\partial z}\right)\theta\,\Delta x\,\Delta y\,\Delta z \qquad (2\text{-}51)$$

Similarly for the y direction the difference between mass inflow and outflow due to dispersion is given by

$$\frac{\partial}{\partial y}\left(D_{yx}\frac{\partial C}{\partial x} + D_{yy}\frac{\partial C}{\partial y} + D_{yz}\frac{\partial C}{\partial z}\right)\theta\,\Delta x\,\Delta y\,\Delta z \qquad (2\text{-}52)$$

and for the z direction:

$$\frac{\partial}{\partial z}\left(D_{zx}\frac{\partial C}{\partial x} + D_{zy}\frac{\partial C}{\partial y} + D_{zz}\frac{\partial C}{\partial z}\right)\theta\,\Delta x\,\Delta y\,\Delta z \qquad (2\text{-}53)$$

The total difference between inflow and outflow of solute mass for the volume element is obtained by summing the advective and dispersive terms in the three coordinate directions. Forming this sum, equating it to the rate of solute mass accumulation in the volume, $\theta\,\Delta x\,\Delta y\,\Delta z\,\partial C/\partial t$, and dividing by the term $\theta\,\Delta x\,\Delta y\,\Delta z$ yields

$$\begin{aligned}\frac{\partial C}{\partial t} = {} & \frac{\partial}{\partial x}\left(D_{xx}\frac{\partial C}{\partial x} + D_{xy}\frac{\partial C}{\partial y} + D_{xz}\frac{\partial C}{\partial z}\right) - \frac{\partial}{\partial x}(v_x C) \\ & + \frac{\partial}{\partial y}\left(D_{yx}\frac{\partial C}{\partial x} + D_{yy}\frac{\partial C}{\partial y} + D_{yz}\frac{\partial C}{\partial z}\right) - \frac{\partial}{\partial y}(v_y C) \\ & + \frac{\partial}{\partial z}\left(D_{zx}\frac{\partial C}{\partial x} + D_{zy}\frac{\partial C}{\partial y} + D_{zz}\frac{\partial C}{\partial z}\right) - \frac{\partial}{\partial z}(v_z C) + \frac{q_s}{\theta}C_s \qquad (2\text{-}54)\end{aligned}$$

where again v_x, v_y, and v_z are components of the seepage velocity, and $q_s = Q_s/(\Delta x\,\Delta y\,\Delta z)$. Equation (2-54) can be written in vector form as

$$\frac{\partial C}{\partial t} = \nabla\cdot(\mathbf{D}\cdot\nabla C) - \nabla\cdot(\mathbf{v}C) + \frac{q_s}{\theta}C_s \qquad (2\text{-}55)$$

or in subscript form as

$$\frac{\partial C}{\partial t} = \frac{\partial}{\partial x_i}\left(D_{ij}\frac{\partial C}{\partial x_j}\right) - \frac{\partial}{\partial x_i}(v_i C) + \frac{q_s}{\theta}C_s \qquad (2\text{-}56)$$

Equation (2-56) describes advective-dispersive solute transport in three dimensions with internal sources or sinks present. Because it is expressed in terms of a fixed coordinate system, equation (2-56) provides a suitable framework for the analysis of problems where velocity and concentration vary in three dimensions. As the development illustrates, however, this form of the equation, rather than equation (2-48), is required even for unidirectional flows, unless one of the coordinate directions coincides with the flow direction.